A functional characterisation of the DNA helicase ChlR1 in DNA replication and repair

LAURA McFARLANE-MAJEED

A thesis submitted to the

UNIVERSITY OF BIRMINGHAM

for the degree of

DOCTOR OF PHILOSOPHY

SCHOOL OF CANCER SCIENCES, COLLEGE OF MEDICAL AND DENTAL SCIENCES

2014

Abstract

ChlR1 is a DNA helicase implicated in diverse cellular processes including sister chromatid cohesion and DNA replication and repair. However, the mechanism by which ChlR1 participates in these processes is unknown. Data presented in this thesis show that siRNA-mediated depletion of ChlR1 causes increased sensitivity to chemically-induced replication stress. Treatment of ChlR1-depleted cells with hydroxyurea results in increased mono-ubiquitination of PCNA and increased chromatin-associated RPA, indicating stalled DNA replication. Furthermore, ChlR1 is recruited to chromatin following hydroxyurea treatment, supporting a role in the stabilisation of forks during replication stress. Fibroblasts derived from a Warsaw Breakage Syndrome (WABS) patient caused by mutation of ChlR1 (G57R) have both defective sister chromatid cohesion and G2 checkpoint following radiation-induced damage. Complementation with wild-type ChlR1 rescued this mutant phenotype while a known helicase dead mutant of ChlR1 (K50R) or the WABS-associated mutants G57R or ΔK897 did not. However, increased and prolonged Chk1 activation was observed in both K50R and ΔK897 complemented cells after treatment with hydroxyurea while the G57R was comparable to wild-type. These data suggest that the novel WABS mutation (G57R) may retain some wild-type ChlR1 activity and offer important insight into the molecular basis of the WABS phenotype.

Acknowledgements

I would like to first of all thank my supervisor Jo for all her support and guidance with this project in particular and during my time in the lab in general. The past 4 years I've spent in the Parish lab have been an absolute pleasure and the atmosphere of camaraderie and collaboration created by all the members and by Jo herself have made all the hard work, long hours and effort that PhD research inevitably entails not only manageable but also extremely enjoyable. For this I would also like to thank the members of the Parish lab, both past and present, for all the advice, help and friendship that they've provided over the years. A special mention must go to Katherine who has laboured along with me on ChlR1 (one day we will know!) and without her technical expertise and invaluable discussion this project could not have progressed to this point. I was very lucky to work with such a great postdoc…especially one who would share a moan with me over a bottle of wine (or two) on a Friday night after a week of terrible western blots. The Court Oak has sadly had to close its doors now that we're no longer supporting it with our custom.

I would also like to extend my thanks to Dr Grant Stewart and Prof Malcolm White for their co-supervision on various aspects of this work and to everyone in the School of Cancer Sciences at the University of Birmingham who has leant me their knowledge, expertise or reagents at some point over the past 2 and a half years. And to all my lovely friends and colleagues in WX1.67 I just want to say how much I appreciate all of your help both during my PhD and during the very stressful writing-up process. I apologise for all the whining and I thank you for all the tea and chocolate!

I would like to thank my family for the support they have shown me during my degree and for never doubting that I would get it done. Finally, I especially want to thank my wonderful husband and best friend Sijad for his unconditional love, support and encouragement that got me through the tough times when nothing else would have.

Table of abbreviations

Abbreviation	Definition
ORC	Origin recognition complex
MCM2-7	Mini-chromosome maintenance 2-7
CDC6	Cell division cycle 6
CDT1	Chromatin licensing and DNA replication factor 1
CDK2	Cyclin-dependent kinase 2
DDK	Dbf4-dependent kinase
GINS	Go-ichi-ni-san
RFC	Replication factor c
PCNA	Proliferating cell nuclear antigen
TLS	Translesion synthesis
DSBs	Double strand breaks
HU	Hydroxyurea
HLTF	Helicase-like transcription factor
ssDNA	Single-stranded DNA
RPA	Replication protein A
ATR	Ataxia telangiectasia and Rad3-related
ATRIP	ATR interacting protein
Topbp1	DNA topoisomerase 2-binding protein 1
FPC	Fork protection complex
UV	Ultraviolet
IR	Ionising radiation
HR	Homologous recombination
NHEJ	Non-homologous end joining
DNA-PK	DNA-dependent protein kinase
BRCA1	Breast cancer associated protein 1
ATM	Ataxia telangiectasia-mutated
MRN complex	Mre11-Rad50-NBS1
Mre11	Meiotic recombination 11 homolog 1
EXO1	Exonuclease 1
D-loop	Displacement loop
HJ	Holliday junction
GEN1	Flap endonuclease GEN homolog 1
FA	Fanconi Anaemia
BLM	Bloom Syndrome helicase
WRN	Werner Syndrome helicase
IF	immunofluorescence
TOP3A	Itopoisomerase 3 alpha
hRMI1	RecQ-mediated genome instability protein 1 or BLAP75
SMC	Structural Maintenance of Chromosomes

SCC1	Sister Chromatid Cohesion
Plk1	Polo-Like kinase 1
Eco1	Establishment of cohesion protein 1
Ctf7	Chromosome transmission fidelity protein 7
POL30	DNA processivity factor PCNA)
FRET	Fluorescence Resonance Energy Transfer
Chl1p	Chromosome loss protein 1
CTCF	CCCTC binding factor
Chl1	Chromosome loss mutation
CTF1	Chromosome transmission fidelity
GST	Glutathione-S transferase
GFP	Green Fluorescent Protein
NER	Nucleotide excision repair
MMS	Methyl methanesulfonate
WABS	Warsaw Breakage Syndrome
TAP	Tandem Affinity Purification
SDS PAGE	Sodium dodecyl sulphate polyacrylamide gel electrophoresis
PCR	Polymerase Chain Reaction
RT	Reverse transcriptase
MPB	Maltose-binding protein
FPLC	Fast performance liquid chromatography
DTT	Dithiothreitol
CPT	Topoisomerase inhibitor camptothecin
UTR	Untranslated region
PCS	Premature chromatid separation
IP	Immunoprecipitation
LB	Luria Broth
kb	Kilobase
EtOH	Ethanol
PVDF	Polyvinylidine fluoride
MeOH	Methanol
FPLC	Fast protein liquid chromatography
TCA	Trichloroacetic acid
FBS	Foetal bovine serum

List of Figures

List of Tables

Contents

Chapter 1

Introduction

1.1 Maintenance of genomic stability is essential for cell survival and proliferation

The ability of a cell to survive, function and replicate depends upon the successful co-ordination of essential cellular processes that enable the integrity of the genome to be maintained. The consistently accurate transmission of genetic information to subsequent generations involves the careful control and regulation of important cellular processes such as DNA replication, DNA damage repair and sister chromatid cohesion.

Cells must accurately synthesise exact copies of the DNA in each chromosome to pass on to their progeny following mitosis. This requires not only accurate, error-free replication of each DNA molecule but also the successful detection and repair of any damage prior to completion of cell division. Additionally, cells must also ensure that chromosomes are correctly segregated so that each daughter cell is genetically identical and has the appropriate chromosomal complement following cytokinesis. This is achieved via the encircling of two newly-replicated DNA molecules, now termed sister chromatids, by a protein complex called cohesin until separation occurs at the onset of anaphase. Disruption or deregulation of any of these processes can result in loss of genomic integrity. In humans this can have serious consequences for cell survival and can lead to severe inherited genetic disorders as well as contributing to both the development and progression of cancer [1, 2].

Consequently, cells have evolved very elegant mechanisms which allow the tight regulation and coupling of these essential processes. This requires the coordination and participation of an army of cellular proteins, many of which function in more than one of these pathways. How diverse cellular processes such as DNA replication, DNA repair and cohesion establishment can function both individually and in collaboration to promote genome stability maintenance will be discussed in subsequent sections.

1.2 DNA replication, DNA damage repair and the maintenance of genetic stability

Accurate transmission of genetic material from a parent cell to its daughter cells during mitosis is absolutely essential if cell viability and genetic stability is to be maintained. This requires that the cell has precisely replicated its DNA such that each of its offspring receives an identical copy of each chromosome following cell division. To ensure this is achieved, cells have evolved sophisticated machinery that allows them to sense mistakes in replication or damage to DNA and to take appropriate action [3].

1.2.1 Overview of eukaryotic DNA replication

In eukaryotic cells, replication initiation occurs at sites across the genome known as origins of replication [4, 5]. The specific factors influencing origin selection as well as origin spacing and distribution throughout the genome, while thought to be sequence independent, still present an area of ongoing study. What is clear however is that origin selection depends upon the binding of the origin recognition complex (ORC), a six subunit complex consisting of ORC1-ORC6, which associates with potential origins in the G1 phase of the cell cycle. Also during G1, components of the pre-replication complex (pre-RC) are recruited to origins by the ORC. These include the replicative helicase MCM2-7 (mini-chromosome maintenance 2-7) as well as CDC6 (cell division cycle 6) and CDT1 (chromatin licensing and DNA replication factor 1). This process is also referred to as origin licencing [6-9]. Replication is then initiated in early S-phase via the specific phosphorylation of various subunits of the pre-RC by cellular kinases CDK2 (cyclin-dependent kinase 2) and DDK (Dbf4-dependent kinase or CDC7 kinase as it is also known) which serves as a signal for subsequent loading of CDC45 and the GINS (go-ichi-ni-san) complex to form the active replicative helicase complex comprised of CDC45,

MCM2-7 and GINS (CMG) [10-12]. This in turn promotes origin firing and replication fork progression [13-16]. In eukaryotes, two individual replication complexes are assembled and activated at each origin and then proceed to move away from the origin in opposite directions (**figure 1.1A**).

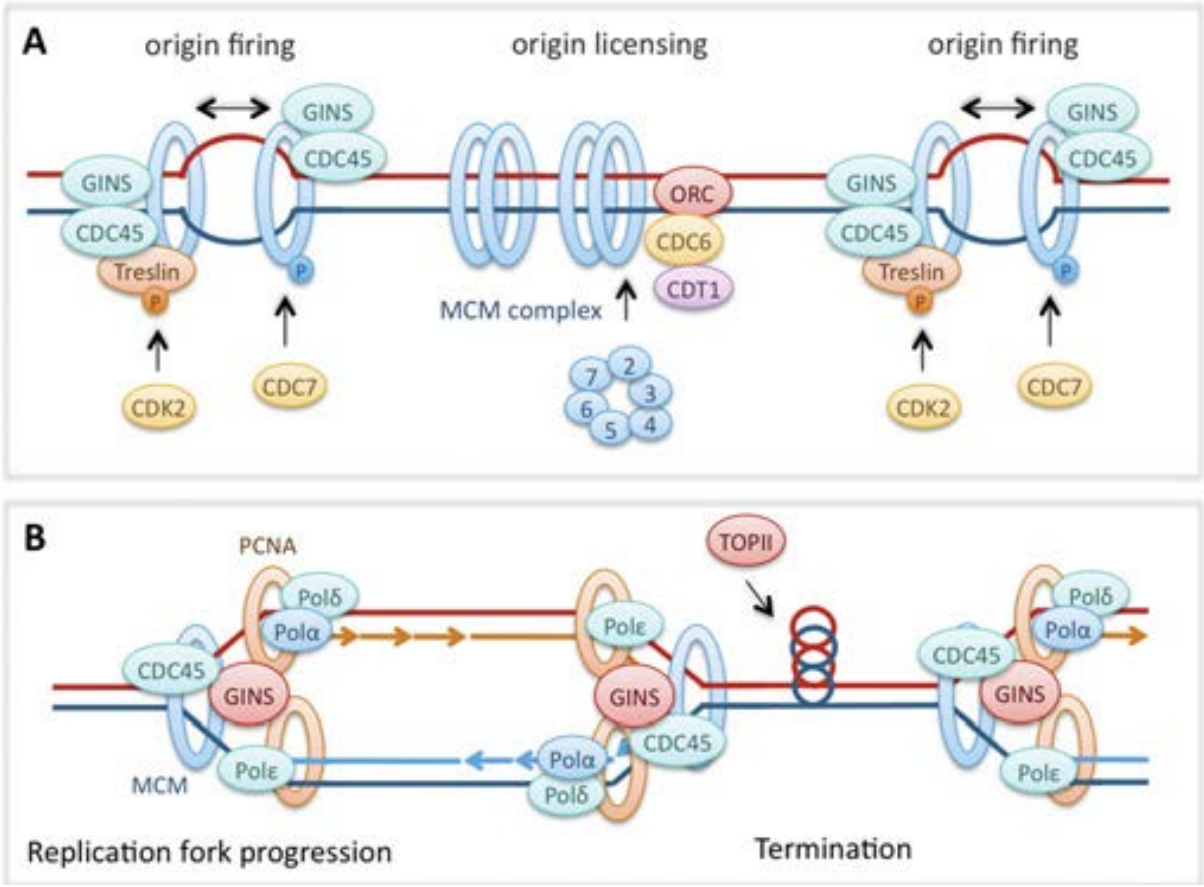

Figure 1.1. Schematic representation of the proteins required for origin licensing and replication initiation (A) and key components of the assembled replication machinery required for subsequent fork progression and replication termination (B). This figure was taken from a review of replication fork dynamics by Jones and Petermann (2012) [17].

Other components of the active replisome at this stage include the clamp loader RFC (replication factor c) as well as the sliding clamp protein PCNA (proliferating cell nuclear antigen) which is responsible for the tethering of the DNA polymerase enzymes to the template and promoting processivity [18]. The replisome actually comprises three polymerase enzymes, each with a specific role to play in the process. Polymerase α synthesises the DNA primer required to kick-start DNA synthesis, polymerase δ is responsible for lagging strand synthesis while polymerase ε replicates the leading strand. The switch between the polymerase α and the replicative polymerases is regulated by PCNA [19]. This polymerase switching mechanism is also important for activation of the translesion synthesis (TLS) pathway where additional specialised low-fidelity polymerases are recruited by PCNA to allow bypass of some DNA lesions (reviewed in [20]). This method of DNA damage tolerance will be discussed further in subsequent sections. RFC and PCNA also act as a scaffold for the loading of other critical replication proteins such as DNA ligase and the flap endocuclease Fen1 which are both essential in the processing of Okazaki fragments generated during lagging strand synthesis [21]. A schematic representation of the proteins involved in replication fork progression is shown in **figure 1.1B.**

While the processes of replication initiation and fork progression have been well-characterised, much remains unknown with regards to how replication is terminated in eukaryotes. It is thought to involve the convergence of two moving replication forks although the precise mechanisms by which the cell co-ordinates this process are not clear. There has been some suggestion that it may ultimately require decatenation of sister chromatids by topoisomerase enzymes with the cooperation of DNA helicases [22]. Termination sites, much like origins of replication, appear to be randomly distributed across the genome in a non-sequence specific manner [23]. Work carried out by Gambus

and colleagues has recently shed new light on the elusive process of replication termination. They show that in Xenopus egg extracts, replisome disassembly at converging replication forks is mediated by the polyubiquitination of the MCM7 subunit of the replicative helicase which then leads to its removal by chromatin remodelling protein p97/VCP/Cdc48 [24].

1.2.2 Replication fork stalling and replication-coupled DNA damage

When replication forks encounter obstacles on the DNA template which impede their progression, this can result in DNA damage and subsequent loss of genome integrity. Barriers to replication fork progression can be endogenous, for example unusual DNA secondary structure or topological entanglements as well as potential collisions with transcription machinery or other chromatin-bound protein complexes. Alternatively, replication stress can be induced by exogenous factors such as DNA damaging agents which cause physical DNA lesions such as DNA crosslinks, DNA-protein complexes or double strand breaks (DSBs) [25]. Sophisticated cellular mechanisms are therefore in place to allow cells to respond to these potential sources of DNA damage and preserve the fidelity of the replication process. The type of damage response initiated by the cell and choice of repair mechanism will depend upon both the type of lesion as well as the cell cycle phase. The successful completion of replication thus requires the coordinated action of proteins from diverse pathways including checkpoint signalling, homologous recombination, DNA repair/damage response as well as proteins directly involved in maintaining replication fork stability or progression. Defects in many of these pathways have been shown to lead to altered replication dynamics and an increase in replication-associated DNA damage [17, 26].

1.2.3 DNA damage tolerance and the translesion synthesis (TLS) pathway

In some instances, when a cell encounters damaged template DNA during replication, PCNA can recruit specialised DNA polymerases that have the flexibility to accommodate the damaged DNA template which allows them to synthesise across lesions [20, 27, 28]. This damage tolerance mechanism is tightly controlled via the monoubiquitination of PCNA by the E3 ubiquitin ligase Rad18 in conjunction with the E2 conjugating enzyme Rad6 [29, 30]. However, as this is an error-prone pathway it is thus carefully regulated at sites of DNA damage. All of the low-fidelity polymerase enzymes which have so far been characterised have been shown to contain a ubiquitin binding domain which allows them to interact specifically with monoubiquitinated PCNA [31, 32]. Interestingly, it has been widely observed that depletion of the cellular nucleotide pool with the replication inhibitor hydroxyurea (HU), also results in PCNA monoubiquitination. In the absence of any actual lesion to bypass, it may be that this monoubiquitin signal also recruits other factors involved in the maintenance of fork stability.

In addition to this error-prone process, a second error-free damage tolerance pathway has been characterised in yeast. This pathway is Rad5-dependent and involves utilisation of the replicated sister chromatid as a template for synthesis of the damaged section of DNA in a process termed ‘template switching’. The initial monoubiquitination of PCNA by the Rad6-Rad18 complex is followed by Rad5 mediated construction of Lysine-63 linked polyubiquitin chains, which appear to act as a signal for the template switching mechanism [33]. Conservation of this pathway has only recently been established in higher eukaryotes [34, 35]. A human homologue of Rad5 has been identified as HLTF (helicase-like transcription factor) which has been shown to have the ability to facilitate PCNA polyubiquitination as well as displaying replication fork regression activity similarly to its yeast counterpart [36].

1.2.4 The intra-S checkpoint

When an active replication fork encounters an obstacle, the fork will initially stall to allow the removal, repair or resolution of the perceived impediment. Following successful removal of the block, the fork may then simply resume replicating. However, if the fork remains stalled for a prolonged period of time, it has been shown that at some point these forks are no longer able to restart and instead collapse [37]. In these instances the replication machinery becomes disassociated from the DNA and a double strand break may be formed which then requires processing and repair.

Often, when a replication fork encounters a block or lesion on the DNA, the helicase activity becomes uncoupled from the polymerase which leads to a scenario whereby the replicative helicase continues to unwind the duplex ahead of the replicon[38]. This results in long tracts of single-stranded DNA (ssDNA) which becomes coated with the single strand binding protein RPA (replication protein A) and can be visualised by immunofluorescence. The generation of single stranded DNA is also a feature of nuclease-mediated DNA resection which occurs during the processing of double strand breaks and other DNA lesions [39].

The primary checkpoint pathway activated in response to replication-coupled damage is the ATR signalling pathway [40]. ATR (ataxia telangiectasia and Rad3-related) is an essential gene in mammalian cells although mutations in ATR which partially abrogate its activity have been linked to Seckel syndrome, a rare genetic disorder which is characterised by growth and developmental defects [41]. ATR and its binding partner ATRIP (ATR interacting protein) recognise and are recruited to RPA coated ssDNA [42]. Activated ATR then mediates phosphorylation of a number of key downstream effectors including other signalling proteins and repair factors including Chk1 [43], the key

downstream effector kinase in the ATR pathway, H2AX [44] and p53 [45, 46]. Chk1 in turn then phosphorylates cellular phosphatases to downregulate CDK activation and inhibit the progression of cells through S-phase which thus allows time for damage repair and/or fork restart to occur [47, 48]. In this capacity Chk1 has also been shown to inhibit new origin firing as well as being able to phosphorylate DNA repair proteins such as BRCA2 and Rad51 [49-52]. Efficient activation of ATR and subsequent phosphorylation of Chk1 also depends upon various other proteins involved in the replication checkpoint pathway including Rad17, Rad9, Topbp1 (DNA topoisomerase 2-binding protein 1) as well as Claspin and components of the replication fork protection complex Timeless and Tipin [53-58].

Checkpoint control of DNA replication is also important in unperturbed replication and components of checkpoint pathways are crucial regulators of replication initiation, progression and fork stability even in the absence of damage [59]. Inhibition of the ATR signaling pathway has been shown to lead to upregulation of origin firing during S-phase as well as an overall reduction in replication fork speeds [60-63]. Even in normal replication, ssDNA is transiently generated upon unwinding of the DNA by the replicative helicase during replication initiation and progression. This is thought to lead to low-level checkpoint activation which in turn regulates cellular levels of CDC25 phosphatases and CDK activity which allows cells to maintain tight control over the replication process by downregulating further origin firing [60]. It has also been shown that CDK2 inhibition in Chk1 deficient cells suppresses the slow replication fork speed phenotype with CDC7 depletion also able to restore normal replication fork speeds in the absence of Chk1. This suggests that control and regulation of replication initiation may be the key to explaining the effects of aberrant checkpoint control on replication fork progression [62]. Higher fork density, as a result of more active origins mediated by a loss of checkpoint control, could

potentially lead to more fork collisions, an increased need for the resolution of replication blocks and subsequent downstream DNA damage.

Additional roles for the checkpoint in promoting efficient replication fork progression have been suggested and could include a role in the maintenance of replicon stability [64-66]. It can be conceived that unstable forks prone to collapse or stalling could also lead to the slower replication fork speed observed in checkpoint deficient cells. There is also some evidence to suggest that activation of the checkpoint in the presence of DNA damage not only leads to a global reduction in origin firing, but actually results in replication fork slowing. Although, precisely how this is achieved remains unclear.

While it is clear that checkpoint proteins play an important role in the control of replication and replication fork stability, the replication fork protection complex (FPC) consisting of Timeless and Tipin is thought to act to promote replication fork stability via a direct interaction with the replication machinery in addition to promoting ATR-dependent checkpoint signalling [54, 55, 65, 67]. Downregulation of either Timeless or Tipin leads to a reduction in protein levels of the other suggesting that formation of the heterodimeric complex is important for protein stability [67, 68]. The FPC has been shown to localise to replication origins and to associate with the replication machinery during DNA replication. It has also been shown that depletion of either protein increases sensitivity to various genotoxic agents including hydroxyurea (HU) and ultraviolet (UV) radiation and that Chk1 phosphorylation is reduced in response to these agents. Conversely, in unperturbed cells that have been depleted of Timeless an increase in basal levels of Chk1 activation has been observed compared to control cells [54, 55, 65]. This indicates that while the FPC is required for a robust checkpoint response to replication stress inducing agents, it also plays a role in the promotion of fork stability under normal conditions which leads to a slightly elevated basal level of checkpoint activation in its absence. This apparent checkpoint

function of the FPC is thought to be dependent on the Tipin subunit which directly binds to RPA coated ssDNA at the replication fork where it then recruits Claspin, a key mediator of checkpoint signalling, and thus promotes Chk1 activation [55]. Work on the yeast functional homologues of these proteins has suggested that the complex also inhibits excessive ssDNA formation by preventing uncoupling of the replicative helicase and polymerase activities perhaps via a direct interaction with MCM subunits [69-71]. In human cells, depletion of Timeless results in slower replication fork progression and spontaneous DNA breaks in undamaged cells as well as displaying downstream sister chromatid cohesion defects [54, 65]. Additionally, elevated Rad51 foci and increased levels of sister chromatid exchanges were observed in Timeless depleted cells which suggests that the FPC may act to prevent fork collapse and/or suppress inappropriate recombination repair at sites of stalled or damaged replication forks [72]. Collectively, this data supports the premise that the FPC has an important role in maintaining the stability of the replication fork during normal DNA replication as well as potentially monitoring, detecting and responding to fork stalling and damage. Cohesion defects that arise as a consequence of FPC depletion may be attributable to loss of coordination between the processes of DNA replication and cohesion establishment due to increased fork instability in the face of endogenous replication challenges.

1.2.5 DNA double strand break repair

Specific DNA repair mechanisms and pathways are employed in cells to deal with particular types of DNA lesion. DSBs are potentially the most deleterious and dangerous lesion a cell can encounter, leading to genome rearrangements and chromosomal instability. DSBs can occur as a result of direct exogenous damage from sources such as

ionising radiation (IR), as a result of damaged replication forks (as discussed above) and can also be generated via the processing of other types of DNA lesions. The two main cellular pathways for repairing DSBs are homologous recombination (HR) repair which occurs preferentially in S and G2 phases of the cell cycle, and non-homologous end joining (NHEJ) which takes place primarily in G1 [73, 74].

NHEJ is the preferred mechanism for DSB repair during G1 when no homologous template is available and the high degree of chromatin compaction inhibits homology searching and resection. DNA DSBs are detected by the Ku heterodimer, a component of the DNA-PK complex, which recognises and binds to the DNA ends [75]. The DNA-PK (DNA-dependent protein kinase) catalytic subunit is then recruited and activated at the break site, facilitating the recruitment and phosphorylation of other repair factors and signalling proteins. Eventually, the process is completed by binding of the XRCC4-DNA ligase IV complex to accomplish annealing of the DNA strands [76]. Often described as an error-prone mechanism of DSB repair, NHEJ is nevertheless a crucial repair pathway in cells with the activity of CDKs ensuring DNA end resection is limited during G1 to minimize the extensive end processing that may result in loss of genomic stability [39, 77]. Several recent studies have also implicated the ATM target protein 53bp1 as a crucial player in determining DSB repair pathway choice [78, 79]. It has been shown that 53bp1 inhibits end resection in G1 and is removed from DNA ends during S-phase in a BRCA1 (breast cancer 1, early onset) dependent process. This leads to inaccurate repair of replication associated DSBs by NHEJ rather than the favoured mechanism of HR repair in BRCA1 deficient cells, which can lead to genomic rearrangements and instability [78].

HR repair makes use of homologous DNA sequences usually from a sister chromatid as a template for repair and re-synthesis of the sequence around a DNA break or lesion. The process is regulated in a cell-cycle dependent manner and is therefore usually restricted to

the S and G2 phases of the cycle when a homologous template is available in the form of a replicated sister chromatid [80]. Inappropriate HR can lead to genomic rearrangements and instability which can have a catastrophic effect on cell survival. HR repair is perhaps best known as one of the key pathways by which cells respond to and repair double strand breaks in DNA, however, components of the HR repair pathway also have roles in the repair of other DNA lesions as well as in the maintenance and repair of replication forks [81].

Just as ATR signalling is primarily responsible for the cellular response to stalled replication forks, a second master checkpoint kinase ATM (Ataxia telangiectasia-mutated) phosphorylates downstream targets in response to DNA double strand breaks. ATM signalling is dependent upon damage sensors such as the MRN complex (Mre11-Rad50-NBS1) which detects a DSB before utilising the intrinsic nuclease activity of Mre11 (Meiotic recombination 11 homolog 1) to resect the DNA at the break site [82]. The binding of Rad51, a crucial mediator of HR repair, requires a 3' overhang to be generated by cellular nucleases such as Mre11 and EXO1 (exonuclease 1), to facilitate its binding to DNA [83-87]. This resection of DNA by nuclease enzymes is regulated by CDKs and also only occurs in S-phase and G2. CtIP, another endonuclease which is essential for efficient Mre11-mediated resection, is activated by CDK phosphorylation at the G1/S transition to promote HR-dependent repair processes [88, 89]. Rad51-coated DNA filaments initiate the process of homology searching for appropriate DNA sequences, subsequently followed by strand invasion and recombination. The resolution of intermediate displacement loop (D-loop) and Holliday junction (HJ) structures is necessary to complete the repair process [84]. A catalogue of important HR repair factors are required for successful completion of each of these steps including BRCA2 which is involved in stabilising Rad51 filaments [90-92] and cellular resolvase enzymes such as GEN1 (Flap endonuclease GEN homolog 1)

which acts to remove HJs [93]. Components of the Fanconi Anaemia (FA) pathway, topoisomerase enzymes and the RecQ-like helicases BLM (Bloom Syndrome helicase) and WRN (Werner Syndrome helicase) are also required for efficient HR repair [93-96].

1.2.6 HR mediated replication fork restart

Evidence using bacterial models initially suggested that the HR machinery is important for replication fork stability and promotion of replication restart after stalling [97]. However, it is clear that HR-dependent modes of replication fork restart are also employed in eukaryotic cells [98-100]. Mutations in proteins involved in HR often exhibit spontaneous DSBs and sensitivity to replication stress and, additionally, cells with defects in the HR pathway have shown slower replication fork progression consistent with an inability to efficiently resolve endogenous replication blocks or with reduced fork stability [101-103]. DNA structures similar to traditional HR intermediates can arise at a stalled fork either because a DSB is generated or via fork processing events and these require resolution by components of the HR machinery.

Furthermore, studies on both Mre11 and Rad51, two key HR proteins, have shown them to be important for effective replication restart after treatment with replication inhibitors. Mre11 is recruited to stalled forks and may be involved in processing the fork via end resection to allow subsequent loading of Rad51 and efficient fork restart [102, 104]. Interestingly, although it has been shown that Rad51 is required for replication fork restart after stalling, this function seems to be distinct from its role in HR repair of DSBs [37]. The latter results in the formation of visible Rad51 foci by IF which are not detectable in cells which have undergone Rad51-dependent replication restart. It is possible that other HR proteins also have alternative functions in replication compared with DSB repair. The

process of HR-mediated replication fork restart is likely to involve the limiting of crossing-over between homologous sequences as this could lead to potentially damaging genomic rearrangements. It is thought that the BLM helicase may function as part of a complex with TOP3A (topoisomerase 3 alpha) and hRMI1 (RecQ-mediated genome instability protein 1 or BLAP75) to dissolve double Holliday junction intermediate structures and suppress recombination events at damaged replication forks [94, 105].

1.3 Sister chromatid cohesion is essential for the maintenance of genomic stability

1.3.1 Cohesion and the cohesin complex

During the process of DNA replication, each newly replicated sister chromatid pair must be physically associated with each other until their separation and subsequent distribution to each daughter cell at mitosis. This is facilitated by a protein complex comprised of both structural and regulatory subunits and collectively known as cohesion factors [106]. Work carried out in yeast identified four genes which, when mutated, resulted in high-frequency chromosome loss. These included two SMC (Structural Maintenance of Chromosomes) family members as well as two uncharacterised genes which were named SCC1 and SCC3 (Sister Chromatid Cohesion) [107]. It was shown in later work that these four proteins are assembled as a large ring-like protein complex in cells, termed the cohesin complex, and that they facilitate the cohesion between newly synthesised sister chromatids by physically linking them together [108] (**figure 1.2**). Interestingly, it was also discovered that the Scc1 subunit of the cohesin complex is specifically degraded at the onset of anaphase which coincides with the dissolution of cohesion and chromosome separation. This led to speculation that removal of Scc1 is the molecular trigger required for chromosome segregation to occur [109, 110].

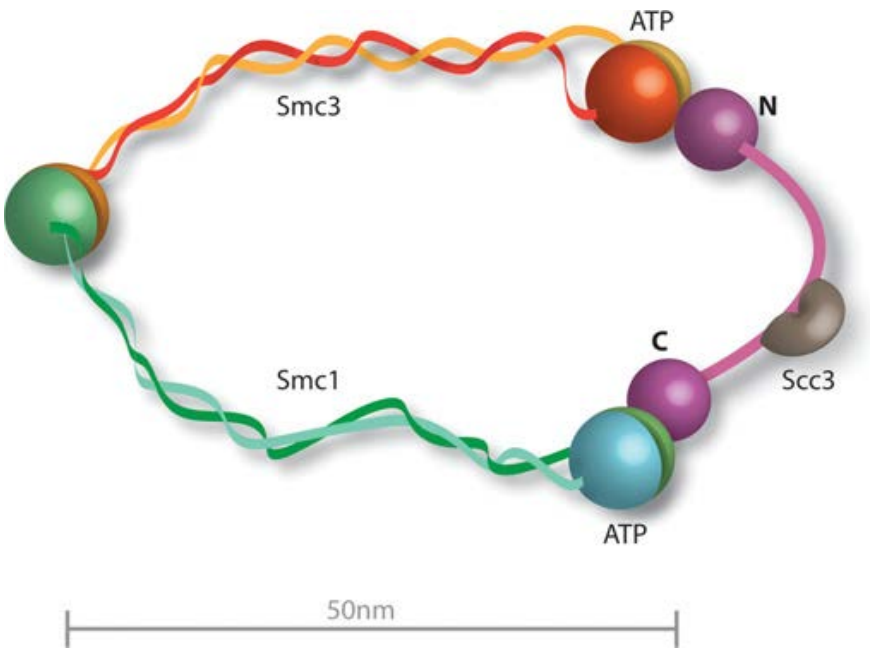

Figure 1.2. Schematic representation of structure of the core cohesin complex. Scc1 is shown in purple and is thought to be degraded at the onset of anaphase to trigger chromatid separation. This figure has been taken from a review by Feeney, Wasson [106].

In higher eukaryotes, however, the picture is somewhat more complicated. While much of the early work in the establishment and regulation of cohesion has been carried out using yeast as a model organism, it is clear that there may be some differences in the way cohesion is regulated in mammalian cells. For instance, while in yeast it has been demonstrated that cohesin remains associated with chromosomes until the metaphase-anaphase transition when segregation occurs, in mammalian cells it seems that cohesin removal is more of a stepwise process that is highly regulated throughout the cell cycle

[111]. During the progression of cells from prophase to metaphase it has been observed that while sister chromatids remained joined at their centromeres, cohesion between chromosome arms is lost [112]. This removal of cohesin from chromosome arms earlier in the cell cycle is thought to be independent of the conventional mechanism of cohesin removal which is mediated by cleavage of the Scc1 subunit (Rad21 in vertebrates) by the cysteine protease separase [110]. Studies have suggested that Polo-Like kinase 1 (Plk1) has a role in the regulation of cohesin removal and it has been shown that Plk1 can phosphorylate cohesin subunits with phosphorylation leading to a reduced affinity of the complex for the chromosome arms during prophase [112, 113]. Nevertheless, a fraction of cohesin does remain associated with chromosomes at their centromeric regions and allows the maintenance of cohesion between sister chromatids until the mitotic spindle checkpoint has been approved. This is then subject to removal via the proteolytic cleavage of the Rad21 subunit by separase, thus supporting the idea that this is a conserved trigger for chromosome segregation [109, 113, 114].

The discovery of two distinct mechanisms for cohesin regulation at different points in the cell cycle supports the idea that cohesin may have more dynamic roles in cell processes in addition to its canonical role in promoting accurate chromosome segregation. Indeed, cohesin has also been implicated in DNA damage repair, possibly via facilitation of homologous recombination, and also in control of gene expression by transcriptional regulation (reviewed in [106]).

1.3.2 Cohesion factors and regulation of sister chromatid cohesion

Although sister chromatid cohesion is established during DNA replication, studies have shown that cohesin actually becomes associated with DNA in G1 phase in the case of

lower eukaryotes while in mammalian cells it has been observed that cohesin re-localises to DNA towards the end of telophase [107, 115, 116]. Loading of cohesin onto DNA molecules is brought about by its interaction with the Scc2-Scc4 cohesin loading complex. The energy driving this process is generated by the ATPase activity of the SMC subunits which is thought to allow either opening of the complex at the hinge region or transient dissociation of Scc1 [117]. Since cohesin is associated with DNA prior to the establishment of sister chromatid cohesion it can be presumed that there must be other cellular factors at work to regulate the actual process of cohesion establishment.

In yeast, several classes of proteins, generally termed cohesion factors, have been identified. These include the proteins discussed above which form the cohesin complex as well as proteins involved in the loading of cohesin onto chromosomes and also cohesion establishment factors [118-120]. Several of these cohesion establishment factors have been shown to interact with components of the DNA replication machinery and thus are essential in ensuring that the processes of DNA replication and sister chromatid cohesion are closely coupled to each other such that newly synthesized sister DNA molecules are tethered together [21, 68, 119, 121].

The cohesion establishment factor Eco1 (establishment of cohesion protein 1), also known in the literature as Ctf7 (Chromosome transmission fidelity protein 7) in yeast and as ESCO1/2 in humans, has been shown to be vital in the establishment of sister chromatid cohesion during S-phase [119, 120]. Skibbens *et al*. identified Ctf7 as an essential protein in *S. cerevisiae* that is highly conserved across species [118]. With the use of temperature sensitive Ctf7 mutants they showed that when placed at the restrictive temperature at S-phase, cells rapidly lost viability and displayed severe chromosome cohesion defects. However, when the cells were placed at the restrictive temperature during mitosis the cells appeared normal, thus suggesting that Ctf7 is required during S-phase for establishment of

cohesion but not for its maintenance during early mitosis. These findings were recapitulated by Toth *et al*. using a different mutant allele of Ctf7, indicating the results are reliable and not allele-specific [118, 120]. Furthermore, genetic interactions between CTF7 and both POL30 (DNA processivity factor PCNA) and CTF18 (a component of yeast Replication Factor C complex) provided tentative evidence that the processes of cohesion establishment and DNA replication are linked [122]. RFC complexes work by using ATP hydrolysis to direct the loading of PCNA onto DNA and drive forward processive replication. It was shown that POL30 was a high-copy suppressor of the CTF7 temperature sensitive mutant phenotype and that both POL30 and CTF18 were synthetically lethal in combination with CTF7. As well as the genetic interaction between CTF7 and genes encoding components of the replication machinery previously described, it was also subsequently confirmed that Ctf7p physically associates with several proteins involved in DNA replication, including PCNA and Ctf18p [119, 122]. Yeast CTF7 mutants unable to bind PCNA were defective in sister chromatid cohesion indicating the interaction between these two proteins is crucial for successful cohesion establishment [122]. Evidence of a connection between replication and cohesion establishment allows for interesting speculation about the implications of this interaction. It is also tempting to speculate about the potential role for these cohesion factors in other aspects of DNA metabolism such as transcription and DNA damage repair, processes which may depend on local remodelling of chromatin structure and the dynamic association of cohesins in order to function successfully.

The actual mechanism by which Ctf7 is involved in the establishment of cohesion still requires some resolution. The ‘handcuff’ model, put forward by Skibbens *et al.*, suggests that Ctf7 associates with the replication machinery and in effect brings together two cohesin complexes associated with individual sister chromatids [123]. This model fits in

with other observations, for example that cohesin is found associated with DNA prior to the development of sister chromatid cohesion and that loading of cohesin is independent of cohesion establishment [116, 124]. It also explains phenotypes that have been observed whereby cohesion is compromised despite the detectable presence of cohesin on the chromosomes [120]. However, work carried out by Lengronne *et al.* using chromatin immunoprecipitation experiments to look at replication-fork associated proteins found only a small amount of Ctf7p was localized to the replication fork compared with other replication factors also known to be important for cohesion such as Ctf18p and Ctf4p [121]. Whether this is due to the potentially transient nature of the association has yet to be determined.

The more established model of sister chromatid cohesion, supported by data from EM studies of cohesin structure, suggests that the ring-like cohesin complex encircles the two sister DNA molecules [108, 125]. It is proposed that the complex forms a V-shaped heterodimer consisting of the Smc1 and Smc3 subunits with the gap bridged by Scc1 to complete the circle. It is suggested that this vast ring-shaped molecule then allows the replication fork to pass through it resulting in efficient pairing of only identical sister chromatids. This model is supported by several studies which showed that no interaction could be detected between differentially tagged subunits of the cohesin complex in FRET (Fluorescence Resonance Energy Transfer) experiments. Additionally, treatment with crosslinking agents generated cohesin-DNA complexes that were not sensitive to degradation by protease treatment which strongly supports the model of a single cohesin molecule that encircles both sister chromatids [108, 126].

The main caveats of the ‘ring’ model, it has been suggested, are firstly that it does not reveal a role for Ctf7p despite previous evidence showing this protein to be required for cohesion establishment and also, as mentioned above, there have been instances where

cohesion defects have been observed in cells without any notable defects in either cohesin deposition or DNA replication. This suggests that there is a missing link between the two processes that results in the defective phenotype. In other words, if the ring model is correct then there are likely to be other factors, perhaps including Ctf7, involved in regulating the passage of the replication machinery through the cohesin ring, a scenario which is extremely plausible in light of the numerous cellular factors which have so far been implicated in both cohesion establishment and replication.

As yet neither of these proposed models has been definitively proven to be correct and there is still much investigation to be carried out in order to fully elucidate the regulation of cohesion. There is still significant controversy surrounding the actual mechanism of cohesion establishment and several groups have published data that seems to contradict the widely accepted 'ring' model of cohesion. For example, in conflict with the FRET study discussed above, Zhang and colleagues were in fact able to detect an association between the Scc1 subunits of individual cohesin complexes [127] while another study suggested that the greater diameter of compact heterochromatic DNA supported a 'handcuff' model of cohesion in these regions [128]. A schematic representation of the proposed models of sister chromatid cohesion is shown below (**figure 1.3**).

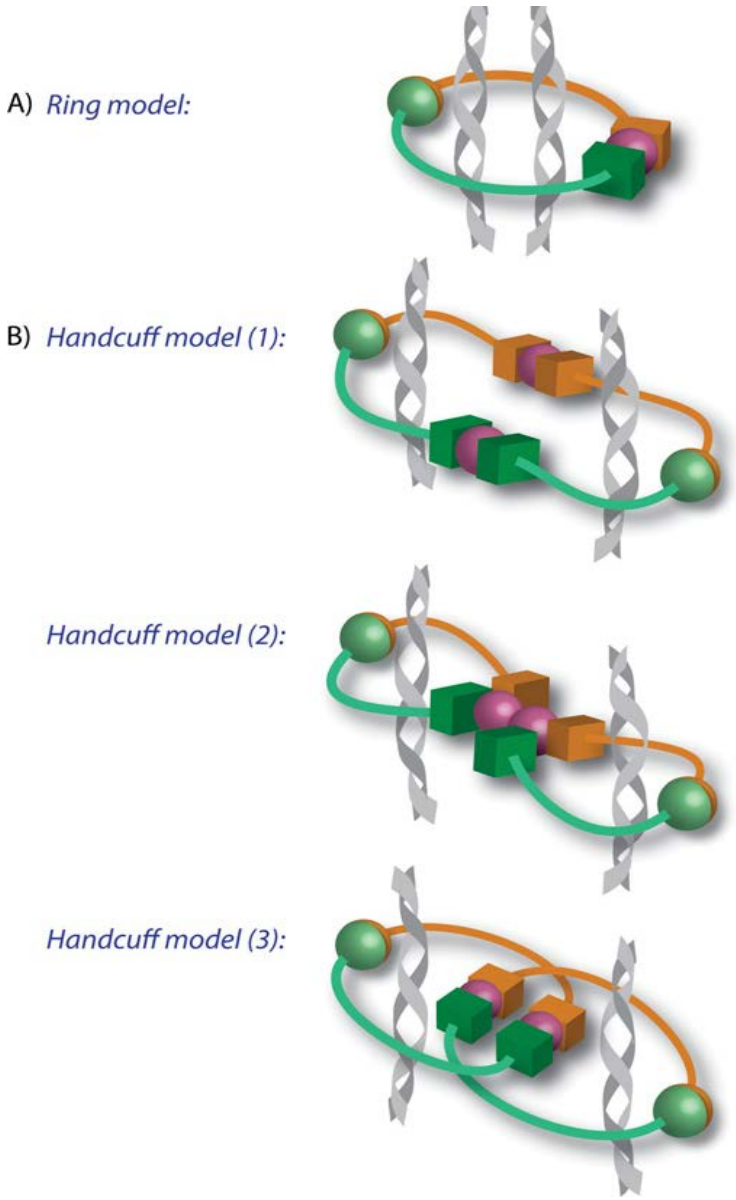

Figure 1.3. Schematic representation of the proposed models of sister chromatid cohesion. The Ring model depicted in (A) suggests that a single cohesin molecule encircles both sister chromatids following replication while the handcuff models depicted in (B) propose that each daughter strand is encircled by single cohesin molecules that are then physically associated with each other via an as yet undetermined mechanism. This figure is taken from a review by Feeney et al (2010) [106].

It has also been shown that Ctf7p interacts with the DNA helicase Chl1p (chromosome loss protein 1) in yeast [129]. Furthermore, as well as an interaction with Ctf7p, the human equivalent of Chl1p, hChlR1 (Chl1-related protein) has been shown to interact with other cohesion and replication factors, including components of the cohesin complex itself, PCNA and Ctf18-RFC [21, 130, 131]. The potential involvement of a DNA helicase in the establishment of cohesion is interesting as it could suggest a mechanism for alteration of DNA topology to allow replication progression in conjunction with establishment or maintenance of sister chromatid cohesion. This, coupled with the discovery that Ctf7p (ESCO1/ESCO2 in humans) functions as an acetyltransferase which acetylates the SMC3 subunit of the cohesin complex [132], suggests that local chromatin remodelling may be an important feature of the mechanisms underlying the establishment of cohesion following replication. Mutation of the two highly conserved lysine residues in SMC3 which are acetylated by Ctf7p results in severe cohesion defects. Conversely, replacing these lysine residues with either glutamine or asparagine residues to mimic acetylation rescues the defect caused by loss of Ctf7p. The acetyltransferase activity of Ctf7p is suppressed during G1, G2 and mitosis, with SMC3 acetylation only occurring only during S-phase. This supports the hypothesis that acetylation of SMC3 is important for converting DNA associated cohesin rings to a cohesive state allowing for replication coupled cohesion establishment [133-135]. It is thought that Ctf7 mediated acetylation functions to promote either dissociation of cohesin rings from DNA or opening of the complex to allow passage of the replication fork. This is supported by evidence which suggests that in the absence of cohesin acetylation replication fork processivity is impaired [136]. It has also been shown that SMC3 acetylation inhibits the Wapl-Pds5 complex, which has a role in suppressing inappropriate cohesion establishment, prior to completion of replication, via a direct interaction with cohesin [137].

1.3.3 Alternative functions of the cohesin complex

Initially there was little evidence of the diversification of cohesin function in lower eukaryotes where early studies had focused on the canonical role of cohesin in sister chromatid cohesion and accurate chromosome segregation. However a publication by Schmidt *et al* provided evidence that, in *S.pombe* at least, not all cellular cohesin participates in chromosome segregation [138]. Using chromatin immunoprecipitation methods followed by analysis on high resolution oligonucleotide microarrays, they were able to show localization of cohesin along fission yeast chromosomes throughout the cell cycle. They show that a fraction of the cellular pool of cohesin does become dissociated from the chromosomes during prophase and that this dissociation is not separase dependent. Their data confirms that in the case of fission yeast there is also more than one pathway for the removal of cohesin and thus suggested that there was scope for further investigation into potentially conserved roles of cohesin using lower eukaryotes as model systems.

Evidence from studies in vertebrate cells indicated that, intriguingly, cohesin re-localises to chromosomes immediately following mitosis and prior to S-phase when it would be assumed that it would again be required for sister chromatid cohesion [116]. This is supportive of the hypothesis that cohesin has more diverse cellular functions. Furthermore, perhaps some of the most compelling evidence supporting alternative roles for cohesin is provided by the phenotypes associated with human diseases that result from mutations of components of the complex [106, 139]. Diseases like Roberts Syndrome and Cornelia de Lange syndrome cause severe developmental defects that include mental retardation and craniofacial abnormalities but sufferers are not predisposed to the development of cancer which might be expected if genomic instability was primarily the cause of these phenotypes. This raises the possibility that it may be the disruption of other functions of

cohesin, such as transcriptional regulation, which lead to the symptoms exhibited in these diseases. Additionally, cohesin has been found to colocalise with the cohesin loading complex Scc2-Scc4 at sites of active transcription in eukaryotic cells suggesting a potential requirement for more dynamic cohesin association within these regions [140, 141].

The observation in *S. cerevisiae* that cohesin molecules tended to accumulate at sites of convergent transcription first suggested that cohesin might have an important role to play in the regulation of this process [115]. It was hypothesised that the transcription machinery was too large to pass through the cohesin ring such that cohesin molecules were somehow translocated along the DNA in front of the transcription machinery until transcription termination [142]. A subsequent study posited that this accumulation of cohesin might act as a boundary between coding regions and have a direct function in successful termination of transcription [143]. However, in mammalian cells cohesin does not accumulate at sites of convergent transcription but instead is enriched at sites of CTCF binding [144]. CTCF (CCCTC binding factor) is a ubiquitously expressed zinc-finger containing protein involved in transcription regulation specifically by facilitating transcriptional insulation of the genes flanked by CTCF binding sites [145, 146]. Depletion of CTCF in mammalian cells alters the positioning of cohesin at these regions and downregulation of either CTCF or Rad21 leads to comparable transcriptional changes as measured by DNA chip technology. This further confirms that the insulator function of CTCF is at least partly mediated by cohesin [147].

In addition to its role in the control of gene expression, it has also been demonstrated in yeast that cohesin is important for effective DNA repair, specifically by homologous recombination. It can be envisaged that for efficient HR repair to occur homologous sister chromatids must be held in close proximity to each other via the establishment of sister chromatid cohesion during S-phase. It was shown that establishment of cohesion in S

phase is essential for DNA repair in G2 while *de novo* loading of cohesin onto DNA in the region of DSBs has also been demonstrated in both yeast and higher eukaryotes. Additionally, DNA damage has been shown to induce genome wide post-replicative cohesion which is dependent upon Ctf7 and Scc2, suggesting that newly loaded cohesin molecules participate in this damage-induced cohesion [148-151]. The function of cohesin in the response to DNA damage is less well characterised in mammalian cells. However, there is evidence that cohesin is recruited to sites of DSBs and that this recruitment is mediated by the Smc5-Smc6 complex which also promotes HR repair [152-154]. It has also been shown that cohesin is specifically recruited to DSBs only in S and G2 phases of the cell cycle and that repair of DSBs was slower in cells depleted of cohesin subunits in G2 but not G1 [155]. This supports a model whereby cohesin facilitates HR mediated repair by inducing localised cohesion bringing sister chromatids into proximity to use as templates for re-synthesis of damaged DNA.

In addition to direct recruitment to sites of DSBs and promotion of HR repair, several studies also support an independent checkpoint function for the cohesin complex. SMC1 and SMC3 are both phosphorylated by checkpoint kinases in response to UV and IR [156-159]. This damage induced phosphorylation causes SMC1 to colocalise with γH2AX DNA damage foci. Mutation of the phosphorylation sites on either cohesin subunit leads to an attenuated damage response [160, 161]. Additionally, the breast cancer susceptibility protein and DNA repair factor BRCA2 has been shown to interact with the cohesin complex via the anti-establishment factor Pds5 and this association was shown to be important for HR repair and efficient DNA damage response [162]. Furthermore, a study by Watrin and colleagues suggests that the cohesin complex may function to recruit various checkpoint proteins to sites of DNA damage, thus promoting effective checkpoint activation [163].

1.4 The DNA helicase Chl1 has a role in sister chromatid cohesion

As discussed above, for cell viability and genome integrity to be maintained, accurate transmission of chromosomes to each daughter cell must occur during mitotic division. The process of chromosome segregation is regulated in eukaryotes by an array of proteins ranging from those involved in the control of vital cellular checkpoints to structural proteins responsible for the establishment and termination of sister chromatid cohesion and association with the mitotic spindle. Studies of chromosomal missegregation using yeast as a model organism have resulted in the identification of many candidate genes with potential roles in the control of correct chromosome segregation as well as in other closely coupled cell cycle processes such as checkpoint regulation, and in DNA replication and repair [164, 165]. One such study, by Haber and colleagues, identified the gene Chl1 (Chromosome loss mutation) as having a putative role in normal segregation of chromosomes at mitosis [166]. The screen was initially designed for the identification of mutants that exhibited abnormal mating phenotypes and thus Chl1 mutants were identified on the basis that they showed a high-frequency rate of missegregation of the yeast chromosome III which harbours the mating type alleles. Later it was determined by Gerring *et al*. that their CTF1 group (chromosome transmission fidelity) mutants, which they had isolated during a screen specifically for genes involved in chromosomal missegregation, were in fact mutants in Chl1 [167]. They then went on to demonstrate that in a Chl1 null mutant there was a significant increase in the rate of missegregation of genetic markers on chromosome III caused by both loss of the chromosome and non-disjunction of sister chromatids [167, 168]. This strongly suggested a role for Chl1 gene product in the maintenance of normal chromosome segregation. Additionally, the study showed that although Chl1 null mutants are viable, indicating Chl1 is a non-essential gene in yeast, clear defects in chromosome segregation were observed and cells were shown to

exhibit a delay in cell cycle progression from G2 through to mitosis. This delay, it was noticed, was independent of the DNA damage checkpoint activation.

Initial sequence analysis of the Chl1 gene showed that it had significant homology to Rad3, an ATP-dependent DNA helicase involved in the nucleotide excision repair pathway [167]. Although extensive biochemical analysis of yeast Chl1p has not thus far been carried out, sequence homology and characterisation of the human homologue ChlR1 strongly suggests that Chl1p is a putative DNA helicase. Work performed by S. Holloway showed that by using site directed mutagenesis to mutate the ATP-binding site on budding yeast Chl1p, thereby abolishing its ATPase activity, that this resulted in loss of Chl1 function [169]. This was demonstrated by transforming Chl1 deletion mutant cells with plasmids expressing either wild-type or ATP-binding site mutants of Chl1. Only wild-type Chl1 was able to rescue the aberrant chromosome segregation phenotype in these cells. Moreover, overexpression of mutant Chl1 in wild-type cells also resulted in abnormal chromosome segregation. This data strongly indicates that Chl1 functions in sister chromatid cohesion and that its role in chromosome segregation is likely to be dependent on its ATPase/helicase activities. One hypothesis from these observations could be that the helicase activity of Chl1p is important for topological modification of DNA to facilitate its interactions with cohesion factors or the cohesin complex itself.

1.4.1 Chl1p interacts with Ctf7p and components of the replication machinery

Further evidence of the role of Chl1p in sister chromatid cohesion was provided by Skibbens *et al.* In this publication it was shown that CHL1 genetically interacts with both CTF7 and CTF18 and that Chl1p co-immunoprecipitates with Ctf7p *in vivo* [129]. It should be noted however that this study uses an overexpression system that utilises tagged

proteins and that a physical interaction between endogenous proteins has not been confirmed. In addition, although this study goes on to suggest that the interaction has been confirmed *in vitro* thereby indicating that there is a direct physical association between the two proteins, the actual methods used cannot completely allow this assertion to be made. Although bacterially expressed GST-tagged Ctf7p is immobilised on glutathione Sepharose resin, the beads are then incubated with clarified yeast cell extract containing Chl1p-13Myc which does not allow us to discount the possibility that other protein cofactors are present and possibly required to mediate the interaction. However, evidence that indicates the involvement of Chl1p in sister chromatid cohesion was provided using a cohesion reporter strain where GFP is used to visualise the positions of the sister chromatids relative to each other. Chl1 mutant cells exhibited a significantly higher percentage of dissociated sister chromatids pre-anaphase compared to wild-type cells.

The proposed human homologue of Chl1p (hChlR1) has been shown to interact with other cohesion and replication factors, including components of the cohesin complex itself, PCNA and Ctf18-RFC [21, 122, 131]. ChlR1, similarly to Ctf7, has been shown to interact with the flap endonuclease Fen1 and to stimulate its activity [21]. Fen1 is important in processing Okazaki fragments during lagging strand synthesis therefore it is tempting to speculate that this association with ChlR1 is somehow functionally important for resolving unusual DNA structures that arise during lagging strand processing events in DNA replication or for coupling lagging strand processing to cohesion establishment.

Additionally, it has also been shown in *S. cerevisiae* that simultaneous deletion of Chl1 and CTF8, another RFC subunit, resulted in cohesion defects and that Chl1 is a high-copy suppressor of the spore lethality caused by missegregation observed in CTF8 null cells, thus providing further evidence that Chl1 has a role in cohesion establishment and that this is coupled to DNA replication [130]. Interestingly, Petronczki *et al.* suggest that the role of

Chl1 in cohesion may be more prominent in meiosis compared with mitosis with a far increased incidence of missegregation observed in the second meiotic division in Chl1 mutant cells [130]. In light of recent evidence suggesting that Chl1 may have a role in DNA damage repair, it is possible that this increased defect observed in meiosis could be due to problems in the HR pathway that results in further chromosomal instability. Alternatively, the increased meiotic missegregation may simply be a downstream consequence of defective HR due to an absence of cohesion rather than a direct result of Chl1 loss of function.

1.4.2 A putative role for Chl1p in response to DNA damage has been proposed

Despite initial observations to the contrary, further investigations into Chl1p function have suggested that Chl1p may have a role in the repair of DNA damage. Chl1 has 23% homology to the nucleotide excision repair (NER) gene RAD3, the human homologue of which is the helicase XPD. Moreover, one of the most closely related human genes to yeast Chl1 is the helicase FANCJ (BACH1) which has been implicated in Fanconi Anaemia (FA), breast cancer susceptibility and in the repair of interstrand crosslinks and double strand breaks in DNA via the homologous recombination pathway [167, 170]. Laha *et al*. show that Chl1p is necessary in S-phase for cell viability either upon exposure of cells to DNA damaging agents or for protection from DNA damage caused by pre-existing gene mutations [165]. The former is evidenced by increased sensitivity of Chl1 mutant strains to DNA damaging agents such as alkylating agents methyl methanesulfonate (MMS) or UV radiation. The mechanism underlying this hypersensitivity to DNA damage inducing agents was shown to be independent of the DNA damage checkpoint pathway as Chl1 mutant cells and wild type cells showed both comparable levels of Rad53p (Chk2 in

humans) phosphorylation and similar progression through S-phase compared to known checkpoint mutants, proving the checkpoint is functional. However, it was shown that Chl1 mutants are less proficient than wild type cells at repairing DNA damage induced by the alkylating agent MMS. DNA was extracted from both wild type and mutant cells, damaged by MMS, and then allowed time to repair prior to analysis of mobility on an agarose gel. DNA from Chl1 mutant cells contained more unrepaired breaks as visualized by its increased mobility on the gel supporting the hypothesis that Chl1p has a role DNA damage repair. Another study showed that the levels of Chl1p associated with chromatin substantially increased in response to induction of DNA damage by MMS and DNA repair was again shown to be deficient in Chl1 mutants [171]. Importantly, it was determined that these mutant cells also had defects in homologous recombination, an important pathway for DNA damage repair.

These studies suggested an emerging role for Chl1p in the response to DNA damage but also raised the question of whether Chl1p is directly involved in the resolution of DNA damage or if defective repair is simply a consequence of impaired sister chromatid cohesion which would undoubtedly inhibit HR repair pathways. As a putative DNA helicase it is certainly conceivable that Chl1p could be involved directly in the repair of DNA lesions either independently or via homologous recombination. How this relates to the canonical function of Chl1p as a cohesion factor has still to be elucidated, although it can be imagined that cohesion between homologous chromosomes is likely to be crucial in the facilitation of DNA repair, particularly by HR. It is however important to note that this work was carried out in yeast and Chl1p shows significant homology to two human proteins, FANCJ and hChlR1. This suggests that Chl1 may be a common ancestor of both proteins which have subsequently diverged and evolved more specialised functions in higher eukaryotes.

1.4.3 The DNA helicase ChlR1 is the proposed human homologue of yeast Chl1

In 1997, Annan *et al* reported the cloning of putative human homologues of yeast Chl1p, hCHLR1 (DDX11) and hCHLR2 (DDX12), and identified them as belonging to the DEAD/DEAH family of DNA helicases [172, 173]. These genes were found to be expressed only in actively proliferating cells. They also showed that hChlR1 protein binds to both single and double stranded DNA in the non-sequence specific manner that might be expected of a DNA helicase. A later biochemical study confirmed that human ChlR1 has both ATPase and helicase activities and that these activities could be abrogated by a point mutation in the ATP binding pocket thus supporting the results of earlier experiments on yeast Chl1 by Holloway [174]. However, complementation of yeast Chl1 mutants with the putative human homologue hCHLR1 could not be achieved. This may signify the evolution of functional specificity by the human homologue or the absence of necessary co-factors in yeast. A recent mouse knock-out of CHLR1 was embryonic lethal which is somewhat in conflict with the non-essential status of the yeast Chl1 gene [175]. The human helicase FANCJ (BACH1,) also exhibits significant homology to Chl1p, however while it has been definitively shown that FANCJ is required for DNA damage repair, early studies maintained that mutations in Chl1p do not result in any discernible DNA repair defects [167, 170]. This initial assertion has now been challenged as some more recent publications have attributed a role to Chl1p in DNA repair via homologous recombination as discussed in the previous section [171].

Studies in yeast have demonstrated that Chl1p is localised to the nucleus as would be expected of a protein with a proposed role in sister chromatid cohesion establishment, a process which occurs during S-phase of the cell cycle [129, 169]. Work in mammalian cells also supports the nuclear localisation of ChlR1 [131]. Immunofluorescence data showed that ChlR1 is associated with condensed chromatin during early mitosis but

dissociates following progression to metaphase. The protein was also found to be localised around the spindle poles throughout mitosis. This dynamic localisation of ChlR1 to chromatin early on in mitosis followed by its subsequent dissociation as the cells enter metaphase corresponds to the observed localisation of the mammalian cohesin complex which is released from chromosome arms prior to metaphase despite remaining bound to centromeres until anaphase onset [111]. This supports the notion that the role of ChlR1 is to promote cohesion establishment rather than maintenance as no centromere associated ChlR1 was observed in metaphase. Additionally, the mitotic delay in Chl1 mutant cells observed by Gerring *et al*. was recapitulated in mammalian cells where hChlR1 protein levels were depleted either by siRNA or in an inducible shRNA system. Morphological analysis showed that a high percentage of cells arrested in pro-metaphase and were unable to complete mitosis normally. It is thought that inability to satisfy the mitotic spindle checkpoint due to cohesion defects could be an explanation for this observation. This, combined with data showing that knock-down of hChlR1 levels results in abnormal loosely paired sister chromatids, is strongly indicative of a role for human ChlR1 in the S-phase establishment of sister chromatid cohesion [131].

1.4.4 ChlR1 is mutated in Warsaw Breakage Syndrome (WABS)

Although the mouse ChlR1 knockout was embryonic lethal, suggesting that this is an essential gene in mammalian development [175], an individual was recently identified with compound heterozygote mutations in ChlR1 which resulted in production of a protein which completely lacked catalytic activity. This led to the first diagnosis of a ChlR1-assoociated genetic disorder that was termed Warsaw Breakage Syndrome (WABS) after the domicile of the affected individual [139]. Clinically, the patient displayed

microcephaly, abnormal skin pigmentation and developmental delay. At the cellular level patient-derived lymphoblasts showed an increased incidence of mitomycin-c (MMC) induced chromosomal breakage. Additionally, patient metaphase spreads also showed evidence of abnormal sister chromatid cohesion in untreated cells which was significantly exacerbated upon drug treatment with either MMC or camptothecin. These cytogenetic phenotypes appeared to combine features of both the DNA repair disorder Fanconi Anaemia and the cohesinopathy Roberts Syndrome [176]. Following the identification of this first patient, three affected individuals from the same Lebanese family were subsequently identified with a homozygotic point mutation which was also shown to result in a helicase-dead protein [177]. Whether this signifies an additional helicase-independent function for mammalian ChlR1 or whether the embryonic lethality exhibited in mice is due to the fact that in humans ChlR2 (or DDX12) has also been identified, which does not exist in mice and could compensate for some functions of ChlR1 [173]. At the sequence level ChlR2 is highly similar to ChlR1 and is thought to have arisen from a gene duplication event, so it is possible that some functional redundancy exists between these two proteins thus allowing the survival of individuals with potentially deleterious ChlR1 mutations. Follow up of these individuals will be important to define the clinical progression of this syndrome and to determine whether WABS patients are predisposed to the development of cancer or the progressive bone marrow failure characteristic of FA patients who have defects in the pathway for repair of DNA crosslinks. It might be expected that if ChlR1 does have a direct role in DNA repair, then patients defective for ChlR1 function could well be susceptible to myelodysplastic syndromes and cancer development as is the case in FA.

1.4.5 ChlR1 and its role in DNA replication and repair

Genetic and biochemical data have suggested that ChlR1 interacts with components of the replication machinery and that it somehow acts to promote the establishment of cohesion in concert with DNA synthesis [21, 131, 174]. More recent work from the Noguchi laboratory has proposed a role for ChlR1 in stabilisation of the replication fork via an interaction with the Timeless-Tipin FPC [65]. They showed that ChlR1 interacts with Timeless and that ChlR1 overexpression can partially rescue the cohesion defect observed in Timeless depleted cells. Whether ChlR1 overexpression rescues the DNA damage sensitivity observed in FPC depleted cells was not tested but could provide potential insight into ChlR1 function at the replication fork. A further study from the same group proposed a role for ChlR1 in recovery from replication-coupled DNA damage [178]. ChlR1 depleted cells were treated with cisplatin, a platinum based compound which causes interstrand crosslinking of DNA. These interstrand crosslinks present a dangerous obstacle to DNA metabolic processes as they link opposing DNA strands together preventing the strand separation that is essential for DNA transcription and replication. It was found that ChlR1 depleted cells were more sensitive to cisplatin treatment in cell survival assays and also accumulated more physical DNA damage as measured by single cell gel electrophoresis. This assay, also known as the comet assay, quantifies broken or fragmented DNA which is able to migrate from the nucleus of a single cell during electrophoresis on an agarose gel. In addition, this study also showed that after stalling replication using HU and releasing into fresh media containing cisplatin, ChlR1 depleted cells were less able to restart replication in comparison to control cells. This was measured by quantifying EdU foci, which will correspond to active replication forks. Fewer EdU foci were observed in ChlR1 depleted cells, indicating less efficient recovery from the replication stalling.

However, whether this is a true measure of replication recovery is somewhat contentious. The addition of cisplatin to the media following release from HU could prevent replication fork progression in ChlR1 depleted cells which is entirely independent of fork restart. It is therefore possible that these results merely support the previous data that shows ChlR1 deficient cells are sensitive to the replication blockages induced by cisplatin. It is possible that ChlR1 depleted cells lack the ability to remove the crosslinks, leading to fork stalling or collapse. Alternatively, in the absence of ChlR1, cells could be unable to stabilise the replication fork at the obstacle to allow time for the relevant repair pathways to resolve the block. Treatment with HU and release into fresh drug-free media would provide a better measure of replication fork recovery and in fact experiments in the Parish lab using the DNA fibre technique have shown that unperturbed replication fork progression is generally slower in ChlR1 depleted cells. This suggests a potential role for ChlR1 in the maintenance of fork stability during normal replication, perhaps via resolution of endogenous lesions or DNA secondary structures that occur during replication. The reported interaction between ChlR1 and the flap endonuclease Fen1 could indicate a role for ChlR1 in the resolution of specific DNA structures associated with lagging strand synthesis whereby absence of ChlR1 leads to problems with Okazaki fragment processing and reduced fork velocity. Biochemical data from Brosh and coworkers has indeed shown that purified recombinant ChlR1 has the potential, at least *in vitro*, to unwind a 5' flap hairpin structure which could occur during lagging strand synthesis and otherwise inhibit Fen1 cleavage [179]. Interestingly, cells derived from the original WABS patient were shown to be sensitive to both MMC and CPT in cell survival assays but not to damage induced by either X-rays or UV radiation [139]. This specific sensitivity to agents which impede DNA replication certainly supports the hypothesis that ChlR1 has a role in replication fork stability or tolerance of replication stress.

1.5 Future directions for the study of ChlR1 function

Recent biochemical studies have revealed a broad panel of *in vitro* DNA substrates for the helicase activity of ChlR1 [179]. While this provides valuable insight into the molecular structures upon which ChlR1 can act, this information must be placed in context with detailed functional and biological studies to provide a more comprehensive understanding of the cellular functions of ChlR1. These studies will also be important for furthering our understanding of the complex mechanisms and pathways that regulate cellular processes like cohesion, replication and DNA repair.

1.6 Aims of this project

The work presented in this thesis aims to investigate the biological role of ChlR1 in DNA replication and repair and to provide insight into how ChlR1 functions in these processes.

Using *S. pombe* as a model system, two different biochemical approaches were initially taken. A tandem affinity purification was used with the aim of identifying novel interacting proteins of Chl1. In parallel, Chl1 was cloned into an *E. coli* expression system in order to express and purify the protein for biochemical characterisation.

Subsequent chapters aim to examine the effects of ChlR1 depletion or mutation on the cellular response to DNA damage and replication stress using siRNA mediated depletion of ChlR1 or complemented WABS patient fibroblast cell lines. The patient cells also provide the opportunity to functionally characterise the effects of a novel WABS mutation on the cellular phenotype. This work aims to further our understanding of the functional relevance of ChlR1 and the mechanism by which ChlR1 mutations can result in genomic instability.

Chapter 2

Materials and Methods

2.1 Molecular biology

2.1.1 Extraction of RNA from *S. pombe*

Wild-type *S. pombe* cells were grown in complete medium (YE4S containing 0.5% yeast extract and 3% D-glucose supplemented with L-leucine, Uracil, Adenine hemisulphate and L-histidine at 0.05% each) and harvested while in the exponential growth phase as determined by an optical density measurement of 0.6 OD on a standard spectrophotometer at a wavelength of 600nM. Cells were harvested by centrifugation and RNA was extracted using Tri-Reagent (Sigma) according to the manufacturer's instructions. Cell pellets were resuspended in 1 ml of Tri-Reagent inside a fume cupboard. Lysate was then transferred to 1.5 ml microcentrifuge tube and allowed to stand for 7 mins at room temperature for complete dissociation of nucleoprotein complexes. Next, 0.2 ml of chloroform was added to the sample which was vortexed for 10 seconds before being allowed to stand for 10 mins at room temperature. The resulting mixture was then centrifuged at 12,000 xg for 15 mins at 4C. This separated the mixture into 3 phases: a red organic phase (protein) in the bottom, an interphase pellet (DNA) in the middle, and a colourless aqueous phase (RNA) at the top.

The aqueous phase from the Tri Reagent extraction was carefully transferred to a new autoclaved microcentrifuge tube and 0.5 ml of isopropanol was added. The sample was mixed well and allowed to stand for 10 mins at room temperature before centrifuging at 12,000 xg for 10mins at 4^{o}C. The RNA precipitate forms a pellet on the bottom of the tube. The supernatant was then removed and the pellet washed with 75% ethanol (~1.5 ml). The sample was then vortexed and centrifuged at 7,500 xg for 5 mins at 4^{o}C. The ethanol was then carefully removed, taking care not to dislodge the pellet and the tubes placed upside down on a Kimwipe to remove traces of ethanol. The RNA pellet was

resuspended in 20 µl RNase free H_2O before it completely dried out. RNA yield was then quantified using a Nanodrop spectrophotometer.

2.1.2 Synthesis of cDNA

Synthesis of cDNA was performed using an AffinityScript qPCR cDNA synthesis kit from Agilent Technologies and carried out according to the manufacturer's protocol. Each reaction contained: 10.0 µl of first strand master mix (2X), 3.0 µl of oligo (dT) primers (0.1 µg/µl), 1.0 µl of AffinityScript RT/ RNase Block enzyme mixture and 0.5 µg of total RNA. Each reaction was made up to a volume of 20 µl with RNase-free H_2O. Reactions were incubated in a thermal cycler programmed as follows: 25^0C for 5 mins to allow primer annealing, 42^0C for 15 mins to allow DNA synthesis and then 95^0C for 5 mins to terminate the reaction.

2.1.3 PCR amplification of cDNA

Amplification of cDNA was carried out using the following reaction conditions: 10µl 5X High-Fidelity buffer (Thermo Scientific) cDNA template (50ng), 1mM dNTPs, 10 pmol of forward and reverse primers (**Table 1**) and 2 units of Phusion High-Fidelity polymerase (Thermo Scientific) in a final reaction volume of 50 µl. The thermal cycle conditions for the PCR reactions were: initial denaturing step of 95^0C for 1minute 30 seconds followed by 25 cycles of 95^0C for 30 seconds, 55^0C for 30 seconds and 72^0C for 1 minute 40 seconds.

2.1.4 Restriction digestion

PCR amplified DNA was digested in parallel with vector DNA (pET24b) using the appropriate restriction enzymes to generate compatible DNA overhangs. The total amount of DNA digested per reaction ranged between 100 ng and 1 µg depending upon PCR and plasmid DNA yields. The reaction conditions were as follows: 2 µl of the appropriate 10X restriction enzyme buffer (Promega), 0.25 µg/µl BSA and 0.5 µl of each 10 U/µl restriction enzyme (Promega). Reactions were made up to 20 µl with sterile nuclease-free H_2O and incubated for 2.5 hours at 37^{o}C. Linearisation of plasmid DNA was checked by agarose gel electrophoresis.

2.1.5 DNA ligation

Ligation of digested DNA inserts into the plasmid backbone was performed by incubating the digested DNA in the presence of T4 DNA ligase (Promega) using a 1:3 molar ratio of vector to insert. Reaction conditions were as follows: 2 µl of 10x DNA ligase buffer (Promega), 1 unit of T4 ligase enzyme, plus the appropriate volume of both vector and insert DNA made up to 15 µl with sterile nuclease-free H_2O. The reaction was then incubated overnight at room temperature.

2.1.6 Transformation of E.coli cells with plasmid DNA

Depending upon the concentration of plasmid DNA, generally 1-2 µl of DNA was added to a 50 µl aliquot of chemically competent *E.coli*, maintaining aseptic conditions to avoid contamination. The mixture was incubated on ice for 20-30 minutes. Each sample was then subjected to a 42^{o}C heat shock for 30 seconds and then incubated on ice for a further 2

minutes. 1 ml of Luria Broth (LB) was then added to the bacteria and the cells placed in a shaking incubator at 37^{o}C and 220 rpm for 30 minutes. 100 µl of the bacterial suspension was plated on an agar plate containing the appropriate selective antibiotic(s) and incubated at 37^{o}C overnight.

2.1.7 Isolation of plasmid DNA from *E.coli*

Following transformation, individual colonies were picked using a sterile pipette tip and used to inoculate 5 mls of LB supplemented with the appropriate antibiotic(s). The culture was then incubated in a shaking incubator at 37^{o}C and 220rpm overnight. Cells were harvested the next day by centrifugation at 4000 xg and cell pellets processed using the QIAprep Spin Miniprep Kit (Qiagen) according to the manufacturer's instructions. DNA yield and purity was analysed using a NanoVue spectrophotometer (GE Healthcare). Plasmids expected to contain cloned DNA were subsequently digested with the restriction enzymes used for cloning and analysed by agarose gel electrophoresis to confirm the presence of the insert before being sequenced to confirm that cloning was successful.

2.1.8 Generating glycerol stocks of plasmid DNA

Glycerol stocks of transformed *E.coli* were generated by removing a 1ml aliquot from an overnight culture and mixing this with 1ml of autoclaved, sterile 40% glycerol solution. Stocks were then stored at -80^{o}C.

2.1.9 Site-directed mutagenesis

Primers were designed to mutate lysine 50 of CHL1 to arginine in order to generate a helicase-dead mutant protein (K50R). The reaction was carried out using the QuickChange II Site-Directed Mutagenesis kit from Agilent Technologies and the sequenced wild type pET24b-CHL1 plasmid as a template. The reaction conditions were as follows: 5 µl 10X reaction buffer, DNA template (50 ng), 1 mM dNTPs, 125 ng each of forward and reverse mutagenesis primers (**Table 1**) and 1 µl of PfuUltra HF DNA polymerase in a final reaction volume of 50 µl. The following cycling conditions were used: initial denaturing step of 95^0C for 1 minute, followed by 15 cycles of 95^0C for 30 seconds, 55^0C for 30 seconds and 68^0C for 5 mins. Extension step was determined by allowing 1 minute per kilobase (kb) of template. A *Dpn*I digestion was performed by adding 1 µl of enzyme to each PCR reaction and incubating for 1 hour to digest the parental template DNA prior to transformation.

Primer description	**Sequence**
Chl1 forward (*Nde*I)	GATGCATCACCATC***CATATG***TGTCATTCGAAAG
Chl1 reverse C-terminal vector (*Xho*I)	CCTGCTGGTG***CTCGAG***ATCACACATCTTTTTAGCCCG
Chl1 reverse N-terminal vector (*Xho*I)	GCGCCTCCTGCTGGTG***CTCGAG***CTAATCACACATC
Chl1 sequencing (529-549)	ATACTTCGGTTGATCCGATG
Chl1 sequencing (1460-1480)	AGTCGATGGTTATACGAAAT
Chl1 forward pHISTEV/pLou 3 (*Nco*I)	CGG***CCATGG***CTTGTCATTCGAAAGAAG
Chl1 reverse pHISTEV (*Xho*I)	GCTGGTG***CTCGAG***CTAATCACACATC
Chl1 reverse pLou3 (*Sal*I)	GCTGGTG***GTCGAC***CTAATCACACATC
Chl1 K50R forward	GAATCACCAACTGGAACGGGACGTAGTTTGAGTTTAATCTGTGC
Chl1 K50R reverse	GCACAGATTAAACTCAAACTACGTCCCGTTCCAGTTGGTGATTC

Table 1: Table of primer sequences used for all PCR, mutagenesis and sequencing reactions. Restriction sites are indicated in bold type where appropriate and the restriction enzyme is shown in brackets.

2.2 Protein expression and biochemical methods

2.2.1 Protein expression in E coli

Sequenced and purified plasmid DNA was transformed into *E.coli* (BL21 or Rosetta 2 strains) for protein expression using the method described in 2.4. An individual colony was once again picked and used to inoculate 5-10 ml of LB containing the appropriate antibiotic(s) before incubating in a shaking incubator at 37^{o}C overnight at 220 rpm. Alternatively, an existing glycerol stock of bacteria containing the expression plasmid could also be used to inoculate a larger starter culture. The following morning, a fraction of the starter culture was used to inoculate a larger volume of LB, depending upon the scale of the experiment.

For small scale analysis of protein expression, usually 0.5 ml of starter culture was used to inoculate 10 mls of LB. This was then grown until mid-log phase as determined by an optical density reading of 0.5 at a wavelength of 600 nm. At this point, a 0.5 ml aliquot of bacterial cell suspension was removed and harvested by centrifugation to represent an uninduced sample. The culture was then induced with 250 µM to 1 mM IPTG and allowed to grow for a further 3.5 hours before harvesting a second 0.5 ml aliquot. The remaining cell suspension was also harvested and the cell pellet stored at -20 ^{o}C for future analysis. The 0.5ml pellets were then resuspended in 100 µl of 1X SDS sample buffer (50 mM Tris-HCl pH 6.8, 2% SDS, 10% glycerol, 100 mM DTT, 0.1% bromophenol blue) and boiled at

95 ^{o}C for 10 mins. 20 µl of each sample was then analysed by SDS PAGE to determine protein expression.

These conditions were subsequently optimized for expression and solubility and it was determined that for the purposes of purifying Chl1, expression overnight at 18-20^{o}C improved the soluble fraction of protein while still achieving a reasonable level of expression (see chapter 3).

2.2.2 Polyacrylamide Gel Electrophoresis (SDS PAGE)

The gel casting apparatus (Bio-Rad) was cleaned thoroughly with 20% ethanol (EtOH) and assembled as per manufacturer's instructions. The resolving gel (375mM Tris-HCl pH 8.8, 8-15% Acrylamide-bis, 1% SDS, 1% ammonium persulphate, 0.1% TEMED) was carefully poured between the casting plates, leaving approximately 1 cm between the resolving gel and the bottom of the gel comb. 20% EtOH was added on top of the resolving gel to remove air bubbles and to allow the gel to set smoothly. The gel was then allowed to set for approximately 30 minutes at room temperature prior to removing the EtOH and pouring the stacking gel. The stacking gel (125mM Tris-HCl pH 6.8, 5% Acrylamide-bis, 1% SDS, 1% ammonium persulphate and 0.1% TEMED) was then poured to within 1-2 mm of the top of the casting plates and the gel comb carefully inserted. The gel was then incubated for a further 10-15 minutes to allow the stacking gel to polymerise.

Following polymerisation of the gel, the comb was removed and the wells washed thoroughly with H_2O to remove any excess or unpolymerised acrylamide. The gel cassette was then assembled in the gel running tanks and the internal chamber filled with running buffer (25 mM Tris-HCl pH 8.5, 192 mM glycine, 0.1 % SDS). Additional running buffer

was added to the outer chamber of the tank up to the indicated fill line. 20-30 µl of pre-prepared protein samples in SDS sample buffer were then loaded into the wells. A commercially available molecular weight marker was always added to the first well (Peqlab Protein Marker V). Electrophoresis was then carried out at 100V for 20-30 mins until the sample has progressed through the stacking gel before increasing to 150-180V until the proteins are sufficiently resolved. Gels can then be stained and proteins visualized with Coomassie Brilliant Blue stain (Bio-Rad) or the proteins can be transferred to a membrane for western blot and immunodetection.

2.2.3 Small-scale nickel affinity purification

For small-scale purifications, 1 ml of an overnight starter culture was used to inoculate 10 mls of LB and the culture was then incubated until an OD of 0.5-0.6 was reached. Expression was induced by adding 0.2 mM IPTG and incubating for a further 3.5 hours at 30^{o}C or overnight at 18-20^{o}C. The bacteria were then harvested by centrifugation, the cell pellets washed in PBS and then lysed in 0.5 ml bacterial lysis buffer (50 mM Tris-HCl pH7.6, 500 mM NaCl, 10 mM imidazole, 0.1% Triton-X 100, 0.5 mM DTT). Lysis buffer was supplemented with 1 protease inhibitor cocktail tablet (Roche) per 20 mls of buffer. Samples were sonicated on ice for 3 x 12 seconds at an amplitude of 50% and the lysate was then clarified by centrifuging at maximum speed on a bench top microcentrifuge (16,000 xg) for 10 minutes. The supernatant was removed to a clean microfuge tube and 20 µl of HIS-Select® Nickel Magnetic Agarose Beads (Sigma) pre-equilibrated in lysis buffer, were added. Samples were incubated on a rotating wheel for 30 mins at room temperature. Beads were collected using a magnetic rack and supernatant removed. The beads were then washed twice with 0.5 ml of wash buffer (50 mM Tris-HCl pH7.6, 500

mM NaCl, 30 mM imidazole, 0.1 % Triton-X 100, 0.5 mM DTT) before eluting the bound protein with 50 µl elution buffer (50 mM Tris-HCl pH7.6, 500 mM NaCl, 250 mM imidazole, 0.1 % Triton-X 100, 0.5 mM DTT). 20 µl aliquots were removed at each of the above steps for quality control checks. For example to check that induction and protein expression was successful and that the protein was soluble in the lysis buffer. All samples were then analysed by SDS PAGE and Coomassie staining as well as immunodetection with anti-HIS antibody to detect the poly histidine tag on the purified proteins.

2.2.4 Nickel affinity chromatography

Bacterial cultures expressing Chl1 were grown and induced as described previously. For initial chromatography purifications 250 ml cultures were harvested by centrifugation and cell pellets were washed in PBS before resuspending in 20 mls of ice cold buffer A (50 mM Tris-HCl pH 7.6, 500 mM NaCl, 20 mM imidazole, 0.5 mM DTT plus protease inhibitor). Lysates were sonicated at 60% amplitude for 30 seconds. This was repeated a total of 4 times with a 15 second break on ice in between. Lysates were then clarified by centrifugation at 20,000 rpm using the fixed-angle Beckman JA-25.50 rotor for 30 minutes at 4^{o}C. The clarified supernatant was then passed through a 0.8 µm filter.

The sample was loaded onto a 1ml Fast Flow HisTrap™ column (GE Healthcare) and then purified by FPLC (fast protein liquid chromatography) using the Akta™ chromatography system (GE Healthcare). The column was washed extensively with Buffer A before the imidazole gradient was increased by altering the ratio of Buffer A to Buffer B (50 mM Tris-HCl pH 7.6, 500 mM NaCl, 250 mM imidazole, 0.5 mM DTT). The column wash volumes, flow rate and the imidazole gradient were optimized over a number of experiments and depended upon the size of the original bacterial culture (see chapter 3).

All flow-through and eluted protein was collected by the automated fraction collector in 1 ml fractions for subsequent analysis by SDS PAGE. All chromatography buffers were filtered and degassed using helium bubbling prior to use on the Akta™ system.

2.2.5 Size exclusion (or Gel Filtration) chromatography

Fractions containing protein for further purification were pooled and concentrated by centrifugation using a Vivaspin sample concentrator spin column (GE healthcare). The protein fractions were concentrated to a volume of 0.5-2 ml suitable for loading onto the gel filtration column. The column was pre-equilibrated in gel filtration buffer (50 mM Tris-HCl, 500 mM NaCl, 0.5 mM DTT). After loading of the sample, the column was washed with gel filtration buffer using a flow rate of 0.5 ml per minute on the Akta™ system. Fractions were once again collected by the automated fraction collector and samples corresponding to absorbance peaks on the chromatogram were analysed for protein by SDS PAGE.

2.2.6 Heparin affinity chromatography

Fractions for further purification on a 1 ml HiTrap Heparin HP column (GE healthcare) were buffer exchanged using Vivaspin sample concentrator spin column into MES buffer A (20 mM MES pH 6.0, 100 mM NaCl, 1 mM DTT) prior to loading onto the column and purifying using the Akta™ system. Bound protein was eluted from the column by increasing the ionic strength. This was achieved by increasing the ratio of MES buffer B (MES pH 6.0, 1 M NaCl, 1 mM DTT) to buffer A and collecting the fractions

corresponding to peaks in the chromatogram. Samples were analysed by SDS PAGE for the presence of purified protein.

2.2.7 Tandem Affinity Purification from S.pombe cells

The protocol for the tandem affinity purification (TAP) of a protein from S. *pombe* was adapted from Gould *et al* [180]. Briefly, S. *pombe* cells were cultured in YE4S medium and grown to an OD at 600 nm of 0.7-0.8 before harvesting by centrifugation. Twenty-four litres of cell culture were required per experiment: 12 litres of the TAP-CHL1 expressing cells and 12 litres of a wild-type (SP322) strain as a control. Cell pellets were then resuspended in 12 mls of 2X lysis buffer (12 mM Na_2HPO_4, 8 mM NaH_2PO_4, 0.3 NaCl, 4 mM EDTA, 100 mM NaF, 0.2 mM Na_3VO4, 0.2% NP-40 plus complete protease inhibitor tablet) and frozen as small pellets by pipetting droplets into liquid nitrogen. These pellets were then mechanically lysed using a Retsch grinding machine, all the while maintaining freezing conditions by immersion in liquid nitrogen to avoid the possibility of the sample thawing.

The resulting powdered lysate was allowed to thaw before cell debris was collected by centrifuging at 14000 xg for 30 minutes. The clarified lysate containing soluble TAP-tagged protein was then incubated for 1 hour with 200 µl of IgG Sepharose resin which had been pre-equilibrated in lysis buffer on a rotating wheel at 4^oC. The sample was then spun down and the beads collected. The unbound supernatant was removed and an aliquot stored at -20^oC for future analysis. The beads were washed 3 times with wash buffer (10 mM Tris-HCl pH 8.0, 150 mM NaCl, 0.1 % NP-40) and once with TEV cleavage buffer (10 mM Tris-HCl pH 8.0, 150 mM NaCl, 0.5 mM EDTA, 1 mM DTT, 0.1 % NP-40) before incubation with 30 µl (10 U/µl) TEV protease (Life Technologies) diluted in 1 ml

of TEV cleavage buffer at 4^{o}C overnight. This cleaves the tag at a specific TEV cleavage site, removing the protein A domain and eluting the protein of interest. Following incubation with TEV protease, the beads were again collected by centrifugation and the supernatant, containing the protein of interest, collected. The beads were washed again in 1 ml of TEV cleavage buffer, spun down and the supernatants pooled to give a total volume of 2 ml.

300 µl of calmodulin Sepharose was prepared by washing 3 times with calmodulin binding buffer (10 mM Tris-HCl pH 8.0, 150 mM NaCl, 1 mM imidazole, 1 mM magnesium acetate, 2 mM $CaCl_{2,}$ 10 mM β-mercaptoethanol, 0.1 % NP-40). 6 mls of calmodulin binding buffer (CBB) was added to the 2 ml of TEV eluted protein. An additional 6 µl of 1 M $CaCl_2$ was also added to quench the EDTA in the TEV cleavage buffer. The eluted protein solution was then incubated with the calmodulin Sepharose for 1 hour at 4^{o}C on a rotating wheel. After incubation the beads were collected and washed twice with CBB. The tagged protein and its interacting partners were then eluted from the beads with 2 x 500 µl of calmodulin elution buffer (10 mM Tris-HCl pH 8.0, 150 mM NaCl, 1 mM imidazole, 1 mM magnesium acetate, 20 mM EGTA, 10 mM β-mercaptoethanol, 0.02 % NP-40).

To the 1 ml elution 333 µl of 100% trichloroacetic acid (TCA) was added and incubated on ice for 30 minutes with periodic vortexing to precipitate the eluted protein. Samples were then spun at 20000 xg on a bench top microcentrifuge at 4^{o}C for 30 minutes before carefully removing the supernatant. The pellet was then washed once in ice cold acetone/0.5 M HCl before centrifuging again at 20000 xg for 5 minutes. The supernatant was again removed and the invisible pellet subjected to a final wash in 1ml of 100 % acetone. The pellet was dried in a heat block at 30^{o}C before resuspending in 20 µl of 1X SDS buffer prior to running on a 4-12 % NuPAGE® Bis-Tris Pre-Cast gel (Life

Technologies). Gels were silver stained using the Bio-Rad Silver Stain Plus kit (Bio-Rad) according to the manufacturer's instructions. Protein bands were then excised and analysed by mass spectrometry.

2.3 Cell biology

2.3.1 Mammalian cell culture

All mammalian cell lines were cultured at 37^{o}C in a humidified incubator with an atmosphere of 5% CO_2. HeLa cells were cultured in DMEM growth medium supplemented with 10% foetal bovine serum (FBS) without antibiotics while hTERT-RPE1 cell lines were cultured in DMEM-F12 supplemented with 10% FBS, no antibiotics. Generally cells were passaged upon reaching ~90% confluence by removing medium, washing in warm PBS and incubating with trypsin-EDTA for 5 minutes until the cells became detached. Fresh medium was added to neutralize the trypsin-EDTA and the appropriate volume of cell suspension seeded into pre-warmed dishes of fresh medium.

2.3.2 Nucleofection of mammalian cells with siRNA

hTERT-RPE1 cells were grown to 60 % confluence prior to transfection with siRNA oligonucleotides. Cells were trypsinized, counted and 0.8 x 10^6 cells were then centrifuged at 250 xg for 10 minutes. Excess growth media was removed from the pellet which was then resuspended in 100 µl of electroporation solution with 20 µl of siRNA (20 µM stock). The suspension was then transferred to a cuvette for electroporation using an Amaxa Nucleofector. Immediately following electroporation, 1 ml of growth media was added to

the cuvette to resuspend the cells which were then plated in 2 x pre-warmed 10 cm dishes with appropriate growth medium.

For all siRNA experiments, cells were cultured for either 48 or 72 hours post-transfection. A commercially available non-targeting control siRNA (Dharmacon) was used in all experiments along with a ChlR1 siRNA specific to the 3' UTR of the gene. Sequences are shown below:

ChlR1 3' UTR siRNA	AGUCACUCCUUCAGUAGAA
non-targeting siRNA	UAAGGCUAUGAAGAGAUAC

2.3.3 Cell synchronization

Cells were synchronized in G1/S by double thymidine block. 2 mM thymidine was added to the growth medium of cells that had been cultured for 8 hours. Cells were then cultured for a further 16 hours and the thymidine was removed by gently washing cells twice in PBS. Fresh growth medium was then added and cells were incubated for a further 8 hours. Once again, 2 mM thymidine was added to the cells and they were cultured for 16 hours before harvesting or releasing into S-phase.

2.3.4 Colony formation assay

HeLa cells transfected with either control or ChlR1 siRNA were cultured for 24 hours post-transfection before trypsinising, counting and re-plating at low density into wells of a 6-well plate. Typically, 150-1000 cells were plated per well depending upon the drug treatment and dose. Untreated wells were seeded at 150 cells/well while the wells

receiving higher doses of DNA damaging drugs were seeded at higher densities. Approximately 4 hours post re-seeding, cells were treated with increasing doses of various DNA damaging agents. Depending upon the drug, treatments ranged in duration from 3 hours to 24 hours before the drug was washed off and fresh medium added. The cells were then incubated at 37^{o}C for 10 days to allow surviving cells to form colonies which could then be stained with methylene blue solution (0.2 % methylene blue, 50 % MeOH) and counted. Each condition was counted in triplicate and an average of the three wells taken.

2.3.5 Cell Counting Kit-8 (CCK-8) proliferation assay

hTERT-RPE1 cells were treated with either control or ChlR1 siRNA and grown for 24 hours post-transfection. They were then harvested by trypsinisation, counted and re-seeded into 96-well plates. Seeding density was typically 500-1000 cells per well in 100 µl of cell suspension. 24 hours later cells were treated with increasing doses of various DNA damaging drugs in triplicate (3 wells per dose). Untreated samples as well as vehicle only samples (i.e. treated with PBS or DMSO) were included on each plate. Following drug treatment for the appropriate length of time, each well was washed gently in warm PBS and fresh medium added. 24-48 hours post-treatment 10 µl of CCK-8 solution was added to each well, taking care not to introduce air bubbles. The plate was incubated with the CCK-8 solution for 1-4 hours and the absorbance measured at 450 nM on a microplate spectrophotometer at 1 hour, 2 hours and 4 hours.

2.3.6 Mammalian cell lysis and determination of protein concentration

Each confluent 10 cm dish of cells was washed once with cold PBS before adding 1 ml of PBS to each dish and gently collecting the cells by scraping. Cells were then transferred to a clean microfuge tube and centrifuged at 1000 xg, for 10 minutes at 4^{o}C. PBS was removed and pellet resuspended in 300 µl of lysis buffer (50 mM Tris-HCl pH 7.4, 100 mM NaCl, 20 mM NaF, 10 mM KH_2PO4, 10 % glycerol,, 1 mM DTT, 1 % TritonX-100 plus 1 % protease inhibitor cocktail (Sigma)) and incubated on ice for 10 minutes. Lysate was sonicated at 40 % amplitude 3 x 10 seconds. The lysate was then clarified by centrifugation at 20,000 xg at 4^{o}C for 10 minutes. Total protein concentration of each sample was determined by Bradford protein assay (Bio-Rad) according to the standard manufacturer's protocol.

2.3.7 Subcellular fractionation

Method 1

Cells were cultured and harvested by centrifugation as previously described in **2.24** and washed once in ice cold PBS. The cytoplasmic protein fraction was removed by incubation in hypotonic buffer (10 mM HEPES pH 7.0, 50 mM NaCl, 0.3 M sucrose, 0.5 % Triton X-100, and protease inhibitor cocktail) for 10 min on ice and centrifugation at 1500 xg for 5 min. The nuclear soluble fraction was removed by incubation with nuclear buffer (10 mM HEPES pH 7.0, 200 mM NaCl, 1 mM EDTA, 0.5 % NP-40 and protease inhibitor cocktail) for 10 min on ice before centrifugation at 20,000 xg for 2 min. Pellets were then resuspended in chromatin extraction buffer (10 mM HEPES pH 7.0, 500 mM NaCl, 1 mM EDTA, 1 % NP-40 and protease inhibitor cocktail), sonicated at 40 % amplitude for 3 x 15

seconds, and then centrifuged for 30 seconds at 20,000 xg. The supernatant represents the chromatin associated fraction.

Method 2

To provide more reliable and consistent fractionation data and to further confirm results obtained via the original method, a commercial sub-cellular fractionation kit (Pierce) was used in later experiments. Cells were harvested and collected by centrifugation as previously described in **2.24**. Packed cell volume was determined after removal of PBS and from this the appropriate volume of CEB buffer was added. For example, a packed cell volume of 10 µl required the addition of 100 µl of CEB, a packed cell volume of 20 µl required 200 µl and so on. The volumes given in this method assumes a packed cell volume of 10 µl. The pellet was resuspended in CEB and incubated on ice for 10 minutes with gentle mixing. The sample was then centrifuged at 500 xg for 5 mins and the supernatant transferred to a clean pre-chilled microfuge tube (cytoplasmic fraction). 100 µl of chilled MEB supplemented with the protease inhibitor cocktail provided (1:100 dilution) was then added to the pellet before incubation on ice for a further 10 mins with gentle mixing. The sample was then centrifuged at 3000 xg for 5 mins and the supernatant once again removed to a clean chilled tube (membrane fraction). The pellet was then resuspended in 50 µl ice cold NEB plus inhibitors and vortexed on the highest setting for 15 seconds. The sample was then incubated for 30 mins on ice with gentle mixing. Following this incubation the sample was centrifuged at 5000 xg for 5 mins at 4^{o}C. The supernatant was transferred to a clean pre-chilled tube and this represents the soluble nuclear fraction. The remaining pellet was then incubated with 50 µl of chromatin

extraction buffer (NEB plus 5 µl of 100 mM $CaCl_2$ and 300 units of Micrococcal Nuclease per 100 µl of buffer). This incubation was carried out at room temperature for 15 mins. After incubation, the sample was vortexed on the highest setting for 15 seconds and then centrifuged at 16000 xg for 5 mins and the supernatant transferred to a clean chilled microfuge tube. This represents the chromatin associated fraction. At this stage, the final pellet was resuspended in 50 µl urea buffer (50 mM Tris-HCl pH 7.5, 9 M Urea, 5 mM DTT) and sonicated at 40% amplitude for 3 x 10s. This represented the cytoskeletal fraction.

2.3.8 Flow cytometry

Fixing

Cells were harvested by trypsinisation and centrifuged for 4 minutes at 500 xg. The supernatant was aspirated to within 1-2 mm of the cell pellet. Cells were resuspended and washed with 5 ml of PBS. PBS was then aspirated off and the cell pellet resuspended in the residual liquid. 3 ml of 1% formaldehyde solution was then slowly added to the resuspended cell pellet while vortexing. This was incubated at room temperature for 20 mins. The sample was then centrifuged at 500 xg and the formaldehyde removed. The cells were resuspended in the residual liquid before slowly adding 3 mls of 70 % EtOH while vortexing. The sample was then left at $4^{o}C$ until ready to stain.

Staining with anti-H3 antibody

When ready to proceed with staining, samples were spun at 500 xg to pellet cells and the EtOH removed. Cell pellets were resuspended in the residual liquid and 3ml of PBS/BSA incubation buffer (PBS containing 0.5 % BSA) was added. The samples were spun again at 500 xg and the supernatant carefully poured off. Cell pellets were resuspended in 90 µl

of incubation buffer plus 2-3 µl Alexa 488 conjugated phosphorylated (serine 10) histone 3 (P-H3) antibody (**table 2**) and incubated in the dark at room temperature for 1 hour. Cells were then washed in 3 mls of incubation buffer, spun at 500 xg and the supernatant removed. Cells were then typically also stained with propidium iodide, although the protocol can be stopped at this point and the cells simply resuspended in 500 µl incubation buffer before analyzing on the flow cytometer.

Staining with propidium iodide (PI)

To stain cells with propidium iodide, cells were washed in incubation buffer following fixation as for P-H3 staining. Cells were then resuspended in 500 µl of staining solution (PBS/BSA containing 50 µg/ml propidium iodide and 5 µg/ml RNAse A) and incubated in the dark at room temperature for 30 mins. Samples were then analysed using a FACSscan flow cytometer (Beckton-Dickinson).

2.3.9 Alkaline comet assay

Cells were transfected with either control or ChlR1-specific siRNA. 72 hours post-transfection cells were harvested and 5 x 10^3 cells were re-suspended in 90 µl of 0.75 % low melting point agarose in PBS at 37^{o}C. This suspension was then spread onto a fully frosted microscope slide pre-coated with 1 % normal melting point agarose that had been allowed to set. Slides were then placed on ice to allow the top agarose layer to solidify before treatment with 5-10 Gy gamma radiation to induce damage. Slides were either lysed immediately in alkaline lysis buffer (10 mM Tris-HCl pH 10, 2.5 M NaCl, 100 mM EDTA and 1 % Triton-X 100) or allowed to recover in appropriate growth medium. For experiments with hydroxyurea (HU), 2 mM HU was added to cell growth media after

suspension on the slides. Lysis was performed overnight at 4°C and the following day slides were incubated in fresh alkaline electrophoresis buffer (0.3 M NaOH, 1 mM EDTA) for 40 minutes to enable unwinding of the DNA molecules. Electrophoresis was carried out for 20 minutes at 300 mA following which the slides were first drained and then washed three times (five minutes per wash) with neutralisation buffer (0.4 M Tris-HCl pH 7.5). Slides were equilibrated in PBS for ten minutes before staining with 1 µg/ml propidium iodide in PBS for 2 hours at 4°C. Comets were visualized using a Zeiss epifluorescence microscope with TRITC filter set and individual cells were scored using the Comet Assay IV software tool. Fifty to one hundred cells were scored for each condition.

2.3.10 Preparation of chromosome spreads

Fibroblast cell lines growing in 10 cm plates were treated with 100 ng/ml of colcemid and incubated at 37°C for 1 hour to enrich for metaphase cells. After this incubation the medium was removed and collected in a 15 ml Falcon tube. The dish was rinsed with 2 ml of warm 1X trypsin-EDTA and this was also collected in the Falcon tube. A further 2 mls of trypsin-EDTA was added to the plate and incubated for 5 mins at 37°C. 2 mls of medium from the falcon tube was added to the plate to neutralize the enzyme and all 4 mls were then collected in the falcon tube to ensure all mitotic cells were collected. The cells were centrifuged at 500 xg for 10 minutes at 4°C. The majority of the medium was then removed leaving just 500 µl and the cells were resuspended in the remaining medium by gentle vortexing. 7 mls of hypotonic solution (0.8 % sodium citrate in deionized H_2O) was then slowly added dropwise to the sample while vortexing before incubating at room temperature for 10 mins. Cells were then collected by centrifugation at 500 xg for 10 mins

at 4^{o}C and the supernatant removed, leaving 500 µl to resuspend the pellet. 7 mls of Carnoy's Fixative (75% MeOH, 25% acetic acid) was then slowly added dropwise to the sample and then incubated for 10 mins at room temperature. Cells were once again centrifuged at 500 xg for 10 mins at 4^{o}C. The addition of the fixative was repeated twice more before removal of as much of the supernatant as possible and adding 300- 500 µl of Carnoy's Fixative to resuspend the pellet. Cells were then dropped onto clean, microscope slides using a water bath set to 37^{o}C to create a warm humid environment for optimal spreading. 3-4 slides were prepared per sample and allowed to dry inside a fume cupboard. Once slides were dry, they were stained with Giemsa stain (Sigma) for 30 mins before rinsing with distilled H_2O and air dried.

2.4 Immunological methods

2.4.1 Western blotting and immunodetection

Sections of polyvinylidine fluoride (PVDF) membrane (Roche) were cut to the required size before being placed in methanol (MeOH) for approximately 10 seconds to allow activation. They were then stored in transfer buffer (25 mM Tris-HCl pH 8.5, 192 mM glycine, 5% MeOH) until needed. Electrophoresed acrylamide gels were removed from the gel cassettes, carefully peeled from the glass plates and allowed to equilibrate in transfer buffer for 5 minutes. Sponges and filter paper sections were also pre-soaked in the buffer prior to assembly of the transfer module. The next steps were all carried out in a shallow plastic container containing a small volume of transfer buffer to keep all components moist throughout the assembly process. The bottom layer of sponge was placed on the black surface of the transfer cassette, followed by a layer of filter paper. Next, the gel was placed on top, taking care to avoid air bubbles. This was followed by the PVDF membrane, another layer of filter paper and finally a second sponge on top. Potential air bubbles were rolled out using a small glass rod and the cassette closed tightly. The cassette was then placed in the transfer tank and fully immersed in buffer. The gel was then transferred at constant 400 mA for 1 hour.

Following transfer, the PVDF membrane was rinsed in dH_2O and stained with Ponceau S solution (0.1% Ponceau S, 5% acetic acid) to ensure even transfer of protein from gel to membrane. The membrane was then rinsed again in dH_2O to destain before blocking in TBS/T (10 mM Tris-HCl pH 7.6, 150 mM $NaCl_2$, 1 % Tween 20) containing 5 % non-fat dry milk powder (blocking buffer). Membranes were typically blocked for 30 mins-1 hour at room temperature or overnight at 4^oC. After blocking, the membranes were incubated with the appropriate primary antibody diluted in blocking buffer for 2-18 hours at room

temperature or 4^{o}C. Membranes were then washed 3-5 times with TBS/T for 10 mins each before incubation with horseradish peroxidase conjugated secondary antibody diluted in blocking buffer for 1 hour at room temperature. TBS/T wash steps were repeated and proteins were detected using commercially available SuperSignal Dura Chemiluminescent Substrate (Pierce). Chemiluminescence signal was digitally detected using the Fusion™ imaging system (Peqlab). **Table 2** shows a list of antibodies along with the appropriate dilution used for immunodetection.

2.4.2 Immunoprecipitation

Cell lysate was mixed 1:1 with binding buffer (50 mM Tris-HCl pH 7.4, 100 mM KCl, 0.1 mM EDTA, 0.1 % BSA, 2.5 % glycerol,, 1 mM DTT, 0.2 % NP-40 plus 1 % protease inhibitor cocktail) along with the appropriate amount of antibody (usually 1 µg per 10 cm dish) plus 10 µl of protein G conjugated Sepharose bead slurry (Sigma) per reaction. Reactions were incubated on a rotating wheel at 4^{o}C for 2-3 hours before collecting beads by centrifugation at 500 xg and washing 3 times with 1 ml of wash buffer (100 mM Tris-HCl pH 7.4, 100 mM NaCl, 1 mM DTT, 0.5 % NP-40). Beads were then boiled in 1 X SDS sample buffer for 5 minutes before analysis by SDS PAGE.

2.4.3 Immunocytochemistry

Cells cultured on 22x22 mm coverslips were fixed in 4 % paraformaldehyde for 10 minutes at room temperature. Cells were washed twice in PBS before permeabilisation in PBS containing 0.2 % Triton-X 100, again for 10 minutes at room temperature. Cells were then blocked in PBS supplemented with 20 % heat inactivated goat serum and 0.1 % BSA for 1 hour. Incubation with primary antibodies at the appropriate dilution was performed overnight at 4^{o}C. Coverslips were then washed in PBS three times prior to incubation with

Alexa Fluor 488 conjugated secondary antibody (Life Technologies) at a 1:500 dilution for 1.5 hours in the dark. Coverslips were washed three times with PBS again and then counterstained with Hoescht 33342. Coverslips were then mounted on microscope slides using Prolong Gold anti-fade reagent (Life Technologies) and stored at -20^{o}C. Slides were imaged using a Zeiss epifluorescence microscope with FITC and UV filter sets. Antibodies and their appropriate dilutions are shown in **table 2.**

Antibody	**Manufacturer**	**Dilution (application)**
ChlR1	Dundee Cell Products*	1:500 (WB)
HA (HA.11 clone, mouse)	Covance (MMS-101P)	1:1000 (WB) 1:500 (IF)
HA (rabbit)	Abcam (ab9110)	1:1000 (WB) 1:500 (IF)
Chk1	Cell signaling (#2360)	1:1000 (WB)
Phospho-Chk1 (S345)	Cell signaling (#2348)	1:1000 (WB)
Chk2	Cell signaling (#2662)	1:1000 (WB)
Phospho-Chk2 (T68)	Cell signaling (#2661)	1:1000 (WB)
Phospho-Histone H2A.X (S139)	Millipore (05-636)	1:1000 (WB) 1:500 (IF)
PCNA	Abcam (ab29)	1:5000 (WB)
RPA34	Calbiochem (NA18)	1:500 (WB) 1:200 (IF)
Rad21	Abcam (ab992)	1:2000 (WB)
SMC1	Abcam (ab9262)	1:2000 (WB)
Timeless	Abcam (ab109512)	1:2000 (WB)
TopBP1	Bethyl Laboratories (A300-111A-1)	1:2000 (WB)
Rad9	Bethyl Laboratories (A300-890A)	1:1000 (WB)
6X his tag® (HIS.H8)	Abcam (ab18184)	1:1000 (WB)
β-actin	Sigma (A5441)	1:5000 (WB)
53BP1	Novus Biologicals (NB100-904)	1:1000 (IF)

Histone H3	Bethyl Laboratories (A300-823A)	1:5000 (WB)
Phospho- Histone H3 (Alexa Fluor® 488 Conjugate)	Cell Signaling (#9708)	1:50 (FC)
GRB2	Cell Signaling (#3972)	1:1000 (WB)
ORC2	Cell Signaling (#4736)	1:1000 (WB)
Fen1	Bethyl Laboratories (A300-256A)	1:1000 (WB)
Cytokeratin No 5/6	Boehringer Mannheim (1273-396)	1:2000 (WB)

Table 2: Table of antibodies used for immunodetection, flow cytometry and immunofluorescence. Supplier and catalogue number are shown in column two. The appropriate dilution for each application is shown in the final column.

Chapter 3

The biochemical purification and proteomic analysis of the DNA helicase Chl1 in *Schizosaccharomyces pombe*

3.1. The role of the DNA helicase Chl1

In yeast several classes of proteins, generally termed cohesion factors, have been identified. These include the proteins which form the cohesin complex as well as proteins involved in the loading of cohesin onto chromosomes and also cohesion establishment factors [118-120]. Several of these cohesion establishment factors have been shown to interact with components of the DNA replication machinery and thus are essential in ensuring that the processes of DNA replication and sister chromatid cohesion are closely coupled to each other such that newly synthesized sister DNA molecules are tethered together. One of these proteins is the DNA helicase Chl1p. Although it is known to be involved in the processes of cohesion establishment and potentially DNA replication, its exact role and mechanism of action is still not fully understood.

It has also been suggested that Chl1p may have a role, either directly or indirectly, in the repair of DNA damage. Laha *et al*. showed that Chl1p is necessary in S-phase for cell viability either upon exposure of cells to DNA damaging agents [165]. As discussed in chapter 1, the mechanism underlying this hypersensitivity to DNA damage inducing agents was shown to be independent of the DNA damage checkpoint. Another study in yeast showed that the levels of Chl1p associated with chromatin increased in response to DNA damage induction by MMS and DNA repair was again shown to be deficient in Chl1 mutants. Importantly, it was determined that these mutant cells also had defects in homologous recombination, an important pathway for DNA damage repair. However whether this HR defect is a consequence of the cohesion defect in these cells or whether Chl1p has a direct role in the HR repair pathway has yet to be determined.

3.2. Aims of Chapter 3

A review of the literature surrounding the yeast Chl1p suggested that while the protein evidently has an important role in cohesion establishment, the exact biological function of Chl1p in chromatid cohesion, cellular DNA replication and DNA repair remained poorly understood. The mechanism by which it interacts with the replication machinery to couple DNA synthesis to sister chromatid cohesion was also unresolved and therefore there was much scope for further functional characterisation of this DNA helicase protein.

Furthermore, work had been carried out in recent years using *Schizosaccharomyces pombe* as a model organism that demonstrated a role for Chl1p in the repair of DNA damage. In addition, while other groups had, at this time, undertaken some limited biochemical analysis of the human homologue ChlR1, the yeast proteins had not been similarly characterised.

To further understand the biological role of Chl1p using *S. pombe* as a model system, two different biochemical approaches were initially taken. Firstly, a tandem affinity purification was used with the aim of identifying novel interacting proteins of *S. pombe* Chl1p. In parallel, *S. pombe* Chl1 was cloned into an *E. coli* expression system in order to express and purify both the wild-type and a helicase-dead mutant protein for subsequent downstream biochemical characterisation.

3.3. Tandem affinity purification of Chl1p to identify novel interacting partners

3.3.1. Tandem Affinity Purification (TAP)

Tandem Affinity Purification (TAP) utilises a modular tag consisting of protein A and calmodulin binding domains to allow the purification of the protein of interest, in this case Chl1p, in a two-step process using IgG and calmodulin Sepharose resins respectively. Following initial binding of the tagged Chl1p to the IgG resin, the protein is then incubated with TEV protease which cleaves the tag at a specific site, removing the protein A domain and eluting the protein of interest. This eluate is bound to calmodulin Sepharose and then washed and eluted with buffer containing EGTA. Protein samples can then be analysed by SDS PAGE followed by mass spectrometry to identify proteins that co-purify with Chl1p.

The process has been shown to be extremely effective in identifying protein interacting partners and components of biological complexes [180, 181]. However, potential problems with the TAP method include the possibility that transient protein interactions may not be detected. It is also possible that the tag itself may affect expression levels of the protein of interest or interfere with protein interactions.

In the case of CHL1, the TAP tag has been cloned at the C-terminus of the CHL1 gene using a PCR-based homologous recombination method [181]. This ensures that Chl1p expression is controlled by the endogenous promoter which may increase the chances of identifying biologically relevant interacting proteins. A disadvantage of this is that endogenous Chl1 expression is fairly low level so the overall yield of the TAP experiment is significantly reduced.

3.3.2. Optimisation of Chl1-TAP expression

The *S. pombe* CHL1-TAP strain was a gift from E. Noguchi, Drexel University College of Medicine. To determine whether Chl1-TAP was indeed expressed in this strain, a western blot was performed on total cell extract using a commercial antibody against the protein A module of the TAP tag to detect the recombinant protein (**figure 3.1**).

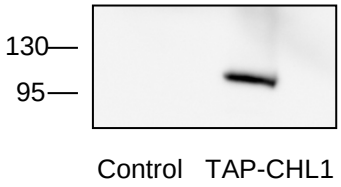

Figure 3.1. Western blot showing expression of TAP-tagged Chl1p detected by an anti-Protein A antibody. The control is total extract from wild-type cells (5 minute exposure). Forty µg of lysate was loaded in each well. Unfortunately no loading control antibody was available.

Forty micrograms of total extract from both TAP-CHL1 expressing cells and wild-type control cells were analysed by SDS PAGE. Expression of the Chl1-TAP fusion protein was confirmed by the western blot analysis, however the five minute exposure time could indicate that the levels of protein expression are quite low. There was no commercially available antibody against endogenous S. *pombe* Chl1p that would have allowed comparison between expression levels of the TAP-tagged protein and the untagged endogenous Chl1. Although the Chl1-TAP protein is expressed under the control of the endogenous promoter it is possible that the large TAP module at the C-terminus of the protein could have an effect on expression or protein stability.

After confirming expression of the TAP-tagged protein, it was then assessed for solubility in the lysis buffer that would be used for carrying out the TAP protocol. Several sodium salts were tested in the buffer to ensure the best possible yield of soluble protein for the particular protein of interest. As the aim of the tandem affinity purification is to identify potential interacting proteins, the salt concentration was kept at 0.15M for each of the sodium salts tested (**figure 3.2**).

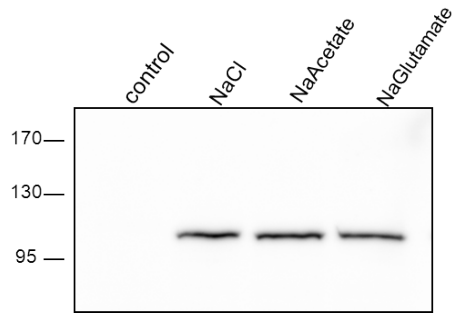

Figure 3.2. Western blot showing soluble TAP-tagged Chl1 in buffers with various salts (15 minute exposure). Anti-protein A antibody was used for detection. The control lane is soluble extract from wild-type cells in NaCl buffer. Protein concentration of soluble extracts was determined by BCA assay and equal amounts loaded for each condition.

No significant difference in solubility was observed between the different buffers. **Figure 3.3** compares Chl1 protein levels in both total cell extract and soluble extract. Equal amounts of total protein were loaded for each sample.

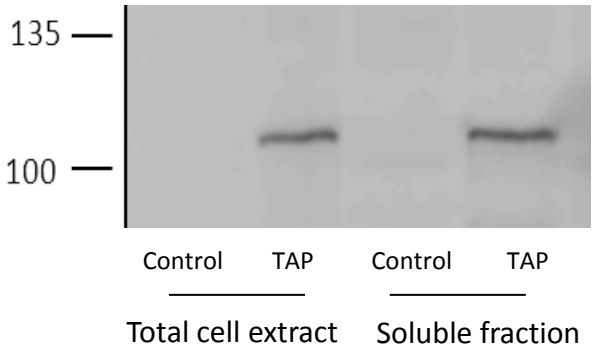

Figure 3.3. Western blot comparing levels of soluble TAP-tagged Chl1p, in NaCl lysis buffer, with Chl1p in total cell extract. Equal amounts of total protein were loaded in each well. Anti-protein A antibody was used for detection.

Comparison of total protein extract with soluble extract indicated that the majority of Chl1p was soluble in the TAP lysis buffer. After the expression and solubility of the Chl1 protein was confirmed the TAP experiment was carried out as previously described. The eluted protein was analysed by SDS PAGE followed by silver-staining of the gel. Precautions were taken at all stages of the staining process to avoid external contamination of the gel by keratins and other exogenous proteins in order to get the best quality data possible from subsequent mass spectrometric analysis.

3.3.3. Tandem Affinity Purification and mass spectrometry analysis

The TAP experiment was repeated four times in total in an attempt to improve the quality of the data and identify interesting interacting partners. **Figure 3.4** shows the silver-stained gel image taken after the second attempt at the tandem affinity purification of Chl1. A control sample was analysed in parallel with the Chl1-TAP cells. The indicated bands that were specific to the Chl1-TAP lane were excised and analysed by mass spectrometry, as were the corresponding regions in the control lane. However, on this occasion the only protein that was identified was Chl1. Further attempts were made to repeat the experiment and have the gel analysed at the in-house mass spectrometry facility at the University of St Andrews but without success.

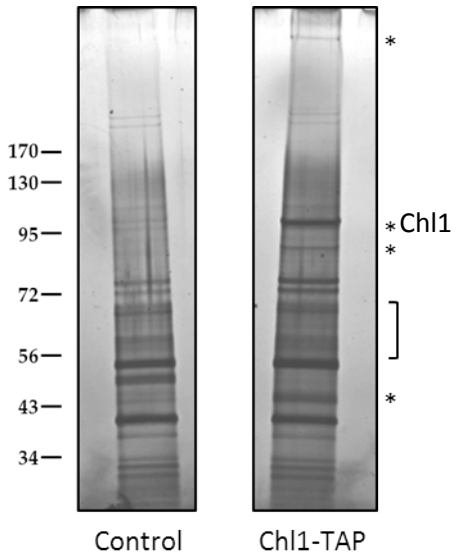

Figure 3.4. Silver-stained gel of eluted protein from Chl1-TAP expressing cells or control wild-type cells expressing untagged protein. The indicated bands/sections were analysed individually by the mass spectrometry facility at the University of St

Andrews. * indicates excised band and] indicates an excised section. The corresponding regions from the control lane were also analysed.

One of the issues raised by the gel images from the TAP experiments was that the band corresponding to Chl1 was fairly low intensity compared to some of the other non-specific bands that were present. This low-yield could be due to a number of reasons, including the probable low-level expression of Chl1. However, it could also be caused by issues such as poor binding of the Chl1-TAP protein to either the IgG or calmodulin resins or by inefficient TEV cleavage which could both result in loss of the protein at various stages of the protocol. Initially the only available antibody was directed against the protein A component of the tag. Upon cleavage by TEV protease the protein A domain remains bound to the IgG Sepharose meaning that, using the protein A antibody, it would not be possible to accurately determine cleavage efficiency.

As a crude method of determining relative Chl1 expression levels compared with other DNA replication-associated proteins in *S. pombe*, I obtained a panel of lysates from Dr Stuart MacNeill, University of St Andrews. These lysates were from three yeast strains containing TAP-tagged endogenous Mcm2, Mlh2 and Psf1 and had previously been used successfully to perform TAP experiments which identified novel binding partners. **Figure 3.5** shows Chl1 expression relative to these proteins. Chl1 expression appears to be significantly lower which could account for the difficulty in using the endogenously expressed protein for the TAP experiment.

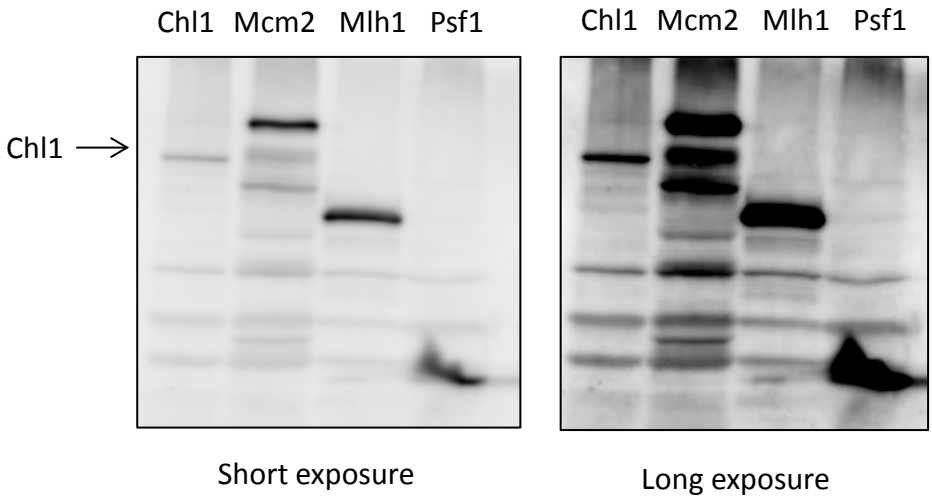

Figure 3.5. Western blot showing the relative expression levels of endogenous TAP-tagged Chl1, as indicated with the arrow, compared with the endogenously expressed TAP-tagged *S. pombe* proteins Mcm2, Mlh2 and Psf1. Anti-protein A antibody was used for detection

It is possible that with such a small amount of bait protein present and the need for silver-staining gels in order to visualise the bands, the mass spectrometry instrumentation in-house was at the limit of its ability to identify peptides and provide meaningful data. Therefore it was decided to repeat the experiment again and have the samples analysed at the proteomics facility at the University of Dundee since the instruments available there are more sensitive. **Figure 3.6** shows the Coomassie stained gel from the fourth TAP experiment.

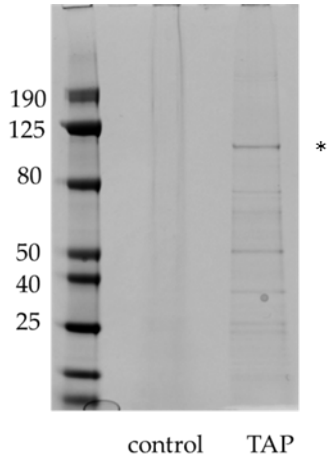

Figure 3.6. Coomassie-stained gel of eluted protein after purification from Chl1-TAP expressing cells or control wild-type cells expressing untagged protein. Only the Chl1-TAP lane was divided into sections and analysed. * indicates Chl1. The corresponding regions from the control lane were retained for analysis at a later date.

Significant protein hits from the analysis of this gel are presented in **table 4**. Proteins that were found, upon review of the literature, either to be known non-specific contaminants of TAP experiments or to be highly abundant cellular proteins with little functional relevance to Chl1 have not been included in the table. For example, elongation factor 1 alpha and glyceraldehyde phosphate dehydrogenase which were also identified in a prior analysis, are both likely to be non-specific contaminants.

Proteins were considered to be significant hits if two or more peptides were present, each with a sufficiently high peptide score. The Mascot score shown in the table is a probability score that is generated based on the number of peptides detected for a particular protein combined with the individual scores of these peptides and taking into account overall sequence coverage of the protein.

Protein ID	Mascot Score	Function
Moc2/Ded1	308	ATP-binding RNA helicase involved in translation initiation. Inactivation of ded1 prevents mitotic cell cycle progression at G1 and G2/M.
Rvb2	212	DNA helicase that is a component of several chromatin remodeling complexes, including the SWR1 and the INO80 complexes.
Rad24	144	Required for the DNA damage checkpoint. It belongs to the 14-3-3 family of proteins.
Rad25	204	Required for the DNA damage checkpoint and also belongs to the 14-3-3 family.

Table 4. A shortlist of potential Chl1 interacting proteins was generated based on the mass spectrometry data as well as using relevant functional data available in the literature.

3.3.4. Novel interacting partners of Chl1p

Without analysis of the corresponding control lane it cannot yet be determined whether these identified proteins are indeed specific interactors. However RuvBL2, the human homologue of Rvb2, was identified independently in a TAP pull-down of human ChlR1 carried out in the Parish lab by Dr Katherine Feeney. In this instance the control was analysed in parallel and RuvBL2 was not found to be present suggesting that it could be a specific interacting partner of ChlR1. Its proposed roles in chromatin remodelling and

DNA repair also suggest some potential functional relevance. Rvb2 is a DNA helicase that is a component of several chromatin remodeling complexes, including the SWR1 and the INO80 complexes [182-184]. The SWR1 complex mediates the ATP-dependent exchange of histone H2A for the H2A variant HZT1, thought to be a mechanism of transcriptional regulation. The INO80 complex remodels chromatin by altering the position of nucleosomes and is also thought to be involved in DNA repair. Both of these remodeling complexes are now considered to have roles beyond their canonical function in transcriptional regulation and have been implicated in other essential cellular processes including DNA repair, replication and checkpoint control [185].

The identification of both Rad24 and Rad25 which are 14-3-3 proteins in S. *pombe* could also be potentially interesting. 14-3-3 proteins are involved in numerous cellular processes as important adaptors and modulators of protein function [186-188]. Although neither Rad24 or Rad25 are essential in *S. pombe*, simultaneous deletion of the two genes is lethal. Rad24 mutants in particular show high sensitivity to DNA damaging agents and cells lacking Rad24 enter mitosis prematurely resulting in a phenotype of abnormally small rounded cells. Selvanathan *et al* published data from a TAP pull-down of Rad24 in *S. pombe* which did not identify Chl1 as an interacting protein, however this could be attributed to the potentially transient nature of such an interaction [187]. Also, as the level of Chl1 expression is not only generally low, but also largely cell-cycle dependent [189] it could be that the interaction is indeed real but that varying experimental conditions have prevented confirmation with the reciprocal pull-down.

Further confirmation by co-immunoprecipitation is still required to validate these putative interacting partners of Chl1. However, with a shift in focus towards the human homologue ChlR1 as a result of recent data generated in the Parish lab (K. feeney, C. Wasson and J.Parish unpublished), coupled with a lack of available biological tools for *S. pombe*, any

attempts to further characterise these interactions will most likely be performed in a mammalian cell system. In light of the mass spectrometry data generated by Dr Katherine Feeney which identified the Rvb2 homologue RuvBL2 as a potential interacting partner of human ChlR1, an attempt was made to co-immunoprecipitate flag-tagged RuvBL2 with endogenous ChlR1 in hTERT-RPE1 cells. This was unfortunately unsuccessful and currently this interaction remains unverified.

3.4. Cloning, expression and purification of *S. pombe* Chl1

In order to express Chl1 for biochemical and structural studies, large amounts of purified protein must be generated. To circumvent problems caused by low expression levels in *S. pombe*, the CHL1 gene was cloned into an *E. coli* expression vector. Bacterial promoters can drive higher gene expression levels and thus allow for the production of much larger amounts of protein. However, to express Chl1 in *E. coli* it was necessary to clone the gene without introns since bacteria lack the necessary RNA splicing machinery to allow the protein to be properly expressed.

This was achieved by extracting total RNA from S.*pombe* cells using a similar Trizol™ extraction method to that described by Chomczynski and Sacchi in 1987 [190]. The method was adapted for *S. pombe* cells which require an additional mechanical lysis step to break open their tough cell wall. After RNA extraction, first-strand cDNA synthesis was carried out using a commercial kit that utilised oligodT primers to specifically synthesise cDNA by priming at the poly-A tail of mRNA. After synthesis of the cDNA, specific primers were used to amplify the CHL1 gene for subsequent cloning.

Chl1 was initially cloned into the pET24b vector which introduced a His-tag at the C-terminus of the protein. Although all expression and purification has been carried out using this construct, work was also undertaken to clone chl1 into several other expression vectors including pHisTev which allows an N-terminal, cleavable hexahistidine tag to be introduced and pLou3, a vector engineered by Dr Huanting Lui (University of St Andrews) which allows expression of the protein as an MBP-His fusion.

Following successful cloning of the Chl1 gene, different *E. coli* expression systems were evaluated with the eventual goal of enabling the purification of full-length, soluble Chl1

protein that could then be used for biochemical studies and potentially for structural analysis.

3.4.1 Cloning of Chl1

Total RNA was extracted from exponentially growing wild type *S. pombe* cells and first-strand cDNA synthesis carried out. A control reaction, without the reverse transcriptase (RT), was included to check for contamination of the RNA preparation with genomic DNA. Using chl1-specific primers containing *Nde*I and *Xho*I restriction sites, the forward and reverse primer respectively, Chl1 was then amplified from the cDNA (**figure 3.7**). No signal was observed in the no RT control PCR. As a positive control, Dcc1-specific primers were used to amplify an 800bp fragment of the *S. pombe* Dcc1 gene. These primers were a gift from Dr Stuart MacNeil.

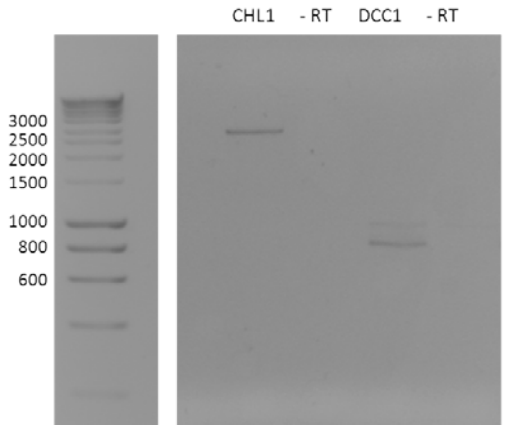

Figure 3.7. Agarose gel image demonstrating the specific amplification of CHL1 from synthesised cDNA. A band corresponding to the expected size of Chl1 (~2500bp) was clearly visible while no band was present in the no RT controls indicating that the RNA preparation was not contaminated with DNA. Dcc1 primers were used as a positive control.

The PCR reaction was purified using a Sigma PCR clean-up kit and the DNA yield was quantified. As the quantity of DNA was quite low several reactions were pooled and then subjected to restriction digest using the appropriate enzymes. In parallel, the pET24b vector was also digested with the same enzymes. Both reactions were once again purified using the commercial clean-up kit and then both the vector and insert were incubated with T4 ligase in the appropriate buffer for 3 hours at a ratio of 1:3.

Several initial attempts at cloning Chl1 failed, possibly due to the low yield of insert DNA. This was overcome by pooling several PCR reactions to increase the quantity of insert DNA available. Although many colonies were screened, almost all appeared to be due

either to re-ligation of the vector or the vector being uncut in the first place. Single digests of the vector were performed to ensure that it was being effectively cut by the restriction enzymes and this was confirmed upon analysis by gel electrophoresis. It is also possible that digestion of the insert itself was inefficient due to the small overhang provided by the primers, although it would not be possible to distinguish undigested from digested insert on a gel.

However, after scaling up the initial PCR reaction to obtain more insert DNA, colonies were screened by restriction digestion and two positive clones were identified and subsequently confirmed by sequencing (**figure 3.8**).

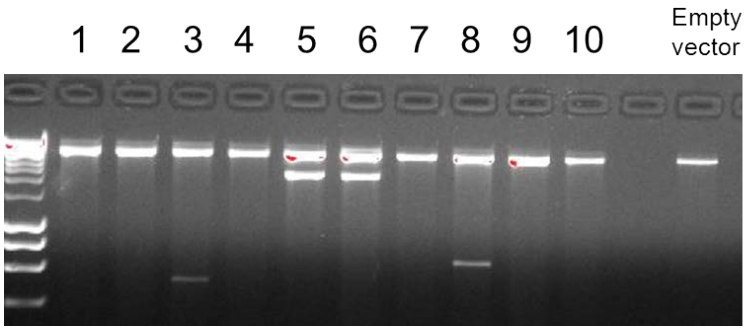

Figure 3.8. Agarose gel image showing the screening of 10 colonies by restriction digest of the extracted plasmid DNA. Colonies 5 and 6 both contained an insert which corresponded to the expected size of Chl1 and which was subsequently confirmed by sequencing.

3.4.2 Expression of Chl1

After confirmation by sequencing, the pET24b-Chl1 construct was transformed into both BL21 and Rosetta 2 cells to check protein expression in these bacterial systems. Transformed cells were then grown in the presence of the appropriate antibiotic to an OD_{600} of around 0.7 prior to induction with 0.5mM IPTG. The pET24b plasmid encodes a kanamycin resistance marker while the Rosetta 2 cells also contain the pRARE plasmid which encodes tRNAs which are rarely used in *E. coli* and which help to optimise eukaryotic protein expression. Therefore Rosetta 2 cells require the addition of chloramphenicol to the growth medium in order to maintain this plasmid. After IPTG induction, cells were then grown for another 3 hours at $30^{o}C$. Samples of cells lysed by boiling in SDS sample buffer were analysed by SDS PAGE followed by Coomassie staining (**figure 3.9**).

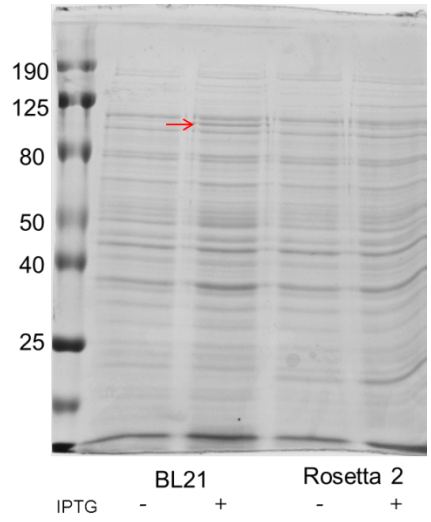

Figure 3.9. Coomassie-stained gel of cell extract from either BL21 or Rosetta 2 strains, -/+ IPTG induction. The red arrow indicates a band potentially corresponding to expressed Chl1.

Upon induction with IPTG there is a faint band visible in the BL21 sample that corresponds to the correct molecular weight for full-length Chl1. There is no corresponding band visible for the Rosetta 2 cells. Western blot analysis confirmed that full-length Chl1 was expressed in both cell systems (**figure 3.10**), however it appeared that expression was higher in BL21 cells. In contrast, although expression in Rosetta 2 cells seems significantly lower than in BL21 there does appear to be less degradation of the protein. Also, in BL21 cells there is some apparent leakage. This indicates that expression of the protein is not as strictly regulated by the addition of IPTG in BL21 cells while in Rosetta 2 cells the expression is more tightly controlled due to the presence of T7 lysozyme which reduces basal levels of expression of the protein of interest. This lack of regulation of protein expression can lead to problems with solubility and also cause protein degradation. It is possible that the relatively low expression level of Chl1 in *E. coli*, particularly in Rosetta 2 cells, could be an advantage. Lower levels of expression may

mean that the protein is less likely either to be degraded by the bacteria or to end up in inclusion bodies and be rendered insoluble.

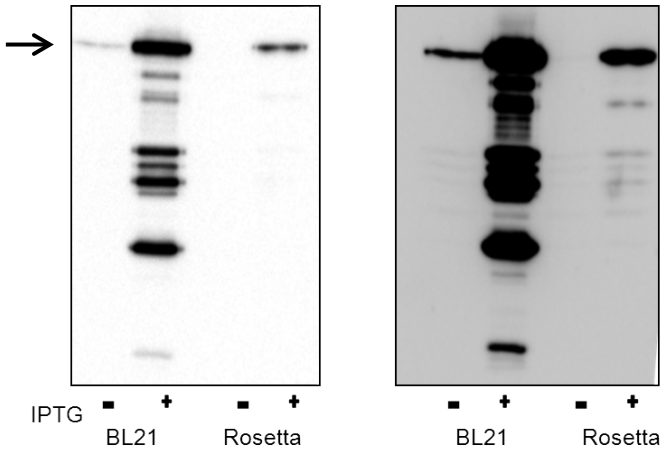

Figure 3.10. Western blot of BL21 and Rosetta 2 cell extract, -/+ IPTG. Anti-His antibody was used for detection. Left-hand panel is a 5 second exposure. Right hand panel shows a long exposure of the same blot. The arrow indicates full-length Chl1.

The next step was to test whether the expressed protein was soluble. Expression of Chl1 was induced for 3.5 hours at 30^{o}C in both BL21 and Rosetta 2 cells and once again samples were taken both prior to and after IPTG induction. Cells were then harvested and pellets were lysed by sonication in lysis buffer (50mM Tris-HCl pH7.6, 500mM NaCl and 0.1% Triton). Total extract and soluble lysate were both loaded on a gel and analysed by western blot (**figure 3.11**). It appeared that Chl1 was more soluble when expressed in Rosetta 2 compared with BL21, under these conditions.

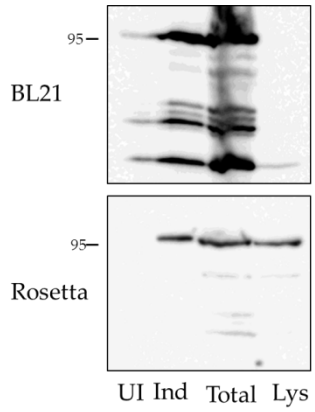

Figure 3.11. Western blot of BL21 (top panel) or Rosetta 2 (bottom panel) cell extract. Samples of uninduced (UI), induced (Ind), total cell extract (Total) and soluble lysate (Lys) were analysed by SDS PAGE and blotted with anti-His antibody. Soluble protein was only detected in Rosetta 2 cell extract.

As it could be demonstrated that Chl1 was soluble when expressed in Rosetta 2 cells but not in BL21, further optimisation of conditions was carried out using the Rosetta 2 expression system. By expressing the protein at 37^{o}C instead of 30^{o}C, it was thought that it might be possible to increase the expression, and subsequently the yield, of Chl1. However, when the western blot analysis was performed it was clear that when expression is carried out at 37^{o}C, Chl1 is not soluble and the majority remains in the pellet after lysis (**figure 3.12**). On the contrary, when Chl1 is expressed at a low temperature (20^{o}C) over a prolonged period of time, in this case overnight, the majority of the protein remains soluble. For the overnight expression a lower concentration of 0.2mM IPTG was used. Different exposures of the western blots are shown for each of these pilot expressions,

therefore they should not be directly compared to each other. The same amount of total protein was loaded compared with soluble lysate so it can be suggested that in the case of the overnight expression the majority of the expressed protein is soluble since the corresponding bands are of approximately equal intensities.

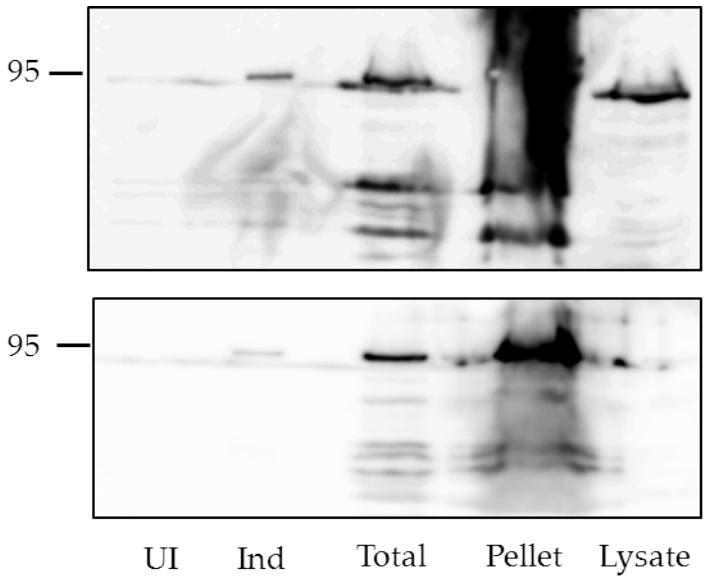

Figure 3.12. Expression of Chl1 carried out at 20^{o}C overnight (top panel) or 37^{o}C for 3.5 hours (bottom panel). The bottom blot clearly shows that the majority of the protein remains in the pellet. This is a very short exposure – in longer exposures the signal from the lane where the pellet has been loaded is too intense to allow appropriate analysis of the blot. A longer exposure is shown for the overnight expression.

3.4.3. Purification of Chl1

Having determined that Chl1 is soluble in Rosetta 2 cells under at least two sets of conditions, some small-scale purification experiments were performed using nickel beads to try to pull-down His-tagged Chl1. Briefly, this method involves induction of protein expression in a 10ml culture of cells. These cells are then harvested, resuspended in lysis buffer (50mM Tris-HCl pH7.6, 500mM NaCl and 0.1% Triton plus 10mM imidazole) and lysed by sonication. The clarified lysate containing soluble protein is then incubated with 20µl of nickel beads for 30 minutes at room temperature on a shaking platform. The beads are washed twice with lysis buffer containing 30mM imidazole and then finally the His-tagged protein is eluted in buffer plus 250mM imidazole. Samples were taken at each stage for analysis by both SDS PAGE and western blot (**figures 3.13** and **3.14**). Purified Chl1 protein is clearly visible on the Coomassie stained gel when the protein is expressed at 20^{o}C overnight while there is no detectable band on the gel when expression is carried out for 3.5 hours at 30^{o}C. Western blot analysis using an anti-His antibody confirms that Chl1 has indeed been purified under the first set of conditions. There is some protein detectable in the eluate of the 30^{o}C expression experiment but in this instance it looks like the majority of the protein remains insoluble, with only a small fraction present in the lysate. From these data it was concluded that a gentle overnight induction of Chl1 expression greatly improved the solubility of the protein and thus these conditions were selected for scaling up the purification process.

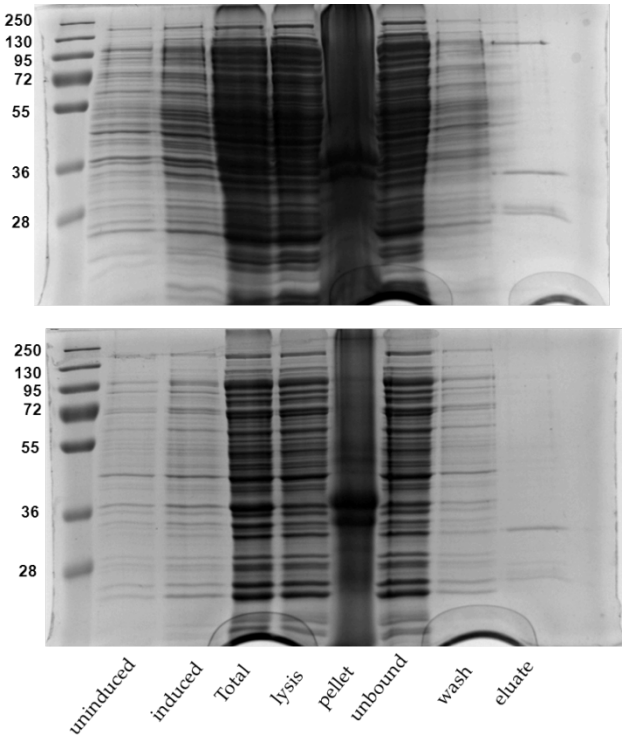

Figure 3.13. The top panel shows the Coomassie gel of samples taken at each step of the small scale purification of Chl1 from an overnight, 20^{o}C expression. Bottom panel shows the same sample set from a 3.5 hour, 30^{o}C expression.

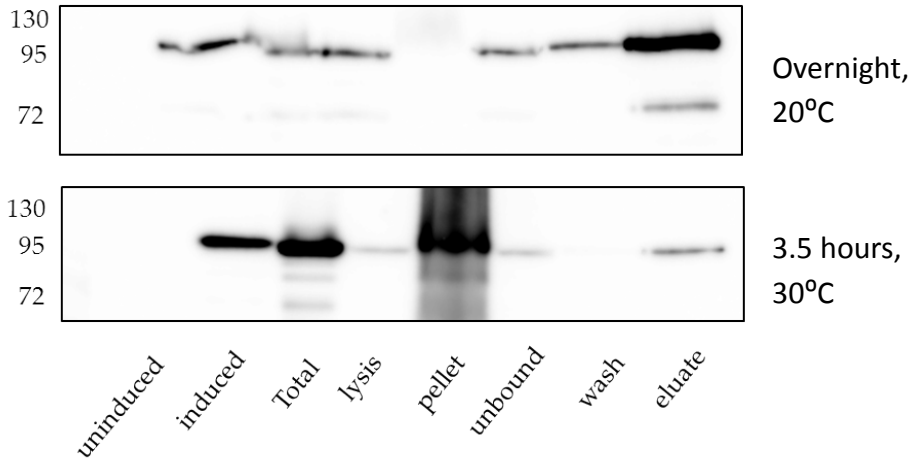

Figure 3.14. The top panel shows the western blot of samples taken at each step of the small scale purification of Chl1 from an overnight, 20°C expression. Bottom panel shows the same sample set from a 3.5 hour, 30°C expression. A 5 second exposure is shown for both.

It is noteworthy that in both small-scale purifications, upon analysis of the western blots, it is apparent that there is very little visible depletion of Chl1-His between the initial lysate and the unbound fraction after removal of the beads. It would be expected that the majority of the His-tagged protein should be bound to the beads and thus there should be less protein detected in the unbound fraction. As this is not the case it should be considered that perhaps Chl1-His does not bind efficiently to the beads. It may be the His-tag is poorly accessible due to the way the protein is folded and this problem could be resolved by

cloning with an N-terminal tag. Alternatively, the addition of a larger tag such as MPB (maltose-binding protein) could also improve binding as the small size of the His-tag compared to the relatively large size of Chl1 might be an issue.

For FPLC purification of Chl1, a 250ml culture of Chl1-His expressing Rosetta 2 cells was grown up and induced overnight at 20^{o}C. Cells were harvested by centrifugation and the pellet was lysed in the same lysis buffer as previously with the addition of a Roche complete protease inhibitor tablet and 0.5mM DTT to prevent possible oxidation of the iron-sulpher cluster of Chl1. Clarified lysate containing the soluble protein was then affinity purified on a 1ml Fast-Flow nickel column. After loading of the lysate, the column was then washed through with several volumes of Buffer A (50mM Tris-HCl pH7.6, 500mM NaCl, 20mM imidazole). Next the concentration of imidazole was increased to 60mM for several more column volumes before increasing in a gradient to 250mM imidazole over a 10 minute period. The chromatography trace is shown in **figure 3.15**. Fractions were collected and analysed by both Coomassie staining and western blot (**figure 3.16**).

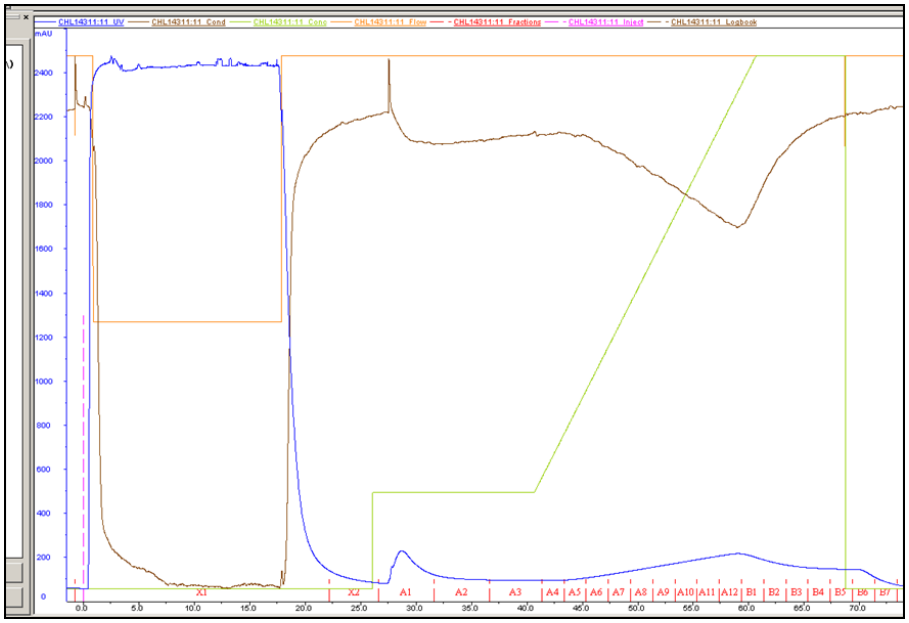

Figure 3.15. Chromatography trace of Chl1 affinity purification. The UV absorbance is shown in blue while the imidazole concentration is indicated by the green line. The brown trace represents conductivity.

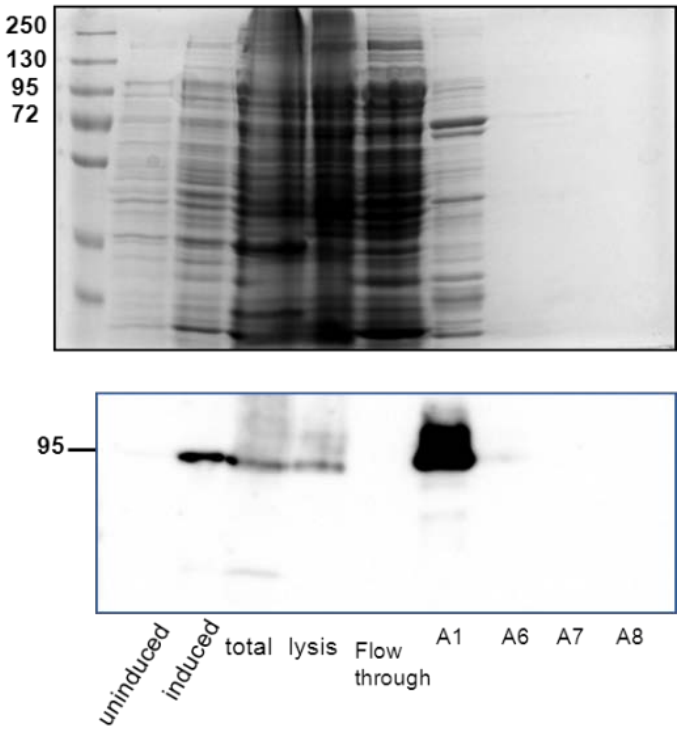

Figure 3.16. Coomassie gel (top) and western blot (bottom) of fractions from purification of Chl1. The Chl1 band is visible on the western blot at around 95 kDa, corresponding to the expected size of His-tagged Chl1 protein.

Fractions A6 to B5 were also analysed, however no protein was detected in any of these fractions. The broad peak in absorbance apparent on the chromatogram could be due to the increasing imidazole concentration rather than protein. Chl1-His is definitely present in fraction A1 which corresponded to the increase in imidazole concentration to 60mM. This step is normally used to eliminate non-specific proteins that have bound weakly to the column, however it seems in this case that Chl1-His also has a low affinity for binding to the column. However, there is no Chl1-His detectable in the flow though which suggests that it does bind to the column albeit with low-affinity. This could be a problem with the

localisation of the His-tag at the C-terminus and could potentially be resolved either by using an N-terminal tag, by using a larger affinity tag such as MBP or by simply optimising the purification protocol to take into account the low affinity binding.

Another attempt was made to purify Chl1 using FPLC, this time washing extensively with 20mM imidazole before introducing a shallow gradient up to 100mM imidazole. This was followed by another steeper gradient to 250mM imidazole to ensure complete elution of bound proteins. The chromatography trace is shown in **figure 3.17.**

Although the trace did not look promising, the zoomed-in view showed a series of very shallow peaks. These fractions were collected and analysed on a Coomassie-stained gel and by western blot. The results are shown in **figure 3.18.**

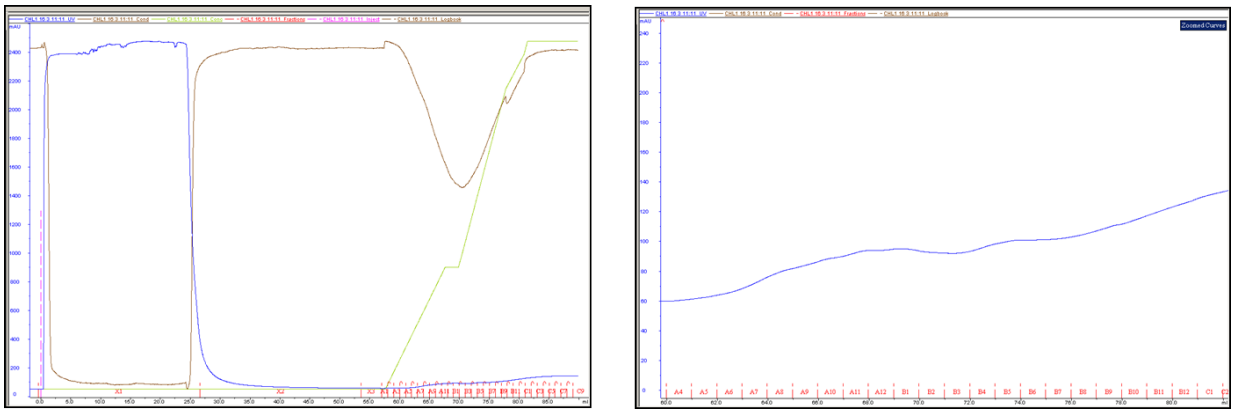

Figure 3.17. Chromatogram of Chl1 purification (left). The concentration of imidazole was increased to 100mM gradually over a 10 minute period before eventually increasing to 250mM. The right panel is a zoomed-in view showing absorbance peaks across fractions A6-B12.

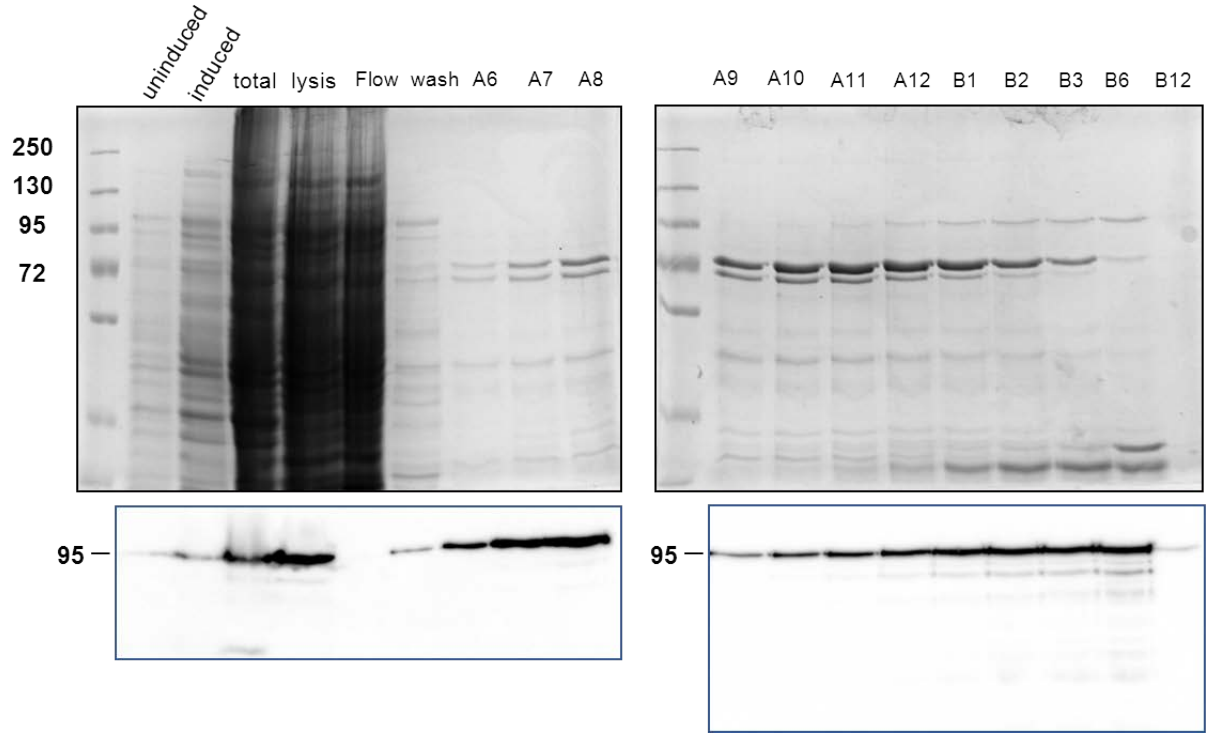

Figure 3.18. Coomassie-stained gels of fractions from Chl1 purification (top). Western blots of the same fractions are shown below (bottom), using anti-His antibody. The western blots shown are each a different exposure. The left hand side is a 1 minute exposure while the right hand side is 4 seconds.

From the Coomassie gels shown in **figure 3.18** there is a band corresponding to full-length Chl1 visible in fractions A11-B6. This was confirmed by western blot to be Chl1-His. Different exposures of the two blots have been shown in order to illustrate that there is also a small amount of Chl1-His present in the other fractions (A6-A8) which suggests that some Chl1-His is eluting from the column at lower concentrations of imidazole. It might be possible to repeat the purification using a shallower gradient to improve resolution of individual peaks. However, if the low-affinty of Chl1 is causing it to elute gradually from the column upon increasing the imidazole concentration, the result might always be a very broad, shallow peak with small amounts of Chl1 present in each fraction. As these purifications were still fairly small-scale, it was thought that increasing the amount of Chl1 in the starting material could improve the results with more Chl1 likely to bind to the column compared with non-specific contaminants.

Thus, larger scale experiments using first 1 litre and then 4-6 litres of bacterial culture were carried out to attempt to optimise the purification conditions. Neither scaling up nor reducing the gradient resulted in a significant improvement in protein purity despite the presence of an obvious peak on the chromatography trace as demonstrated in **figure 3.19**. However, this optimisation process did result in the development of a purification strategy which consistently provided acceptable yields of partially purified Chl1-His protein. A typical example of a Coomassie stained gel from a nickel affinity purification from 6 litres of bacterial culture is shown (**figure 3.19**). A 5ml Fast-flow nickel column (GE healthcare) was used and the imidazole gradient was increased from 10mM to 250mM over 25 column volumes. These conditions were used as the first step in all subsequent purification attempts and the purest Chl1-containing fractions were then pooled for further downstream purification. For example, the fractions highlighted in red in **figure 3.19** were considered sufficiently pure to be carried forward.

It was determined that the pooled and dialysed fractions from the nickel affinity chromatography could be concentrated and stored at 4°C for up to 1 week without significant protein precipitation or visible degradation of Chl1 as determined by Coomassie staining. The dialysis buffer used was 50mM Tris-HCl pH 7.6, 500mM NaCl, 10% glycerol plus 1mM DTT. Encouragingly, following concentration of the nickel purified fractions the soluble protein had a yellowish appearance which can often be observed in iron-binding proteins. This suggested that the iron-sulpher cluster remained intact and protected from oxidative damage due to the precautions taken during the purification process. However, after storage at 4°C for 2 weeks, some degradation did become apparent by Coomassie staining and the protein solution had lost its yellow tinge (data not shown), suggesting oxidation of the iron sulphur cluster.

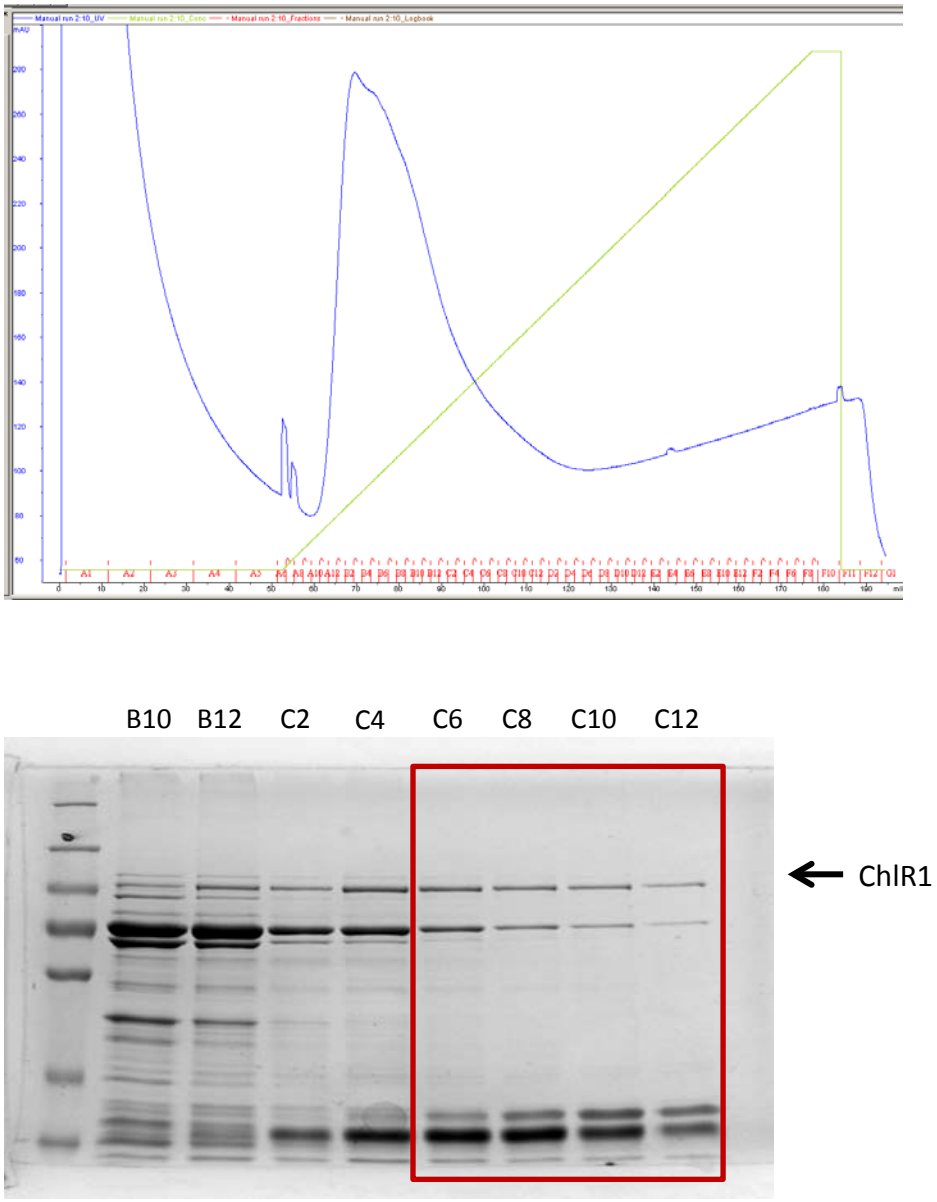

Figure 3.19. Top: Chromatogram of Chl1 purification from 6 litres of bacterial culture. The concentration of imidazole was increased from 10mM to 250mM gradually over 25 column volumes. Bottom: Coomassie stained gel showing alternate fractions from B10-C12 where the majority of Chl1 protein eluted. Several co-purifying bands were still visible even in the cleanest fractions. The highlighted

fractions were chosen as the most promising fractions for further purification based on purity.

It is common for nickel affinity chromatography to be merely the first step in the purification process and therefore it was not unexpected that additional steps had to be considered to enable the protein to be used for downstream applications. However, further purification steps must be carried out quickly and with exceptional care in order to maximise the chances of producing adequate quantities of stable, active enzyme of sufficient purity for biochemical assays.

Heparin is a very highly negatively charged polysaccharide molecule which is often used in affinity chromatography as an intermediate step in the purification of DNA binding proteins due to its charge and structural similarity to nuceic acids. Heparin therefore has the capacity to act as both an affinity ligand as well as a cation exchanger. However with regards to Chl1, which has a theoretical isoelectric point of 4.8, a relatively acidic buffer pH would need to be used to generate a net positive charge on the protein. This was considered inadvisable as it could detrimentally affect the function of the protein for downstream applications. Nevertheless, as Chl1 is a DNA helicase which evidently binds to DNA, the potential still remained to utiise heparin as an additional affinity chromatography step in the hope of further purifying the protein.

The pooled fractions from the nickel column were dialysed to remove the imidazole as well as to carry out a buffer exchange to promote binding to the heparin column. The binding was performed in a buffer containing 20mM MES pH 6.0, 0.1M NaCl with 1mM DTT and elution was achieved by gradually increasing the ionic strength of the buffer from 0.1M NaCl up to 1M NaCl. The chromatography trace and accompanying

Commassie gels are shown in **figure 3.20.** It is clear that Chl1 does indeed bind to the heparin column as the corresponding band is absent in the flow through fraction. Unfortunately, many of the contaminating proteins also appear to bind to the column and it was not possible to separate Chl1 from these co-purifying proteins using this method. In fact this suggests that it is probable that these contaminating proteins may actually be binding specifically to Chl1, not simply to the column. This could be problematic and might indicate that using this bacterial system it may not be possible to achieve the level of purity required to carry out biochemical studies on Chl1. The major bands highlighted on the gel in **figure 3.20** were excised and sent for identification by mass spectrometry.

The mass spectrometry analysis confirmed the band 1 as Chl1, however interestingly band 2 running around 70kDa was also identified as Chl1. This would normally suggest that the protein is cleaved, probably towards the C-terminus due to the fact that this band is not picked up on western blots by the anti-his antibody. Rather counter-intuitively however, when a closer inspection of the peptide coverage was undertaken, peptides were in fact identified at both the N and the extreme C-terminus of the protein in this sample. The only explanation for this is cross-sample contamination, either from the gel itself or from carry over from the previous mass spectrometry sample run. Bands 3-5 were confirmed to be contaminating bacterial ribosomal proteins.

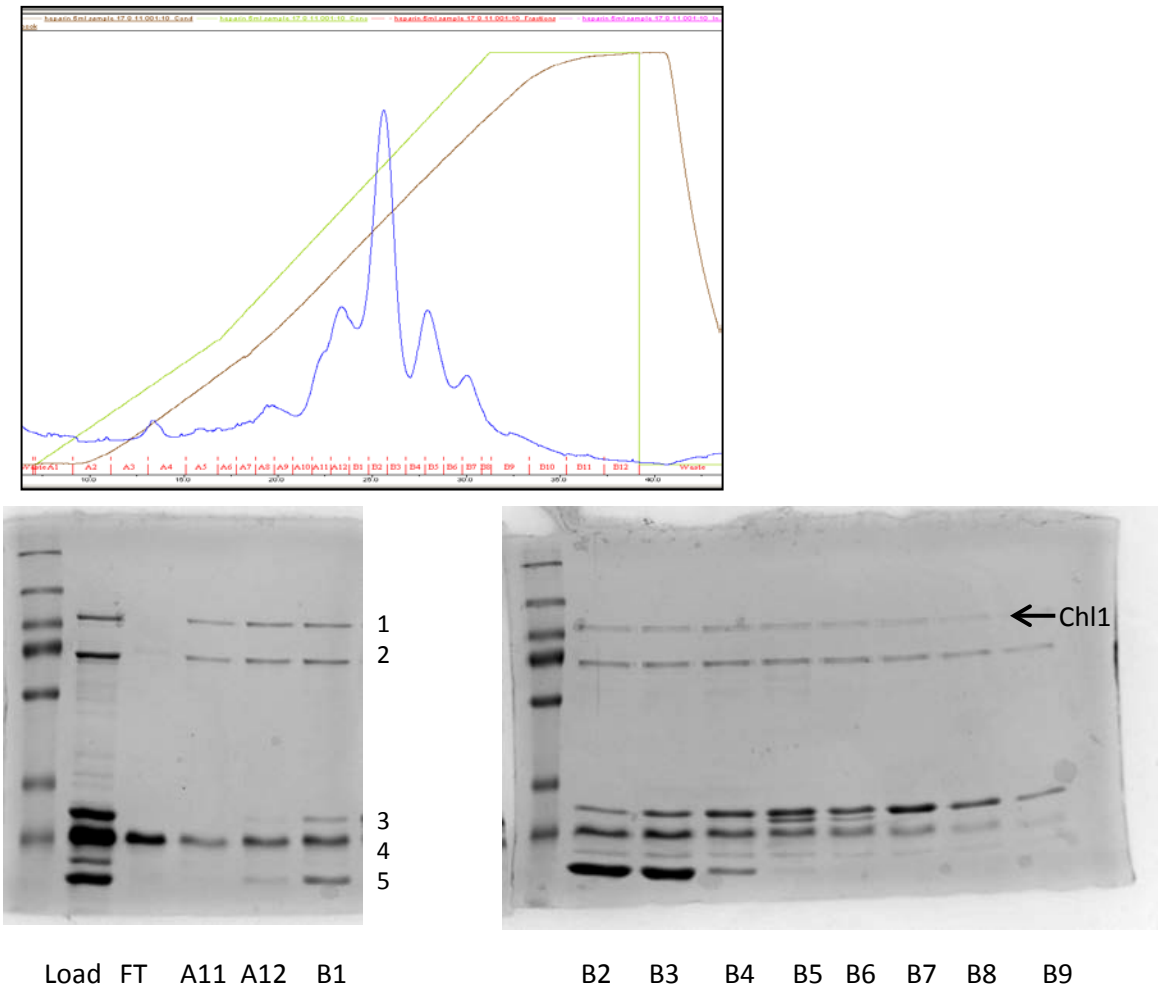

Figure 3.20. Top: Chromatogram of Chl1 nickel-purified fractions run on a heparin affinity column. The concentration of NaCl in the buffer was increased from 100mM to 1M gradually over 25 column volumes. Bottom: Coomassie stained gel showing fractions from A11-B9 corresponding to the major chromatogram peaks. Again, several co-purifying bands were still visible even in the cleanest fractions. The numbered bands were excised and sent for analysis by mass spectrometry.

Despite the issues with the contaminating proteins, it was felt that the nickel-affinity purification scheme was robust enough that it was worth going ahead and attempting to purify both the wild type Chl1 and the helicase dead K50R mutant in parallel. The idea being that with a helicase-dead Chl1 protein purified using the same method, to act as a biological control in any downstream biochemical assays, it might still be possible to generate some data even without optimal levels of purity being reached.

Cloning of the K50R mutant was carried out by site-directed mutagenesis of the original Chl1 wild type construct in the usual way, as described in materials and methods, and confirmed by sequencing. A Rosetta 2 expression strain was then generated as previously described and expression and solubility confirmed by western blot analyisis before purification was attempted.

Figure 3.21 shows the chromatography trace and Coomassie stained gels from the purification of the Chl1 K50R helicase-dead protein. The trace shows more of a bump than the peak that was usually observed with the wild type protein, however after analysis of alternating fractions by Coomassie staining it was clear that the purification had been successful. The representative gels shown in **figure 3.21** were unfortunately allowed to run for slightly too long and therefore the usual low molecular weight contaminating proteins are not visible although they are still present.

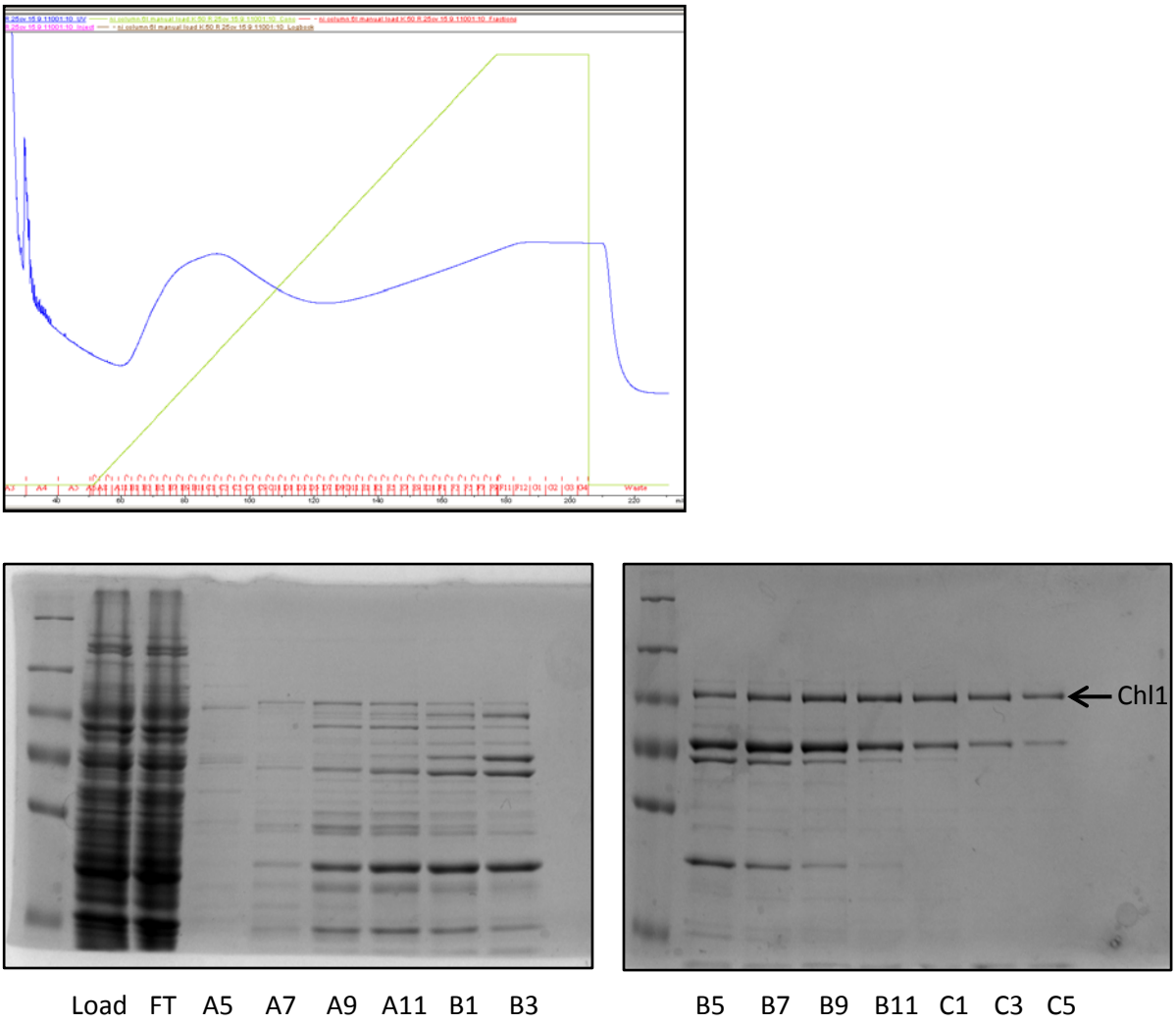

Figure 3.21. Top: Chromatogram of Chl1 K50R helicase-dead mutant purification from 6 litres of bacterial culture. The concentration of imidazole was increased from 10mM to 250mM gradually over 25 column volumes. Bottom: Coomassie stained gel showing alternate fractions from A5-C5 to determine where the Chl1 K50R protein eluted.

Having demonstrated that both the wild type protein and the K50R mutant can be partially purified by nickel-affiinity chromatography to the level where it should theoretically be possible to separate the smaller contaminating proteins via size exclusion chromatography, the purest fractions were pooled and concentrated preps of both proteins were run on a Superose 6 gel filtration column. Chromatography traces and Coomassie stained gels are shown in **figure 3.22.** In size exclusion chromatography, high molecular weight molecules and complexes are too large to enter the pores of the stationary matrix and thus elute more quickly than smaller molecules which will enter the matrix pores and therfore take longer to travel through the column. It would be expected that using this method, which essentially separates protein mixtures based on size, Chl1 should elute earlier than the low molecular weight bacterial ribosomal proteins. While this appears true to some extent based on the Coomassie gels shown in **figure 3.22**, there is still a significant proportion of Chl1 which co-elutes with these contaminants. This is even more prominent in the K50R mutant. The caveat with this approach, as in the case of the heparin column, is that if the contaminating proteins are actually binding directly to your protein of interest, then it becomes extremely difficult to separate them using any sort of conventional chromatography method. For some proteins there remains the option of attempting purification under denaturing conditions which could potentially circumvent this problem. For an iron-sulphur cluster containing enzyme like Chl1 however this would not be recommended as it would be potentially difficult, if not impossible, to re-fold the protein successfully and for it to retain its helicase activity.

WT Chl1

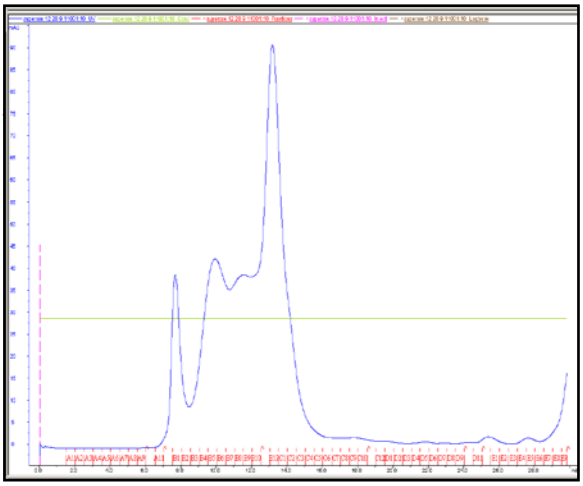

K50R Chl1

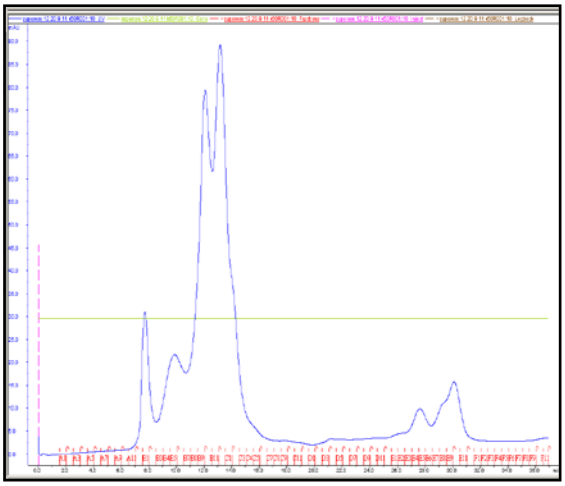

WT Chl1

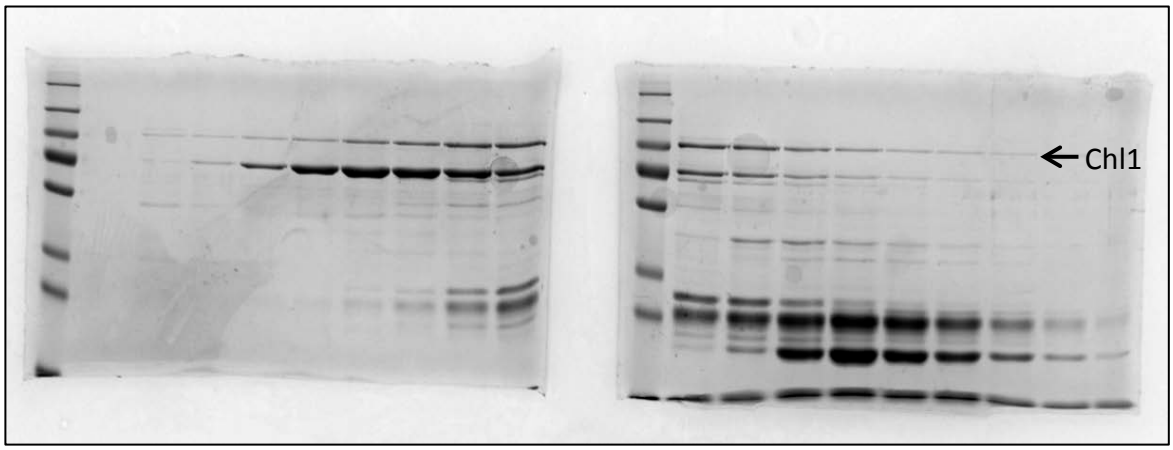

K50R Chl1

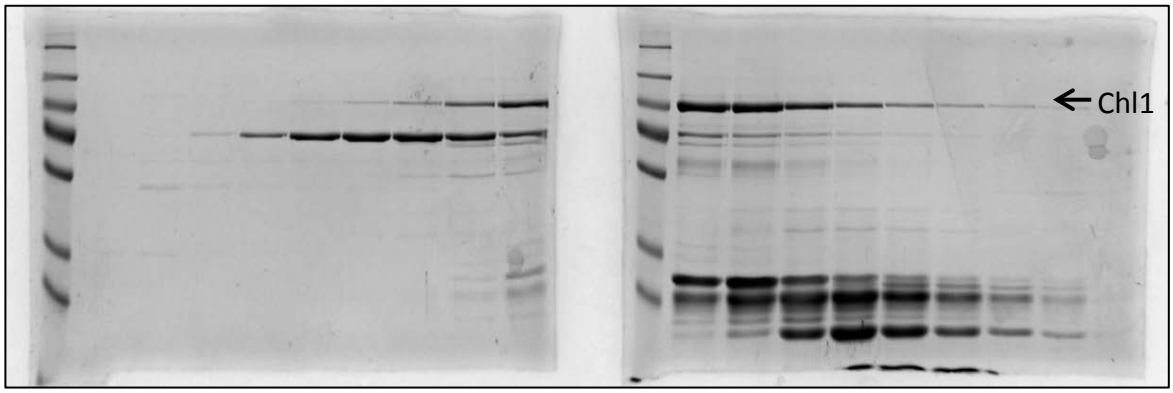

Figure 3.22. Top: Chromatogram of Chl1 and Chl1 K50R helicase-dead mutant gel filtration using a Superose 6 column. Bottom: Coomassie stained gels showing fractions A12-C6 from each purification were used to determine whether Chl1 could be resolved from the contaminating bacterial proteins via size exclusion chromatography.

At this point a number of options were considered. From the gels in **figure 3.22**, it looked like it may have been possible to isolate and pool a few of the purest fractions, even although it would likely yield only a small amount of protein. From 6 litres of bacterial culture only approximately 4mg of partially purified protein was obtained following nickel affinity chromatography as calculated by bradford assay of the pooled and concentrated samples. Visual inspection of the Coomassie stained gels however suggests that at best the sample is 10-20% pure, indicating a much lower yield of approximately 400-800µg of total ChlR1 protein. For the downstream biochemical applications such as DNA helicase assays, only very tiny amounts of active enzyme are required, thus it might still have been possible to perform some of these experiments with the inclusion of the helicase dead mutant as the appropriate control. However, after seeking advice from experts in these types of assay, it was decided that the purity was still unlikely to be sufficient for the generation of meaningful data. Moreover, the publication of a comprehensive biochemical characterisation of the human homologue ChlR1, in combination with some exciting functional data generated in the Parish group in human cell systems, resulted in further attempts to purify the yeast Chl1 protein being put on hold as the focus of the project shifted to a more functional approach in determining the role of ChlR1 in mammalian cells.

3.5. Discussion

3.5.1. The use of Tandem Affinity Purification of Chl1 to identify novel interacting partners

At the time this work was undertaken, much of data concerning the function of Chl1 had been generated using yeast as a model organism. While parallel work in the Parish lab focused on dissecting the biological role of human ChlR1, it was thought that using a yeast system to identify novel interacting proteins would lend itself further down the line to potential genetic studies in *S. pombe* that would provide novel insight into the cellular function of this conserved protein.

However, there were several caveats to the approach initially adopted which limited the success of this aspect of the project. Firstly, *S. pombe* as a model organism for carrying out large scale proteomic experiments are not ideal due to their tough outer cell wall that makes cell lysis extremely difficult on a large scale. In fact, mechanical lysis is required in order to effectively break open the cells. This was accomplished by first pelleting the yeast grown in culture, resuspending in lysis buffer before snap freezing droplets of the suspension in liquid nitrogen. These frozen pellets then had to be transferred to a pre-chilled mechanical grinding machine to be ground to a very fine powder. When this thawed it could then be spun down just like normal cell lysate and the supernatant would contain the soluble proteins. Because it is necessary to keep the lysate cold and because the grinding generates heat, the grinder itself is cooled in liquid nitrogen prior to use. On several occasions malfunctions of this equipment resulted in loss of sample due to thawing of barely or partially lysed cellular material. And because each experiment required the growth of 12 litres of yeast culture per sample, this proved both costly and time-consuming each time this occurred.

Another issue with the experiment was the relatively low expression of endogenous Chl1 as shown in **figure 3.5**. The protocol was developed based on proteins with a slightly higher level of endogenous expression in yeast, thus despite good solubility there was very little Chl1 visible on the gel post-purification. When the abundance of the bait protein itself is so low it is very difficult to then detect interacting partners which are expected to be present at even lower levels of abundance.

Scaling up the experiment to increase the yield was not an option as 24 litres of total cultures per experiment was already at the limit of what was practically feasible. A possible solution could have been to clone the TAP-tagged Chl1 gene into a S. *pombe* expression vector with a promoter driving overexpression of the gene. In fact, this was attempted but without success. It proved difficult to successfully PCR out the TAP-tagged Chl1 gene from the *S. pombe* strain gifted by Prof E. Noguchi so therefore several attempts were made to achieve success with the original method.

Low yield of the bait protein could also be caused by poor binding of the Chl1-TAP protein to the resins or inefficient TEV cleavage. Samples were taken after each step of the purification process and stored for analysis however as previously stated, only an anti-protein A antibody was initially available which allowed testing of the first binding step only. The majority of TAP-Chl1 bound to the IgG resin with very little detectable in the lysate following incubation. To test for efficient TEV cleavage an anti-CBP antibody was purchased, however several attempts to use it for western blot analysis resulted in very dirty blots with multiple bands that could not be interpreted. The TEV protease used in the protocol was commercially purchased from Invitrogen rather than in-house purified so it seems unlikely that this would be a significant factor in explaining the low yield of Chl1, although it remains a possibility.

Finally, although several attempts were made to analyse protein gels using the in-house mass spectrometry facility, only the bait protein was ever positively identified. External analysis at the University of Dundee did however yield some positive hits, following careful exclusion of known contaminants or highly abundant cellular proteins with no functional relevance. The most promising of these was Rvb2, the human homologue of which, RuvBL2, was also identified in a parallel TAP pulldown of ChlR1. Verification of this interaction by co-immunoprecipitation was not successful however. It has to be said that the data generated from the human TAP experiment has been far more interesting. Replication proteins such as PCNA and Mcm7 were identified as well as the catalytic subunit of the DNA repair kinase DNA-PK supporting the hypothesis that ChlR1 has a role in these cellular processes.

With the focus of this project now shifting towards the human ChlR1 protein, there remains scope for further utilisation of the tandem affinity approach or perhaps SILAC (Stable Isotope Labelling of Cells in Culture) quantitative proteomics using the established human cell system. It would be interesting, for example, to see whether under conditions of replication stress novel interacting proteins could be identified.

3.5.2. Purification of Chl1 for biochemical studies

Until the Brosh lab published their detailed biochemical analysis of the human ChlR1 protein in 2012 [179], there was very little data available regarding the functional biochemical properties of the protein. Hirota and Lahti provided evidence that ChlR1 was indeed a DNA-dependent helicase which could unwind both DNA:DNA and DNA:RNA duplexes [174] while Farina *et al* followed this up in 2008 with a biochemical study that conclusively demonstrated the ATPase and helicase activities of the protein [21]. Hirota

and Lahti also showed that the enzymatic activity of ChlR1 could be abolished by mutating a crucial lysine residue in the Walker A box which is responsible for the binding and hydrolysis of ATP, thus generating the K50R helicase-dead mutant which is now frequently used as an essential control for assaying ChlR1 activity or biological function [174].

The initial aim of this project was to purify the yeast Chl1 in order to carry out a detailed biochemical study using various available DNA substrates to further elucidate the function of ChlR1 in DNA metabolism. Previous biochemical studies using the human ChlR1 had yielded only very tiny quantities of protein using both baculovirus and human expression systems. A secondary aim of the project was therefore to potentially generate larger quantities of the yeast protein that could be used for structural studies. It was hoped that some of the difficulties associated with previous attempts to purify human ChlR1 would be circumvented by focusing on yeast Chl1.

Bacteria were chosen as an initial expression system due to their propensity to produce higher protein yields than in eukaryotic systems. However, after cloning Chl1 into the pET24b expression vector and transforming into both BL21 and Rosetta 2 cells it was clear from initial optimisation experiments that there would need to be a trade-off between yield and solubility (**figures 3.10-3.14**). While expression appeared higher in the BL21 system, the protein showed increased degradation and lower solubility. Rosetta 2 cells were chosen as the preferred expression system despite the lower expression. It should be noted that the very fact that a western blot was required to detect expression of the Chl1 protein after IPTG induction rather than the visualisation of a strong Coomassie stained band is indicative of a low yield by bacterial expression standards.

Nevertheless, despite the relatively low level of expression the first step purification of Chl1 by nickel affinity purification was successful. Although it did not yield pure protein, when the Chl1 containing fractions were pooled and concentrated, the protein remained relatively stable in solution, once 10% glycerol was added to the storage buffer, which allowed for further purification strategies to be attempted. However, the most effective purification schemes are those which yield protein of the required purity with the minimum amount of manipulation. Each additional step in the process introduces more handling time, during which the protein can become degraded, oxidised or precipitate out of solution which means starting again from scratch. Unfortunately, after establishing a consistent and robust technique for the nickel affinity purification of Chl1 it was apparent that it could not be significantly improved upon in terms of resolving the contaminating bands any further using this method alone.

Both heparin affinity and size exclusion chromatography techniques were utilised as secondary purification steps with neither yielding protein of the necessary purity for the intended downstream applications. With regards to the size exclusion, increasing the size of the gel filtration column also increases the resolution of proteins and this was considered an option. However, when proteins of such drastically different masses appear in the same fractions after size exclusion chromatography it does strongly suggest that these proteins exist in complex with each other. Furthermore, previous attempts to use a larger gel filtration column to increase resolution resulted in fractions so dilute that Chl1 could not be detected on the gel and could only be visualised by western blot. This was however from a smaller culture size. Ion-exchange chromatography using a Mono-Q column was also attempted on some pooled fractions post-size exclusion. These had been stored at 4°C for a few days but were used in order to have a quick assessment of whether

it might be useful as an alternative step in the process. The Mono-Q column also failed to resolve the co-purifying proteins.

In addition to the pET24b C-terminal His-tagged Chl1, other Chl1 expression constructs were generated which have only been partially characterised thus far. Chl1 was cloned into a pHisTev vector which introduces an N-terminal, cleavable His tag and also into pLou3 which expresses Chl1 as a cleavable MBP-His fusion protein. Both of these constructs are expressed, although solubility and stability have not been fully determined. The advantage of a cleavable tag is that the His tag can be cleaved from affinity purified Chl1 fractions which can then be passed back through the nickel column. This would in theory re-bind the contaminating proteins, leaving purified Chl1 in the flow through. As with the other methods already described however, this is not helpful if the contaminating proteins are binding directly to Chl1.

It does seem from all the purification strategies attempted thus far, that at least a proportion of the contaminating bacterial proteins are associating with Chl1. The only way to circumvent this problem would be to change the expression system. Given that previous biochemical studies have used alternative eukaryotic systems to purify ChlR1, it is possible that even in the case of the yeast homologue, bacterial expression and purification to a satisfactory standard is not feasible. With the recent publication by Brosh and colleagues, which elegantly characterises not only the wild-type ChlR1 protein but also describes the biochemical properties and substrate specificity of a patient-derived mutated form of the protein [179], the decision was made to set aside this branch of the project in favour of taking a functional approach to investigating the role of ChlR1 in mammalian cells.

Chapter 4

Investigating the role of ChlR1 in DNA Replication and Repair

4.0 Introduction and Aims of Chapter 4

Cellular processes including DNA replication, DNA damage repair and cell cycle checkpoint control all play important and fundamental roles in the ability of cells to survive and replicate. Control and regulation of these vital processes requires the coordinated action of an array of cellular proteins, many of which will have functions in more than one of these essential pathways.

ChlR1 is known to be involved in the process of establishing sister chromatid cohesion and has also been implicated in DNA replication [21, 65, 129, 131] although it's exact role and mechanism of action is still not fully understood. Furthermore, there is evidence from studies in yeast that indicates a possible role for yeast homologue Chl1 in DNA repair pathways [165] and, in fact, the identification of ChlR1 mutations in patients with a unique cellular phenotype combining features of both Fanconi anaemia and the cohesinopathy Roberts syndrome has also suggested for ChlR1 in the DNA damage response [139]. The recognition of Warsaw breakage syndrome as a distinct disease seen specifically in patients with ChlR1 mutations seems to lend credence to the assertion that the protein may have some involvement in the mammalian response to DNA damage and could perhaps function in coordinating the processes of DNA repair and chromatid cohesion in response to DNA damage. This taken together with the interaction of ChlR1 with various components of the replication machinery, including PCNA, the Ctf18-RFC complex and FEN1 [21], is suggestive that the ChlR1 helicase could be important in situations where cells encounter replication stress resulting in fork stalling, ultimately leading to DNA strand breaks. ChlR1-deficient cells typically progress normally through the cell cycle (K. Feeney, unpublished data) so it could be hypothesised that the function of the protein becomes more significant when cells encounter damage or stress that results in the stalling of replication and the need for the DNA damage response pathways to be activated.

The aim of this chapter was to further characterise the effects of ChlR1 depletion on the cellular response to DNA damage, in particular to agents that cause replication stress, in order to better understand the function of ChlR1 in the processes of DNA replication and/or in DNA repair pathways.

4.1 siRNA mediated depletion of ChlR1 has little effect on cell survival in response to various DNA damaging agents

As mentioned above, several publications characterising ChlR1 mutations in WBS patient cell lines have suggested a role for ChlR1 in the DNA damage response [191]. Patient derived cell lines were shown to have sensitivity to a variety of DNA damaging agents including the DNA crosslinking agent mitomycin-C (MMC) and topoisomerase inhibitor camptothecin (CPT) as well as a slight sensitivity to ionising radiation (IR) [139]. Additionally, Noguchi and colleagues have recently shown that ChlR1 has a role in recovery from replication stress and that ChlR1 deficient HeLa cells appear to be sensitive to the effects of interstrand crosslinking agent cisplatin [178].

In order to further understand the role of ChlR1 in the cellular response to DNA damage, ChlR1 was first depleted in hTERT-RPE1 cells using a specific siRNA targeting the 3' UTR of the ChlR1 transcript. Cells were transfected with either ChlR1 specific siRNA or a commercially available non-targetting siRNA as a control. The western blot in **figure 4.1** confirms the successful knockdown of ChlR1 at the protein level. β-actin serves as a loading control.

Using the standard nucleofection protocol for the siRNA knockdown of ChlR1 described in the methods section, a >90% reduction in ChlR1 protein level was consistently achieved. **Figure 4.1** represents a typical result of a siRNA knockdown experiment.

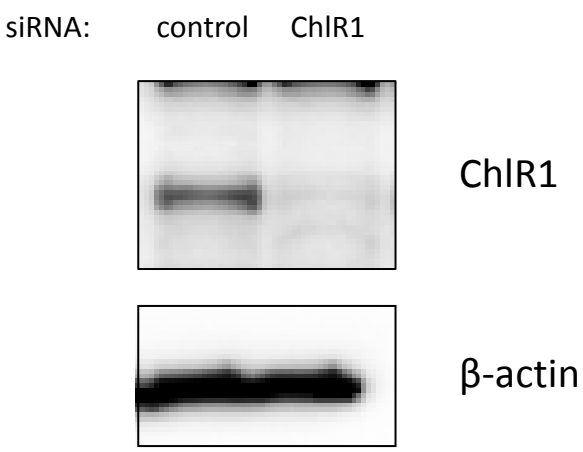

Figure 4.1. Western blot of hTERT-RPE1 cell lysate showing siRNA knock down of endogenous ChlR1. Cells were transfected with either ChlR1 specific siRNA or a non-targetting control oligo. 20ug of total protein was loaded in each lane as determined by Bradford assay. Lysates were probed with the indicated antibodies.

To determine the sensitivity of ChlR1 depleted cells to various DNA damaging agents, two different methods were used to assay cell survival. The first method employed was the cck-8 cell viability assay (Dojindo Molecular Technologies) which measures the reduction of a water soluble tetrazolium salt to an orange coloured formazen compound, a reaction which is mediated by cellular dehydrogenase enzymes. This colour change can then be measured and used to determine cell viability or survival.

Graphs plotting cell survival for ChlR1 depleted cells versus control cells following treatment with several DNA damaging agents are shown in **figure 4.2**. Although Van der Lilij et al showed that the WBS patient cells were sensitive to camptothecin, in our knockdown system there was little difference in cell survival between the control and the ChlR1 knockdown except at the lowest dose (**figure 4.2A**). The overall trend does suggest that the ChlR1 depleted cells are more sensitive; however the large error bars reflect the high level of variability within this particular experiment. It is also possible that the doses of CPT used in this experiment were too high and may have had an effect on the accuracy of the readings at the higher doses. Interestingly, a recent study has shown that lower doses of CPT, while still inducing replication fork stalling, can lead to lesions which resolve by fork regression without the need for activation of the double strand break repair pathway. As it appears that ChlR1 depleted cells may be more sensitive to CPT than control cells at the lower doses, a role for ChlR1 in replication fork stability or in the resolution of replication coupled DNA damage could be supported.

ChlR1-depleted cells showed no significant sensitivity to either ionising radiation or to the replication inhibitor hydroxyurea (HU) compared with control siRNA treated cells using this assay (**figure 4.2B and C**). In order to consolidate these results, the more traditional colony formation assay was also employed. In this case, HeLa cells were substituted for hTERT-RPE1 cells as the latter lack the ability to form colonies.

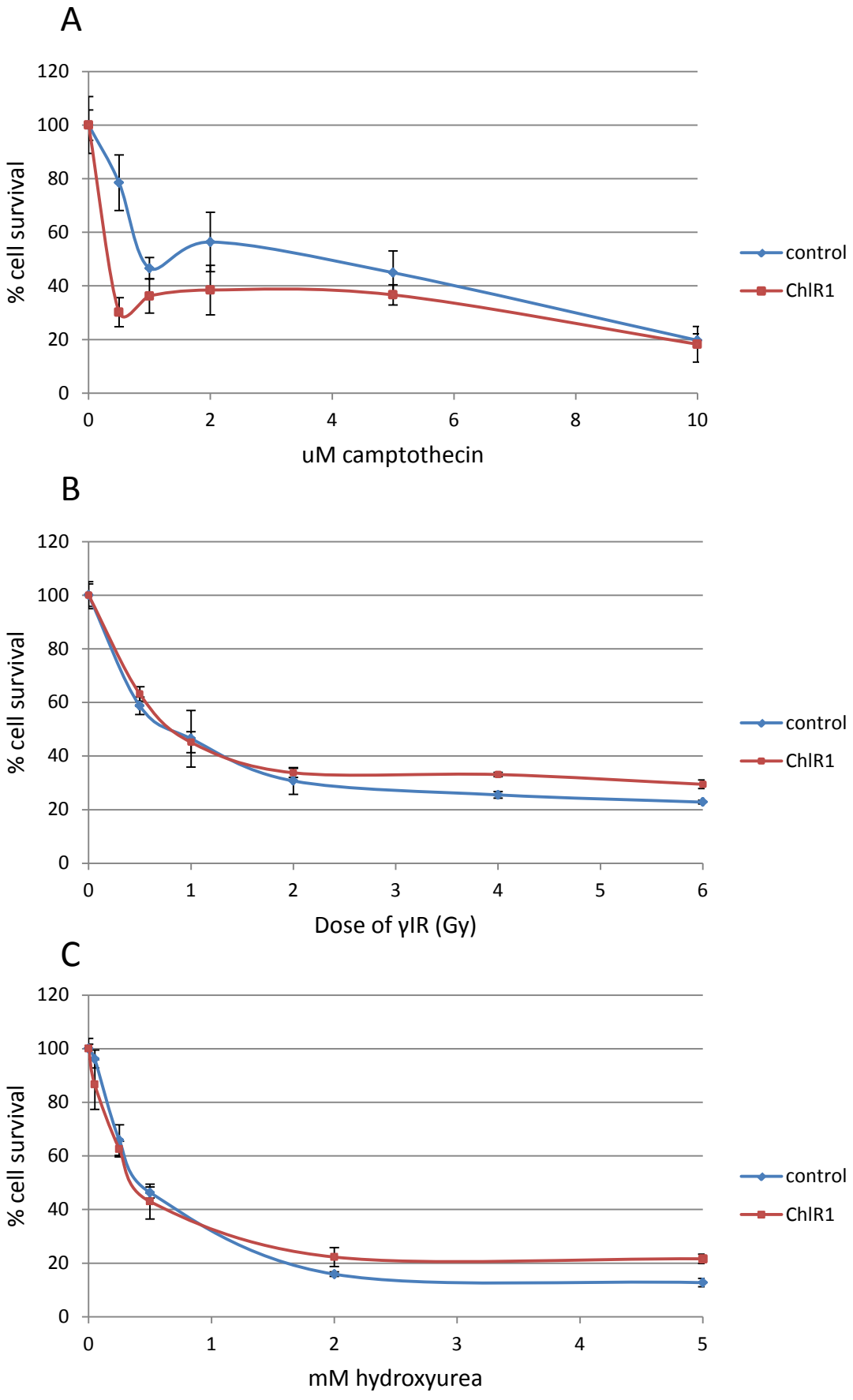
A
120
100
80
60
40
20
0
% cell survival
0
2
4
6
8
10
uM camptothecin
control
ChlR1
B
120
100
80
60
40
20
0
% cell survival
0
1
2
3
4
5
6
Dose of γIR (Gy)
control
ChlR1
C
120
100
80
60
40
20
0
% cell survival
0
1
2
3
4
5
mM hydroxyurea
control
ChlR1

Figure 4.2. Graphs showing cell survival of ChlR1 depleted HTERT-RPE1 cells versus control siRNA treated cells. Cells were treated with increasing doses of the indicated DNA damaging agent and assayed using using the cck-8 cell viability assay as described in the methods section. Cells were treated with (A) camptothecin, 3 hour drug treatment followed by 2 washes (B) ionising radiation and (C) hydroxyurea, 24 hour drug treatment followed by 2 washes. Following the drug treatments, cells were incubated for 72 hours before the assay was performed. Each graph represents a single representative experiment performed in triplicate with error bars representing +/- SEM. Each experiment was independently carried out at least twice.

Figure 4.3 shows graphs of cell survival as determined by the colony forming ability of either ChlR1 depleted or control cells treated with the indicated DNA damaging agents. The data from the colony formation experiments largely corroborated the previous data using the cck-8 assay. A treatment with mitomycin-C was included in these experiments in order to determine whether siRNA-mediated reduced expression of ChlR1 results in the same sensitivity to DNA crosslinking agents that had been previously reported in the patient-derived cells. The data generated from the colony survival assays strongly suggested that in fact, ChlR1-depleted HeLa cells were not sensitive to mitomycin-C (**figure 4.3A**). Additionally, no significant sensitivity to camptothecin was observed and only a very subtle sensitivity to higher doses of hydroxyurea (**figures 4.3B and C**) was apparent using this assay.

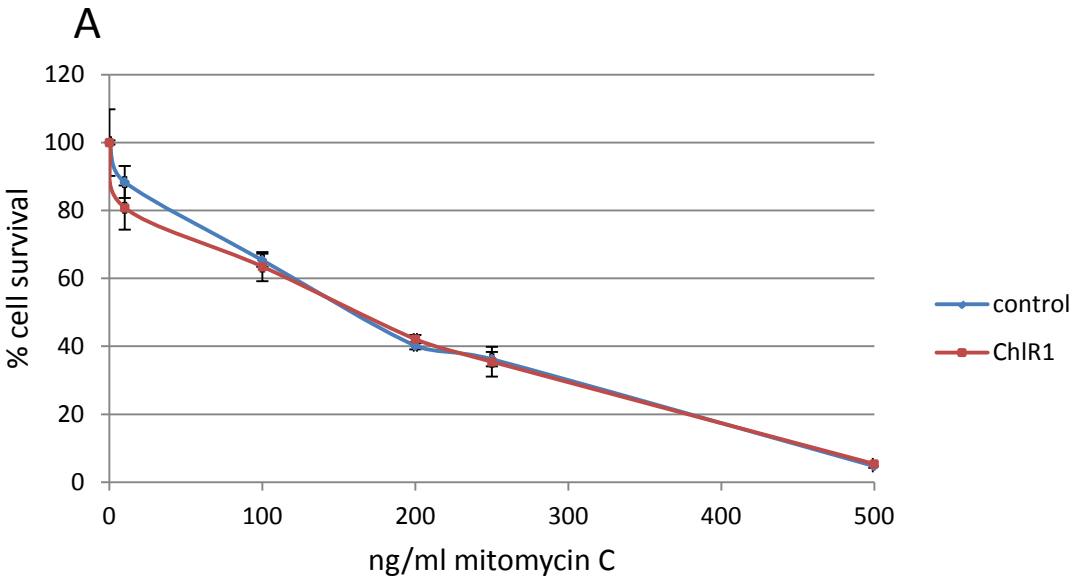
A
120
100
80
60
40
20
0
% cell survival
0
100
200
300
400
500
ng/ml mitomycin C
control
ChlR1

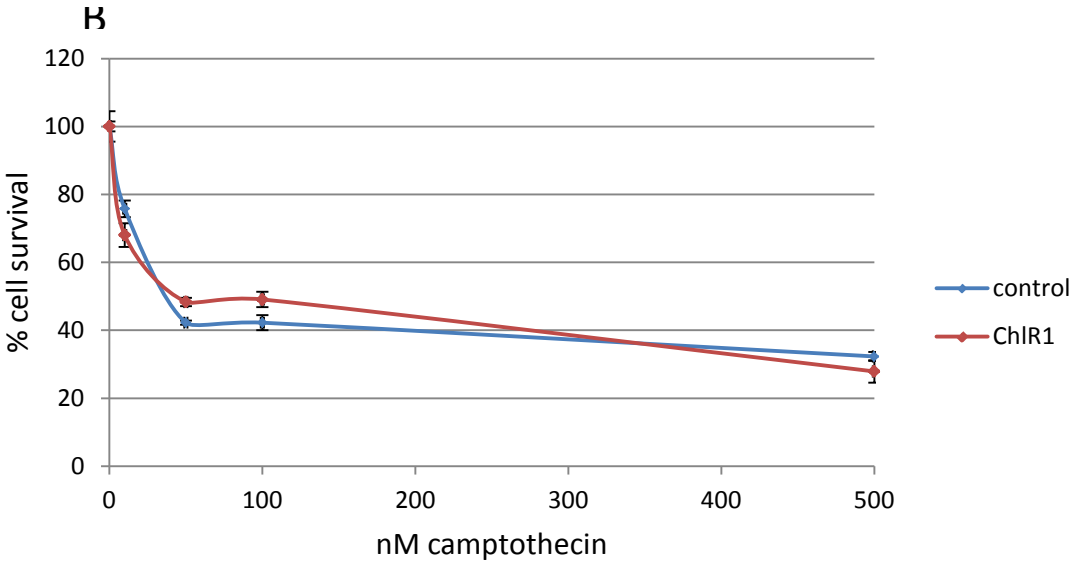
B
120
100
80
60
40
20
0
% cell survival
0
100
200
300
400
500
nM camptothecin
control
ChlR1

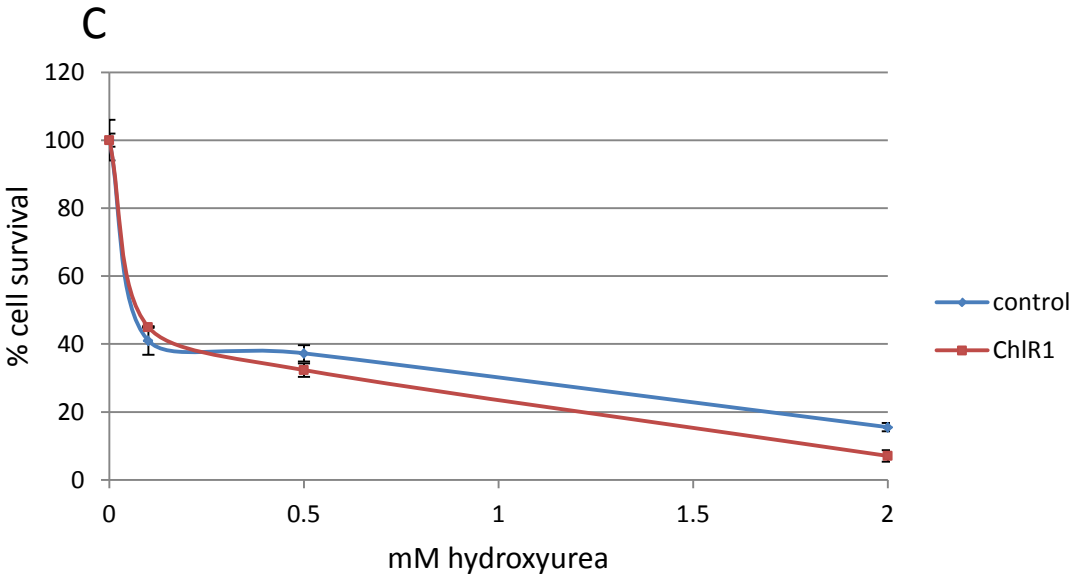
C
120
100
80
60
40
20
0
% cell survival
0
0.5
1
1.5
2
mM hydroxyurea
control
ChlR1

Figure 4.3. Graphs showing cell survival of ChlR1 depleted HeLa cells versus control siRNA treated cells. Cells were treated with increasing doses of the indicated DNA damaging agent and assayed for their ability to subsequently form colonies. Colonies were stained and counted 10 days post-treatment. Cells were treated with (A) mitomycin-C for 3 hours (B) camptothecin for 3 hours and (C) hydroxyurea for 24 hours. Each graph represents a single representative experiment performed in triplicate with error bars representing +/- SEM. Each experiment was independently carried out at least twice.

Taken collectively, the results described in **figures 4.2** and **4.3**, suggest that at best ChlR1-depleted cells show only a very slight sensitivity to any of the DNA damaging agents used in these cell survival assays. Unfortunately, this does little to shed further light on the potential role of ChlR1 in the DNA damage response. However, although ChlR1 depleted cells do not appear particularly sensitive to any of the specific cytotoxic agents that have thus far been tested, this does not necessarily preclude a role for ChlR1 in the response to DNA damage or replication stress. For example cells lacking ChlR1 may utilise alternative pathways under conditions of stress that result in no visible reduction in viability. Additionally, it should be noted that the majority of previous cell survival data has been generated using primary patient-derived cells which may behave differently to our knock-down system.

4.2 ChlR1 depleted cells are less efficient at repairing damaged DNA after exposure to ionising radiation

To further analyse the potential role of ChlR1 in the DNA damage response, the alkaline comet assay, or single cell gel electrophoresis as it is sometimes known, was used to determine whether ChlR1 cells could effectively repair IR-induced DNA damage. From the data above, ChlR1 depleted cells showed no sensitivity to IR which correlates with published data showing patient-derived cells also showed only a slight sensitivity to this type of DNA damage. However, the comet assay directly quantifies the amount of damage present in a single cell, offering a much clearer insight into the kinetics of the DNA repair process when compared with cell viability assays alone. The hypothesis being that ChlR1 deficient cells could still have a DNA repair defect that does not necessarily lead to a reduction in viability.

The comet assay or single cell gel electrophoresis assay is used to detect fragmented DNA in individual cells by subjecting the cells to electrophoresis to draw the fragmented, damaged DNA out of the nuclei resulting in a distinctive 'comet' tail when stained and visualized. The larger the percentage of DNA in the comet tail the more fragmented DNA has migrated from the nucleus and the greater the amount of damage. If cells are allowed to recover in growth medium after damage has been induced it is possible to measure the extent of the recovery and to determine the efficiency of repair in control versus ChlR1-depleted cells.

Previous data generated in the Parish lab had suggested that ChlR1-depleted HeLa cells were less efficient in their ability to repair IR-induced DNA damage (C.Wasson, unpublished data). To confirm this HeLa cells were nucleofected with either non-targeting or ChlR1 specific siRNA and harvested 72 hours post-transfection. Briefly, cells were immobilised on a microscope slide in a thin layer of low melting temperature agarose prior to irradiation. Cells were then allowed to recover in growth medium for the indicated times post-damage before being subjected to single cell gel electrophoresis as described. **Figure 4.4A** shows representative images of cells that are either undamaged or cells subjected to 5gy of γ irradiation. The characteristic 'comet' tail is visible in the damaged cells and is composed of fragmented, damaged DNA which migrates from the nucleus during electrophoresis and can be quantified using specialist software. **Figure 4.4B** is a screen shot of a cell which has been scored by the software. For simplicity, the measurement of comet head intensity will be used throughout to express the % of undamaged DNA in a cell.

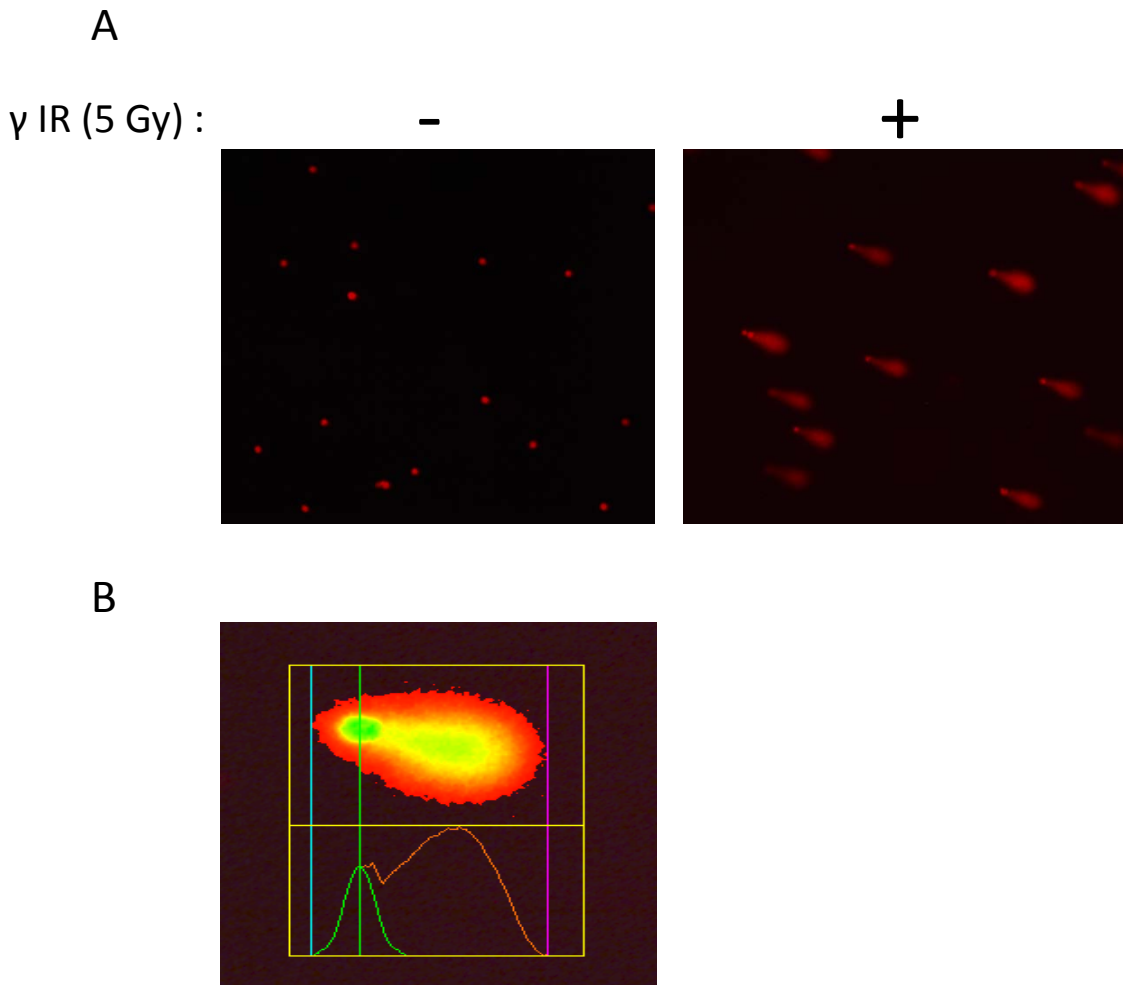

Figure 4.4. Representative epifluorescent images of undamaged and irradiated cells after single cell gel electrophoresis. The DNA has been stained with propidium iodide for visualisation (A). (B) is an example of a cell which has been scored by the Comet IV software with the green peak corresponding to head intensity while the red peak represents tail intensity.

HeLa cells that are depleted for ChlR1 show an impaired capacity to repair the damage induced by IR compared with cells transfected with the control siRNA (**figure 4.5**). **Figures 4.5A** and **4.5B** represent two independent experiments each showing the same trend. The average head intensity of 100 cells is plotted for each sample. In agreement with data previously obtained in the Parish Lab (Wasson, Parish unpublished), the data indicate that the ChlR1 deficient cells are less efficient at repairing the DNA damage. However, after 3 hours recovery the ChlR1 depleted cells do seem to have reached the same level of repair as the control cells suggesting that there is a delay in repair rather than an inability to recover. This could explain why very little sensitivity is observed in the cell survival assays.

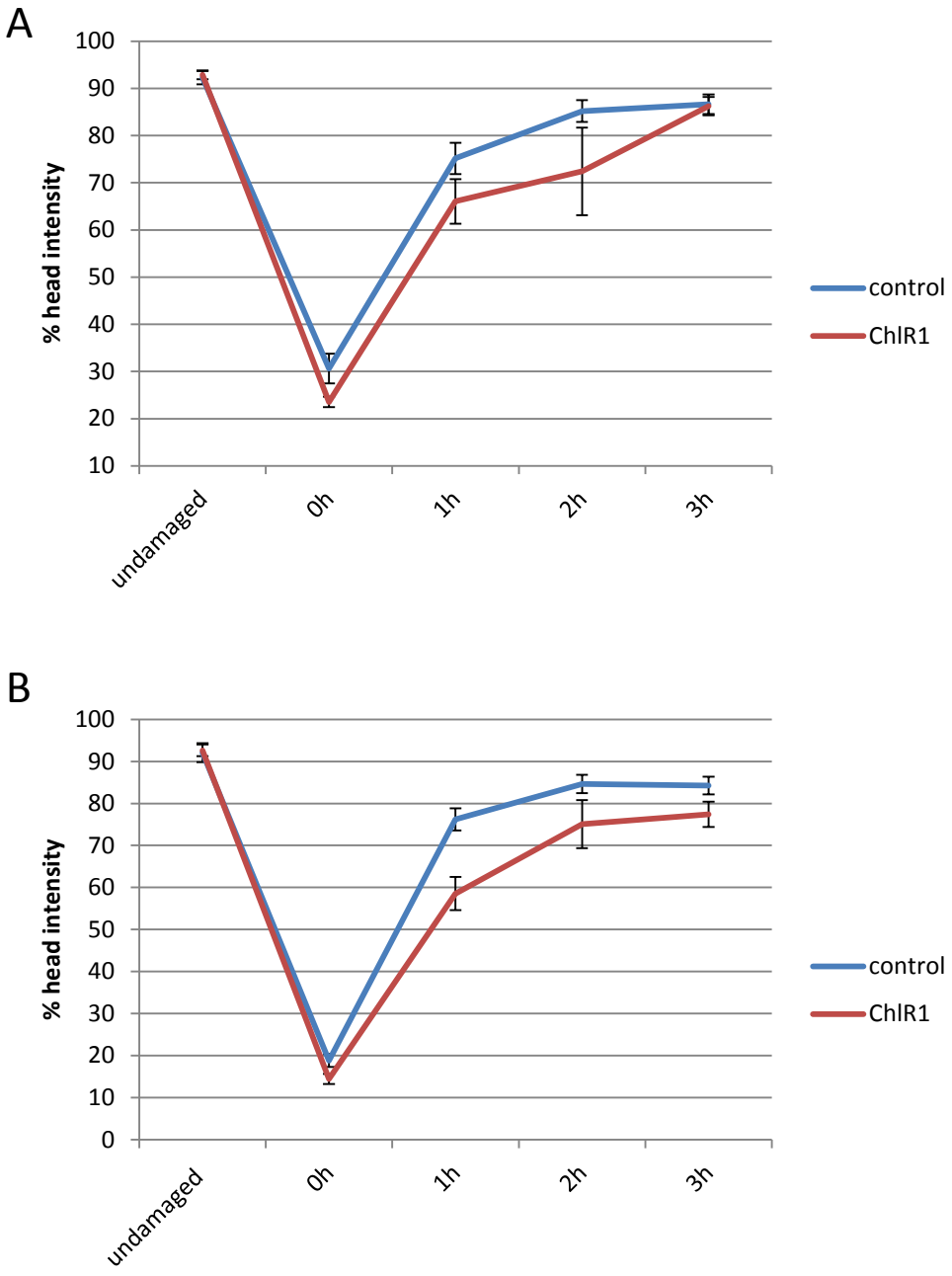

Figure 4.5. Alkaline comet assay performed on HeLa cells damaged with 5gy γ-radiation. Data is plotted as percentage of DNA remaining in the 'head' or nucleus after electrophoresis. 100 nuclei were scored per time point. Error bars represent 95% confidence intervals. A and B are the results of two independent experiments.

This repair defect, while not as prominent, was recapitulated to some extent in hTERT-RPE1 cells (**Figure 4.6A and 4.6B**). The statistical significance varied between experiments and therefore in the hTERT-RPE1 cells the data supporting a repair defect in ChlR1 depleted cells was less convincing. Two representative experiments are shown in **figure 4.6A** and **4.6B.** The discrepancy in the results between the two cell types could be attributed to hTERT-RPE1 cells being representative of a more 'normal' cell type that may be able to repair the damage more efficiently than HeLa cells in the absence of ChlR1. To achieve the same level of damage in the hTERT-RPE1 cells 10gy of IR was required which suggests a general increased tolerance to IR compared with HeLa cells. HeLa cells are a well-established cancer-derived cell line and as such it is possible that these cells harbor additional mutations in other proteins involved in the DNA damage response which exacerbates the effect of ChlR1 depletion.

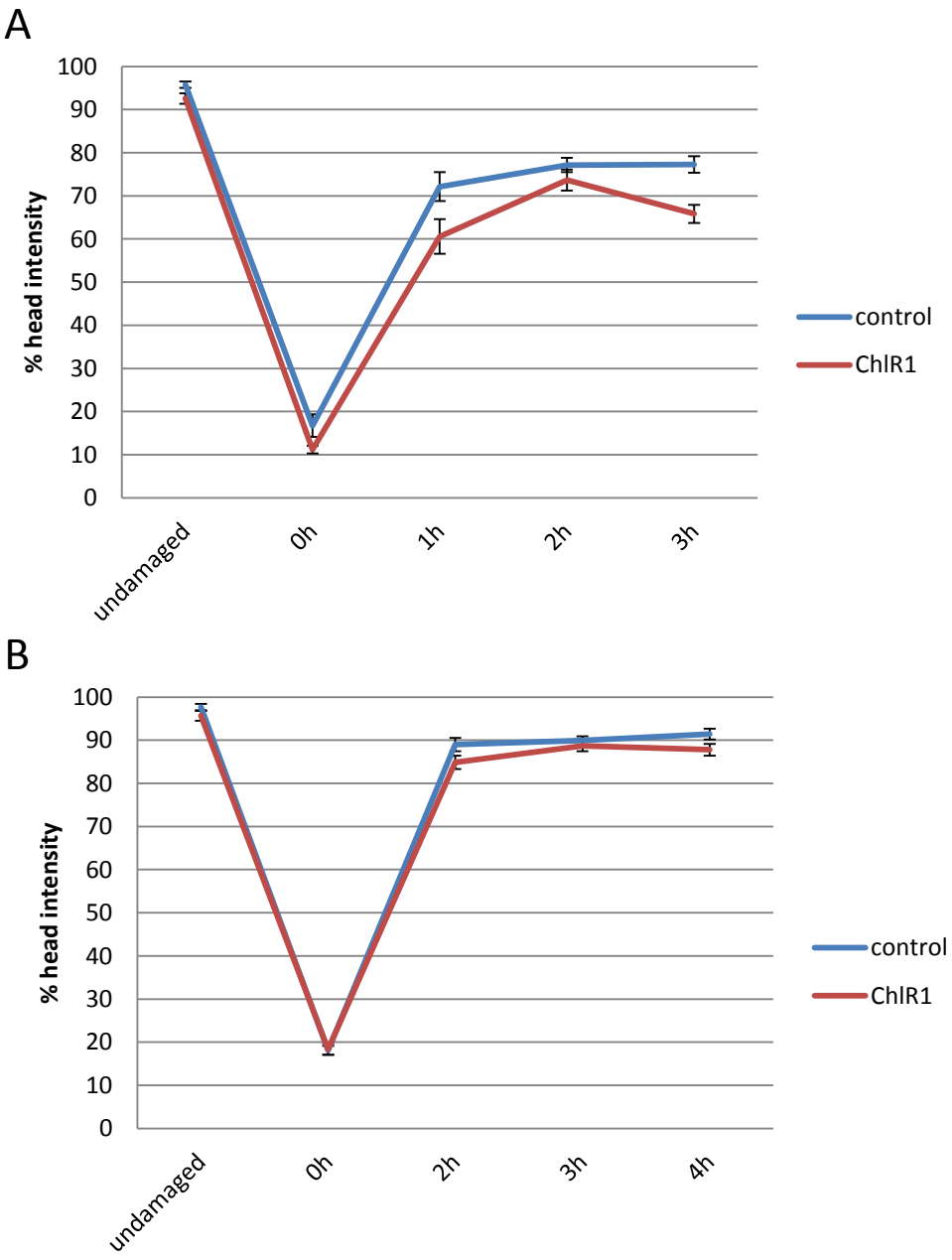

Figure 4.6. Alkaline comet assay performed on hTERT-RPE1 cells damaged with 10gy γ-radiation. Data is plotted as percentage of DNA remaining in the 'head' or nucleus after electrophoresis. 100 nuclei were scored per time point. Error bars represent 95% confidence intervals. A and B represent two independent experiments with a later 4 hour time point substituted for the 1 hour time point in experiment B.

It was hypothesised that in order to see a more dramatic effect of ChlR1-depletion in hTERT-RPE1 cells it might be necessary to look at earlier time points since the results in **figure 4.6A** show that the most significant difference is observed at the 1 hour time point. If ChlR1 functions early on in the damage response any difference might then be more evident (**figure 4.7).** In this instance no statistically significant difference between control and ChlR1-depleted cells was observed although the data did follow the general trend of a slightly poorer efficiency of repair in the ChlR1 knock down cells.

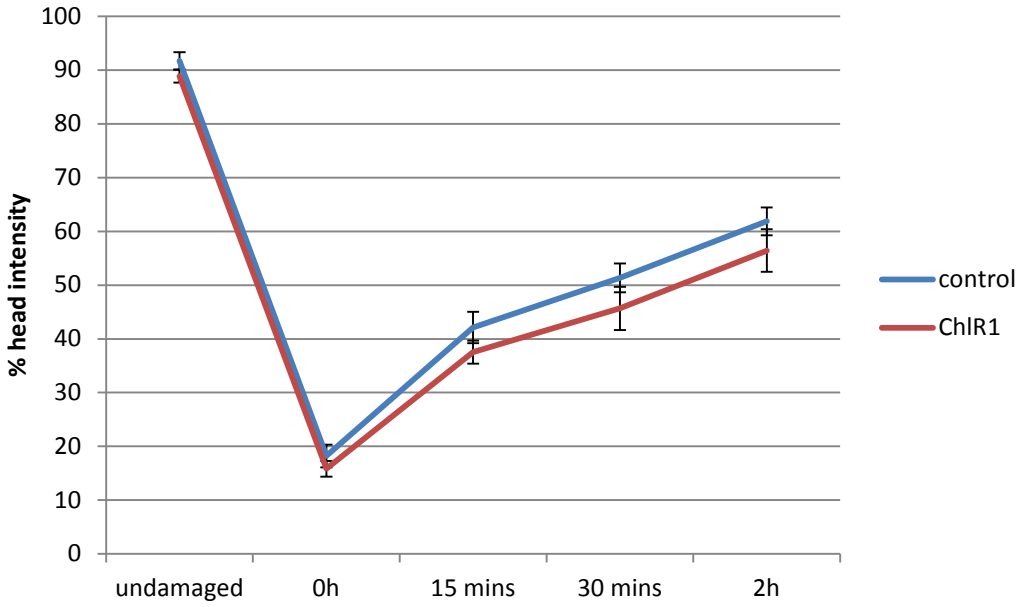

Figure 4.7. Alkaline comet assay performed on hTERT-RPE1 cells damaged with 10gy γ-radiation. Data is plotted as percentage of DNA remaining in the 'head' or nucleus after electrophoresis. 100 nuclei were scored per time point. Error bars represent 95% confidence intervals. Cells were analysed at shorter intervals post-recovery in this experiment. The graph shown is representative of two independent experiments.

Evidence has suggested that ChlR1 may have a role in DNA replication and work in the Parish lab has shown that ChlR1 deficient cells are less able to restart stalled replication forks when cells are treated with hydroxyurea (K. Feeney, unpublished). It was therefore proposed that ChlR1 function may be specific to damage encountered during DNA replication, for example, it might be involved in the resolution of stalled forks and/or prevention of the collapse of these forks into double strand breaks. To determine whether cells in S-phase were more susceptible to the effect of ChlR1 depletion, hTERT-RPE1 cells were synchronized using the double thymidine block method. The cells were then released into S-phase prior to inducing damage and performing the comet assay (**Figure 4.8**). Results indicated no significant difference between the control and ChlR1-deficient cells in an S-phase synchronized population.

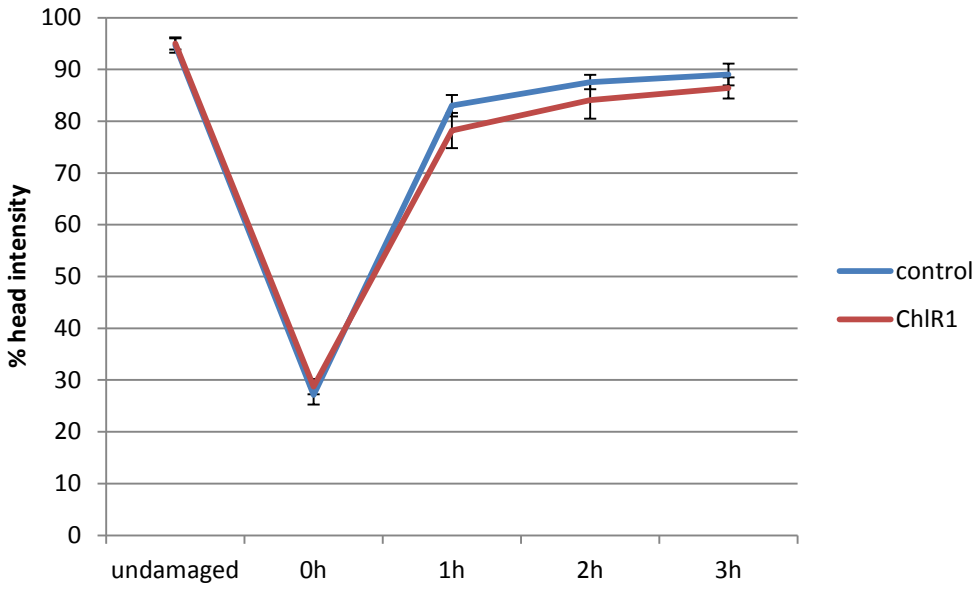

Figure 4.8. Alkaline comet assay performed on hTERT-RPE1 cells synchronised in S-phase and damaged with 10gy γ-radiation. Data is plotted as percentage of DNA remaining in the 'head' or nucleus after electrophoresis. 100 nuclei were scored per time point. Error bars represent 95% confidence intervals. The graph shown is representative of two independent experiments.

4.3 G2 checkpoint remains intact in cells treated with ChlR1 siRNA

Following the observation of a DNA repair defect in response to IR, assessment of the IR-induced G2 checkpoint function in ChlR1 depleted cells was carried out. Under normal circumstances, cells exposed to ionising radiation will arrest at G2 to allow for the damage to be repaired which prevents cells entering mitosis with unrepaired DNA damage, subsequently contributing to genomic instability. It was thought that if ChlR1-depleted cells fail to activate this checkpoint and progress through mitosis without efficient repair of the damage, this could partially explain the genomic instability observed in ChlR1

deficient cells. To assess G2 checkpoint activation, hTERT-RPE1 cells were damaged with 3 Gy of γ-IR and then harvested at the indicated time points post-irradiation. Cells were fixed and stained with an Alexa488 conjugated antibody against phosphorylated histone 3, a marker of mitotic cells, before being subjected to analysis by flow cytometry and the percentage mitotic cells determined (**Table 3**). As expected, following exposure to ionising radiation the control cells exhibited an arrest at G2 as indicated by the drop in the number of cells progressing to mitosis. There was no significant difference observed between control cells and cells treated with ChlR1 siRNA in terms of mitotic entry across two independent experiments, which suggests that the IR-induced G2 checkpoint remains intact in ChlR1 depleted cells.

	% mitotic cells			
	Experiment 1		Experiment 2	
	Control siRNA	ChlR1 siRNA	Control siRNA	ChlR1 siRNA
Untreated	1.97	1.85	1.43	1.05
4h post-IR	0.023	0.002	0.003	0.006
8h post-IR	0.5	0.73	0.46	0.43
10h post-IR	0.62	0.6	0.43	0.42

Table 3. The percentage of mitotic cells in control siRNA treated hTERT-RPE1 cells versus ChlR1 depleted cells as determined by flow cytometric analysis. Phospho-H3 positive cells were gated and expressed as a percentage of the total cell population.

Approximately 30000 events were counted per condition. The data is representative of three independent experiments.

4.4 ChlR1 depleted cells show an increased level of DNA damage in response to treatment with the replication inhibitor hydroxyurea

Data generated in the Parish lab by K. Feeney has shown using DNA fibre analysis that while ChlR1-depleted hTERT-RPE1 cells progress normally through the cell cycle with no S-phase delay, these cells have a significantly reduced replication fork speed when compared to controls. These cells also show an impaired ability to restart replication after induction of fork stalling by treatment with hydroxyurea (K. Feeney, unpublished). While data from the comet assays in **figures 4.5-4.8** indicates a mild repair defect in response to ionizing radiation, it is possible that the primary role of ChlR1 is in the repair of replication-coupled DNA damage or in the promotion of replication fork stability under conditions of replication stress. To investigate this, the comet assay was performed on ChlR1-depleted cells which had been treated for 2 hours with 2mM hydroxyurea to inhibit DNA replication. The results shown in **figure 4.9** suggest that in the ChlR1 depleted cells there is a significant increase in the amount of DNA damage accumulated after exposure to hydroxyurea compared to control siRNA treated cells.

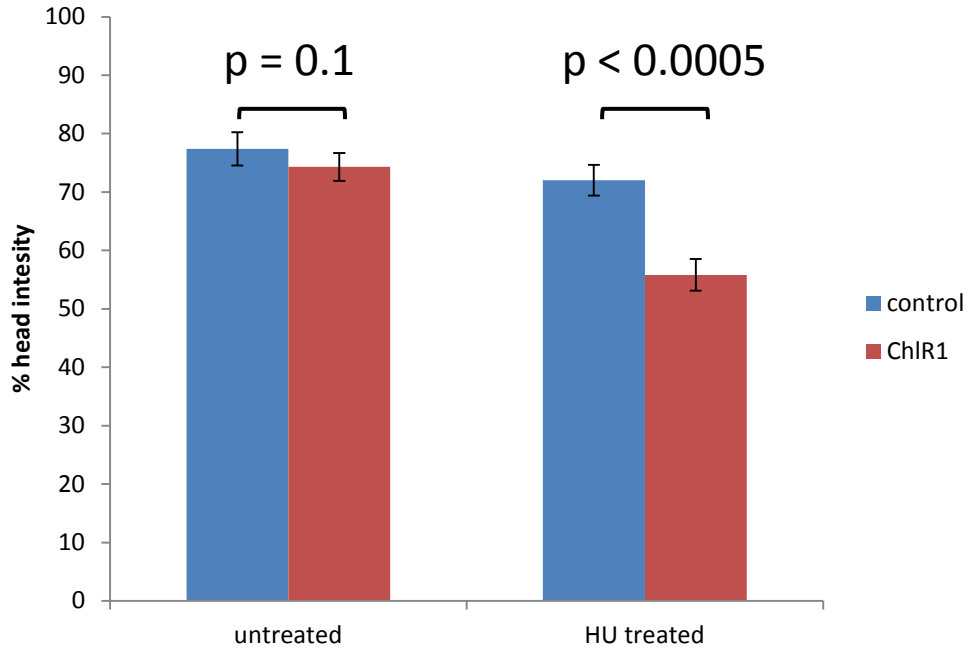

Figure 4.9. Alkaline comet assay performed on hTERT-RPE1 cells treated with 2mM hydroxyurea. Data is plotted as percentage of DNA remaining in the 'head' or nucleus after electrophoresis. 100 nuclei were scored per time point. Statistical significance was determined using a students' T test and the relevant p values indicated on the graph. This experiment was independently repeated twice.

It is worth noting that the alkaline comet assay quantifies all types of DNA damage in a cell including single strand breaks and alkali labile sites in addition to double strand breaks. This is an important consideration when interpreting the results in **figure 4.9** as it cannot be concluded from this data whether the absence of ChlR1 results in more collapsed replication forks or an increase in stalled forks which result in the accumulation of single stranded DNA tracts.

In an attempt to determine whether ChlR1 depletion results in an increase in replication fork collapse leading to DNA double strand breaks following treatment with hydroxyurea, hTERT-RPE1 cells were treated with 2mM HU for 2 hours and then assessed for 53bp1 foci formation, a key marker of double strand break repair. Cells treated with either control or ChlR1 specific siRNA were grown on coverslips, treated with 2mM hydroxyurea for 2 hours and then allowed to recover for either 1, 4 or 8 hours before fixing with 4% paraformaldehyde and staining with the appropriate antibodies for the immunofluorescent (IF) detection of 53bp1. Cells with >10 foci were scored and expressed as a % of the total cells counted (**figure 4.10A**). 150-200 cells were counted for each time point. A representative graph is shown in **figure 4.10B**. This experiment was repeated three times and while the overall trend remained the same, due to significant variation in the actual foci numbers it was not possible to average all the data sets to determine statistical significance.

A

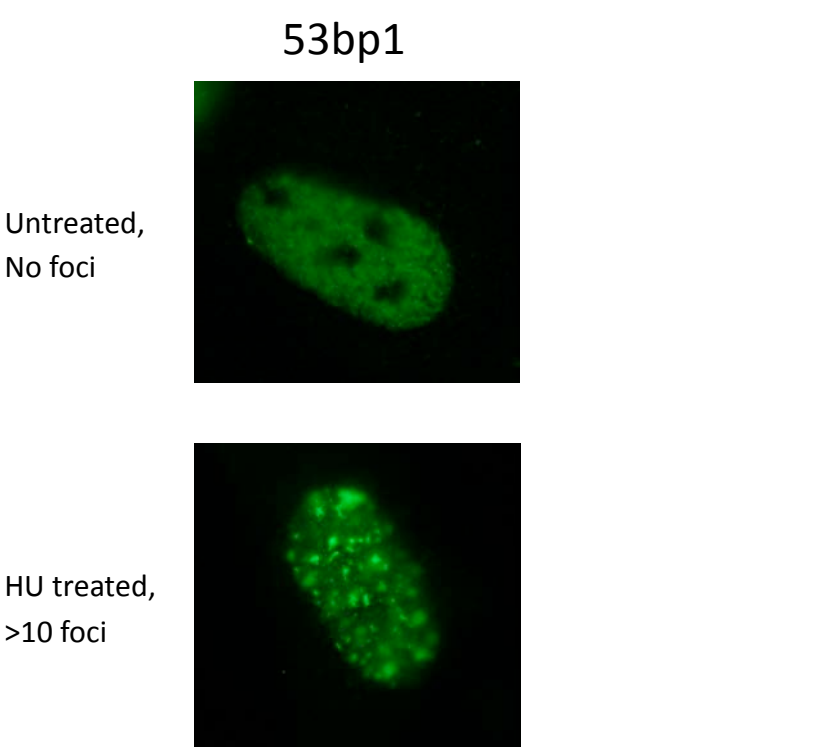
53bp1
Untreated,
No foci
HU treated,
>10 foci

B

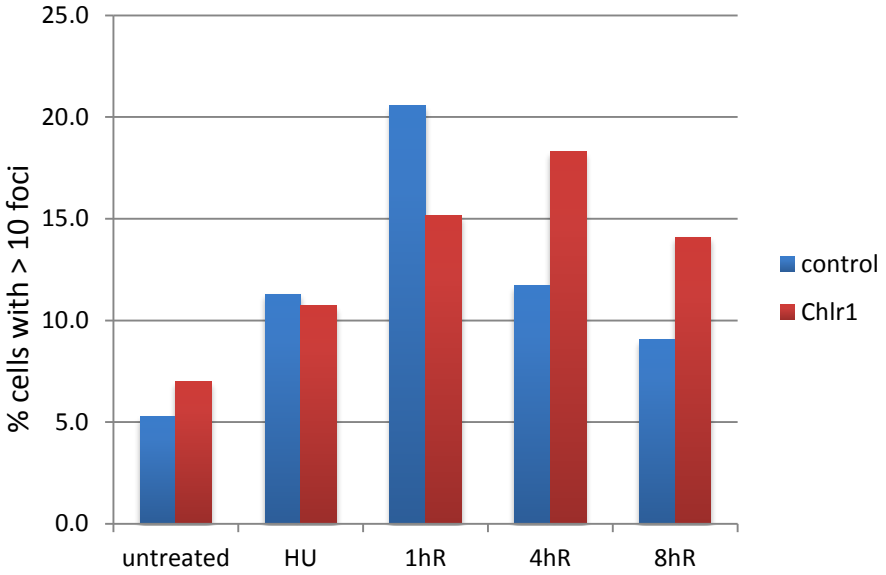
25.0
20.0
15.0
10.0
5.0
0.0
% cells with > 10 foci
untreated
HU
1hR
4hR
8hR
control
Chlr1

Figure 4.10. Representative IF images showing cells stained with anti-53bp1 primary antibody, detected using an Alexa 488 conjugated secondary antibody and imaged by epifluorescent microscopy. Examples of an undamaged cell and a cell with >10 damage induced foci are shown in (A). Cells with >10 foci were scored and expressed as a % of total cells counted (B). 150-200 cells were counted per time point. Cells were either untreated, treated with HU for 2h (HU) or treated, washed and allowed to recover for the indicated times: 1hR, 4hR and 8hR. The histogram shown is representative of three independent experiments.

While the numbers of 53bp1 foci immediately following the 2h HU treatment increase slightly for both the control and the ChlR1 depleted cells, at the 1h post-HU time point there is a considerable increase in foci formation in the controls. While the ChlR1 depleted cells also show elevated foci formation at the 1h time point, the increase is less dramatic. In contrast, after 4h the numbers of foci in the control cells appear to have reduced substantially from the peak observed at 1h, while the ChlR1 depleted cells show a definite increase. By 8h post-HU, there still appears to be an elevated number of foci present in the ChlR1 deficient cells compared to in the controls. This data could indicate a potential delay in the ability of ChlR1 cells to repair double strand breaks; a result which seems to be supported by the previous comet assay data analyzing the capacity of ChlR1 cells to repair IR-induced DNA damage (**figure 4.5**).

It is still unclear from this data however whether or not ChlR1 has a role in replication fork stability. While the increased level of physical damage apparent after HU treatment suggests more stalled or collapsed forks (**figure 4.9**), the 53bp1 foci formation assay seems to indicate that there is also a potential delay in the damage response. There does not seem to be any great overall increase in 53bp1 foci numbers in ChlR1 deficient cells, rather the kinetics of foci formation post-HU treatment would appear to indicate a delay in the DNA

damage response pathway. This is perhaps unsurprising as it is well established that even in the absence of any exogenous stress or damage the most obvious phenotype of ChlR1-deficient cells is their abnormal sister chromatid cohesion. This is likely to have a detrimental impact on homologous recombination; a major pathway for repair of double strand breaks in late S-phase and G2.

4.5 ChlR1 depleted cells are sensitive to hydroxyurea-induced replication fork stalling

Mono-ubiquitination of PCNA by the Rad18 ubiquitin ligase occurs in response to DNA damage or stalled replication. This mono-ubiquitination activates the translesion synthesis pathway (TLS) responsible for bypassing lesions caused by damaged DNA via recruitment of specialised low-fidelity DNA polymerases [30, 86, 192-195]. While it is widely acknowledged that PCNA becomes ubiquitinated in response to hydroxyurea treatment, the absence of any physical lesion to bypass this has meant that the role of PCNA mono-ubiquitation during this type of replication stress is less well understood. It is possible that the stalled replication machinery itself acts as an obstacle and the ubiquitination of PCNA acts to recruit proteins responsible either for its subsequent removal to allow repair of the lesion or for the promotion of fork restart.

While it is still unclear whether ChlR1 depletion leads to decreased replication fork stability, western blot analysis of chromatin-associated PCNA indicates a distinct increase in the levels of mono-ubiquitinated protein after treatment with HU which is amplified in the ChlR1 depleted cells (**figure 11**). Additionally, while the levels of total PCNA remain relatively constant, there is a reduction in the amount of chromatin bound PCNA following HU treatment which is again more apparent in the ChlR1 depleted cells versus the

controls. Both the increased ubiquitination and reduction of the chromatin bound fraction of PCNA is to be expected following stalled replication and the fact that both of these phenotypes are exacerbated in the ChlR1 knockdown suggest that these cells are more sensitive to hydroxyurea induced replication stress. Sustained PCNA ubiquitination after release from HU treatment is also evident in ChlR1-depleted cells compared to controls again suggesting a deficiency in the ability of these cells to repair the damage caused by replication stalling.

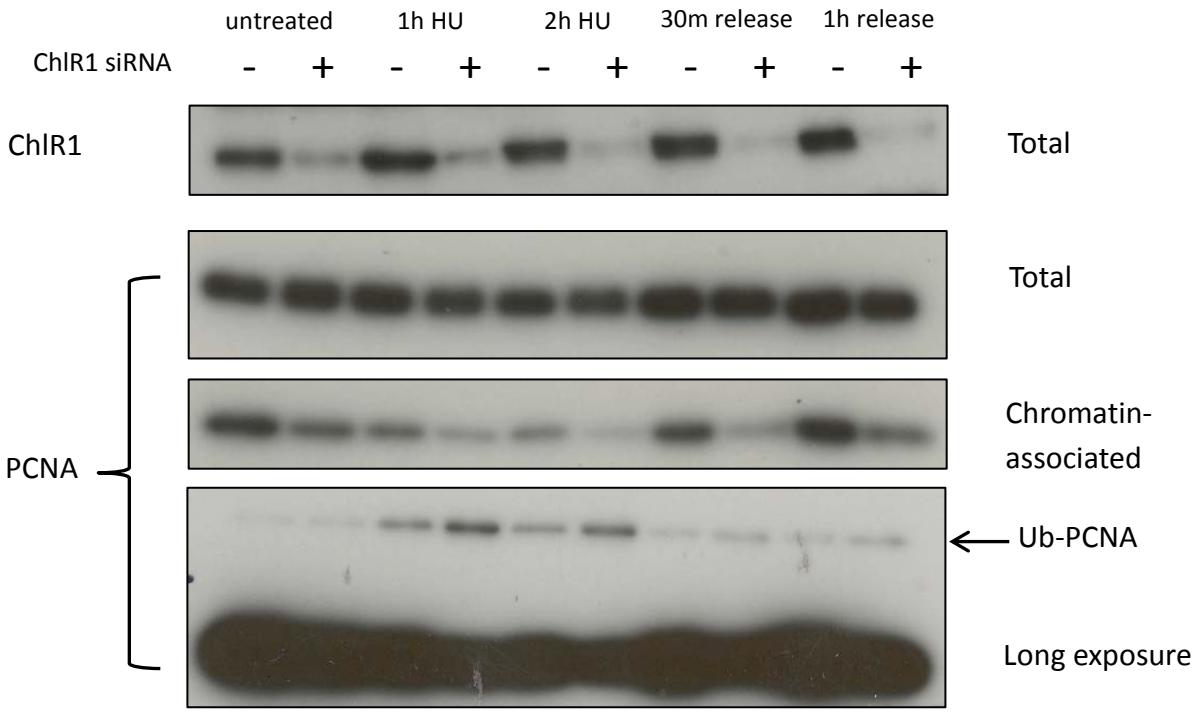

Figure 4.11. Western blot indicating an increase in mono-ubiquitinated PCNA in hTERT-RPE1 cells that have been transfected with ChlR1-specific siRNA compared with cells transfected with control siRNA. Cells were treated with 2mM HU for 1 or 2 hours or then washed and released for the times indicated. The top two panels show total protein while the bottom two panels show just the chromatin associated fraction. The western blot shown is representative of at least three independent experiments.

In addition to ubiquitination of PCNA another marker of stalled replication is an accumulation of RPA-coated single stranded DNA. This can be visualised by immunofluorescence as discrete nuclear foci which become apparent after exposure to DNA damaging agents or agents that cause replication stress. Control or ChlR1-depleted cells were grown on coverslips and treated for 2 hours with 2mM HU before fixing and staining with an antibody specific to RPA34 subunit of the RPA complex. Cells were scored as foci-positive if they contained more than 10 discrete RPA foci present in the nucleus. **Figure 4.12A** shows representative images of an untreated cell and an RPA positive cell following hydroxyurea treatment. The percentage of RPA positive cells was quantified in the control and the ChlR1-depleted samples before and after hydroxyurea treatment and the results are shown in **figure 4.12B.** The data indicates that there are an increased number of RPA positive cells in the ChlR1-depleted cells. Furthermore, sub-cellular fractionation was performed on cells subjected to the same hydroxyurea treatment and the chromatin associated fraction was isolated and probed with an anti-RPA34 antibody as an alternative method of quantifying the chromatin bound fraction of cellular RPA. The western blot is shown in **figure 4.12C.** It is evident that there is more chromatin-associated RPA in the ChlR1 depleted cell compared to the controls which further corroborates the hypothesis that ChlR1 deficient cells are more sensitive to replication fork stalling in the presence of hydroxyurea. From the western blot data it also looks like after 1 hour release from hydroxyurea, ChlR1 depleted cell have recovered from the replication stalling to a level comparable to control cells. This also concurs with the immunofluorescence foci data and suggests that while the cells seem more sensitive to fork stalling they may still be able to eventually restart the stalled fork or to resolve the damage induced by fork stalling. If this were the case it would be assumed that the intra S-phase replication checkpoint is likely to be activated normally in these cells.

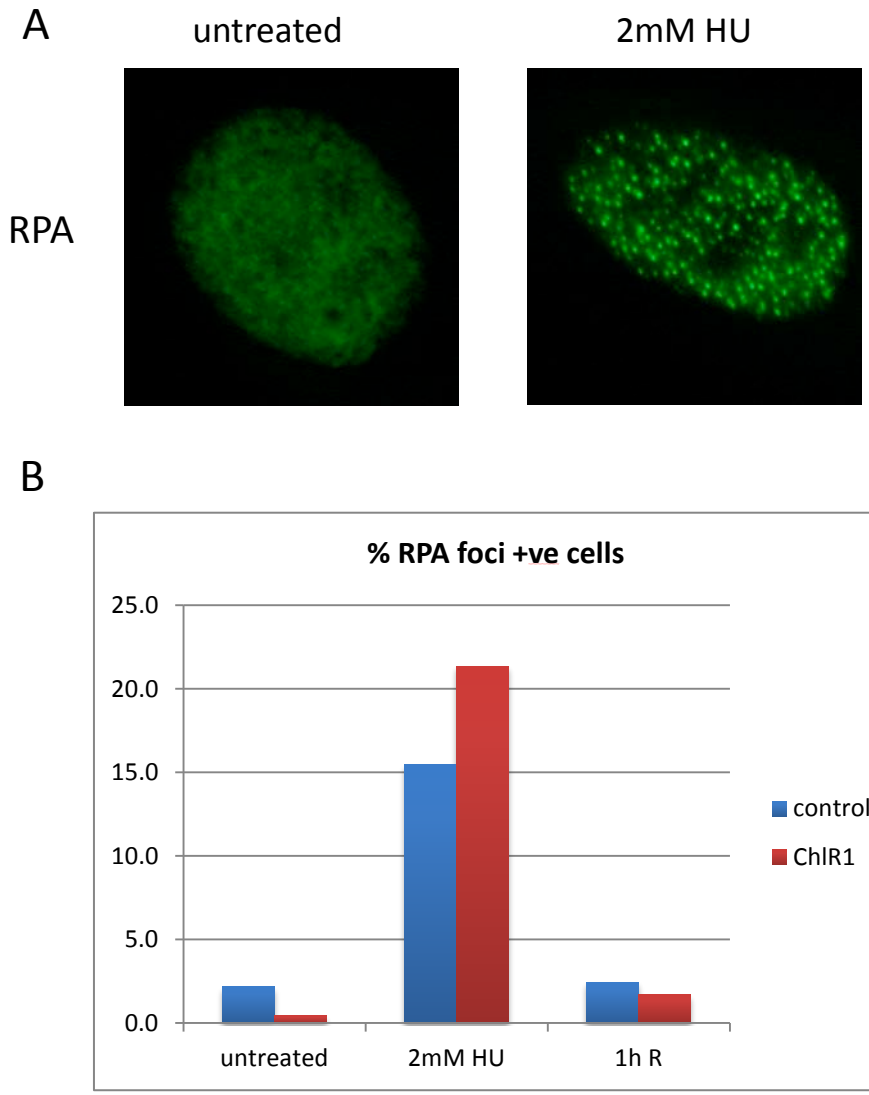
A
untreated
2mM HU
RPA
B
% RPA foci +ve cells
25.0
20.0
15.0
10.0
5.0
0.0
untreated
2mM HU
1h R
control
ChlR1
C
untreated
1h HU
2h HU
30m release
1h release
ChlR1 siRNA
- + - + - + - + - +
RPA
H3

Figure 4.12. (A) Representative immunofluorescent image of a nucleus stained with anti-RPA32 antibody, followed by an Alexa 488 coupled secondary antibody for detection. Top image shows an untreated foci-negative cell with diffuse nuclear staining while the bottom image shows a foci-positive cell following 2mM HU treatment for 2 hours (B) Quantification of foci positive cells in either untreated, hydroxyurea treated or hydroxyurea treated cells that were allowed to recover for 1 hour. 200 cells were counted per condition and the graph shown is representative of two independent experiments (C) Western blot showing the chromatin associated fraction of RPA in hTERT-RPE1 cells treated with hydroxyurea for the indicated time points. Histone 3 (H3) is shown as a loading control.

4.6 Checkpoint activation and cell cycle progression is normal in ChlR1 depleted cells that have been exposed to replication stress

Previous work in the Parish lab has shown that in the absence of exogenous stress ChlR1-depleted cells progress normally through the cell cycle despite an observed reduction in replication fork speed. However, it has also been observed that ChlR1-depleted cells are less efficient at restarting stalled replication forks (K. Feeney, unpublished) as well as showing an increase in hydroxyurea-induced DNA damage and an increase in PCNA ubiquitination (**figures 4.9 and 4.11**). It was therefore of interest to determine whether ChlR1 deficient cells were capable of activating the intra-S phase DNA damage checkpoint as efficiently as control cells, thus allowing the cell to effectively repair replication-coupled DNA damage. When replication fork stalling occurs, the single strand DNA binding protein RPA accumulates ahead of the stalled fork and results in activation of the ATR checkpoint pathway. ATR in turn phosphorylates Chk1, the major effector kinase of this pathway. In normal cells, this will trigger cell cycle arrest until the damage can be resolved. **Figure 4.13** shows western blots of hTERT-RPE1 whole cell lysates which have been treated with 2mM HU and allowed to recover for the indicated times. Checkpoint activation was assessed by probing with a phospho-specific antibody for Chk1 at residue serine 345. Activation of the ATM pathway, which is primarily involved in the response to DNA double strand breaks, was also investigated using phosphorylated Chk2 as a read-out. The data suggests that not only does checkpoint activation appear normal upon treatment with HU, it also seems that recovery from the induced replication stress occurs just as efficiently in the ChlR1-depleted cells. This is somewhat at odds with both the increased amount of DNA damage observed in the hydroxyurea comet assay as well as the observed increase in ubiquitinated PCNA.

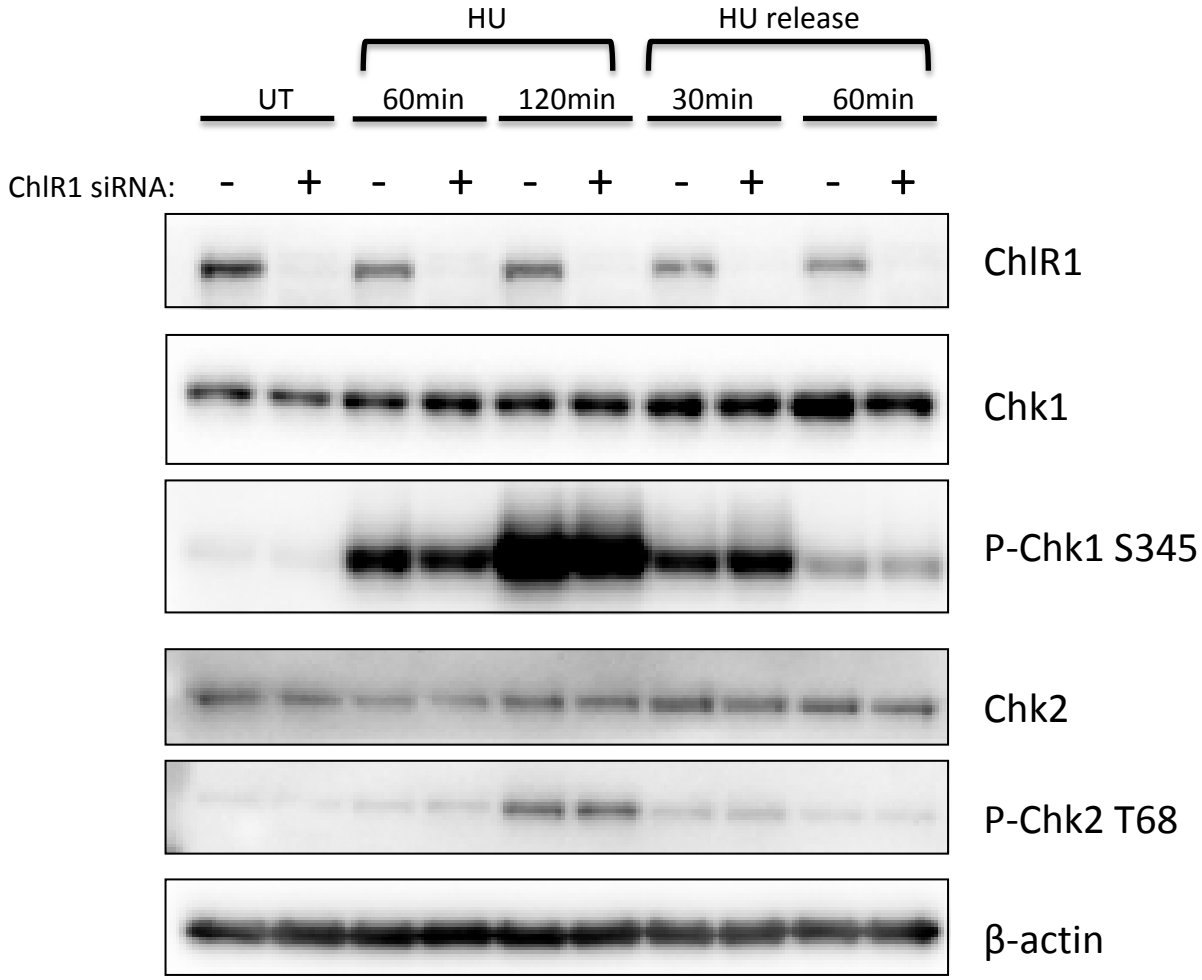

Figure 4.13. Representative western blot showing HU induced checkpoint activation in hTERT-RPE1 cells that have been transfected with ChlR1-specific siRNA compared with cells transfected with control siRNA. Cells were treated with 2mM HU for 1 or 2 hours, then washed and released for the times indicated. Whole cell lysates were probed for both total and phosphorylated forms of the checkpoint proteins Chk1 and Chk2 with β-actin as a loading control. The western blot shown is representative of at least three independent experiments.

To confirm that cell cycle progression and checkpoint activation was normal in ChlR1 depleted cells after induction of replication stress, flow cytometry analysis of DNA content was carried out on cells which had been treated with increasing doses of either hydroxyurea or camptothecin for 24 hours. Both of these agents cause replication stress via different mechanisms. Hydroxyurea acts as an inhibitor of the enzyme ribonucleotide reductase which is involved in dNTP synthesis, thereby depleting the cellular pool of dNTPs available for replication to proceed while camptothecin is a topoisomerase I inhibitor which results is the formation of DNA-topoisomerase covalent complexes that act as a physical block to the replication machinery. Cells were simultaneously treated with nocodazole which prevents spindle formation and thus arrests cells in prometaphase. This allowed analysis of one single cell cycle. The experiment was attempted without the addition of nocodazole but this proved very difficult to analyse, particularly at the lower drug doses, as cells continued to cycle making the interpretation of the data problematic. **Figure 4.14A** shows control and ChlR1 siRNA treated hTERT-RPE1 cells either asynchronously growing or treated with 250ng/ml nocodazole for 24 hours. The graphs of DNA content, as determined by propidium iodide staining, versus cell number indicate that in cells treated with nocodazole only, the same proportion of cells are arrested at G2/M in the control and ChlR1 depleted samples. There is also no difference in relative cell cycle distribution in the asynchronous cells which supports previous data generated in the lab indicating ChlR1 depleted cells show normal cell cycle progression. Following treatment with increasing doses of hydroxyurea for 24 hours (50uM-1mM) both the control and ChlR1 depleted cells show an accumulation of cells in S-phase and eventually in G1 at the higher doses which would be expected as cells arrest following inhibition of replication (**figure 4.14B**). There appears to be little difference between the control RPE1 cells and

ChlR1 depleted cells in this respect which supports the previous western blot data showing that ChlR1 deficient cells have normal checkpoint activation in response to hydroxyurea-induced replication stress (**figure 4.13**). To check whether this also applied to damage induced by camptothecin, which causes a physical lesion that blocks replication and therefore requires resolution and/or repair, the same experiment was carried out using increasing doses of this drug (10nM-500nM). Again, no difference was observed in relative cell cycle distribution between control and ChlR1 depleted cells (**figure 4.14C**). Taken together this would suggest that the intra S-phase replication checkpoint is intact in ChlR1 deficient cells and that additionally these cells do not appear to arrest more readily or be more sensitive to the effects of these drugs, at least in terms of checkpoint response.

A

asynchronous

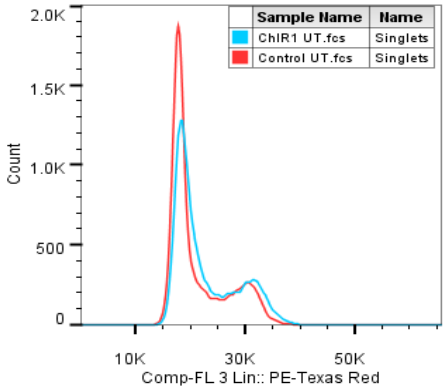

24h nocodazole

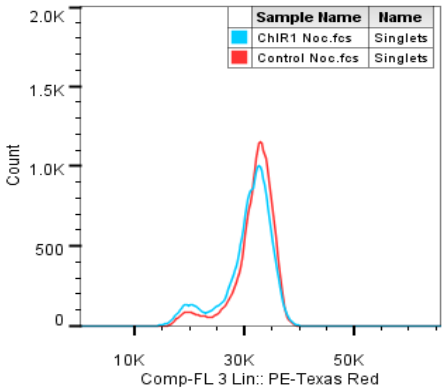

B

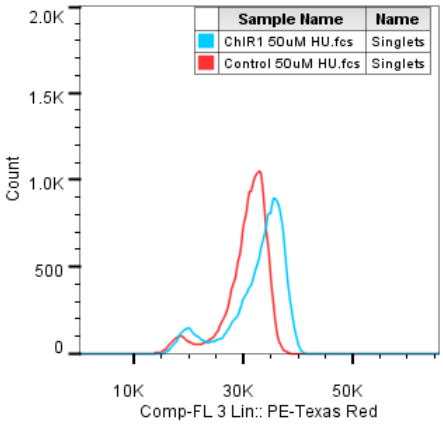

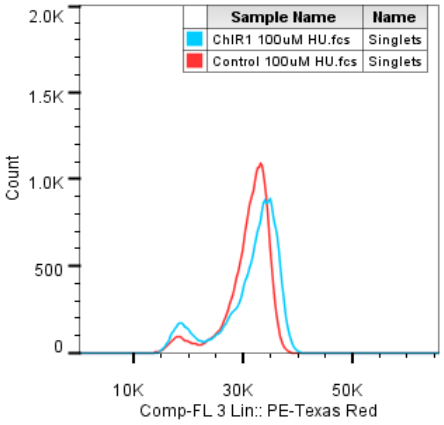

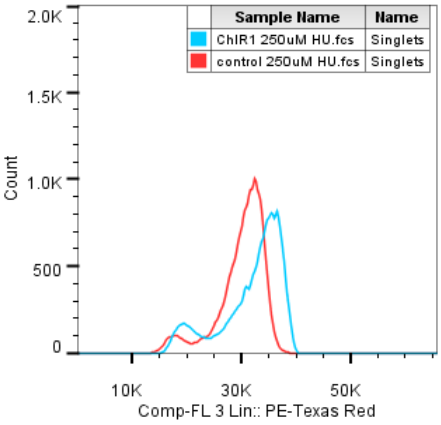

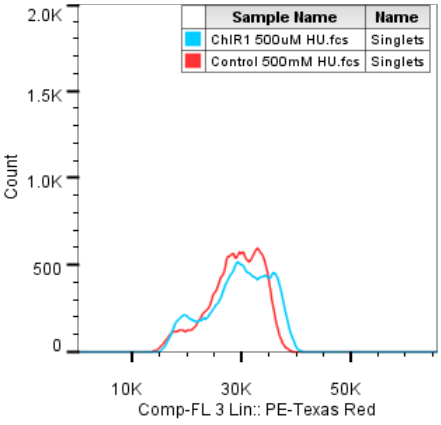

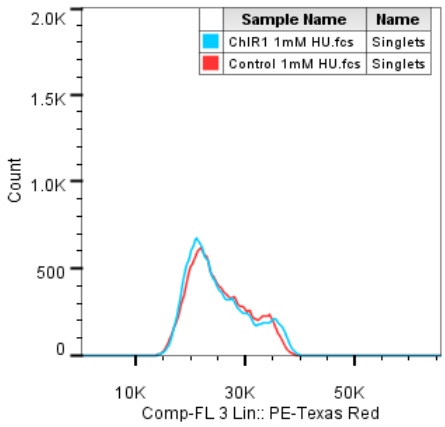

C

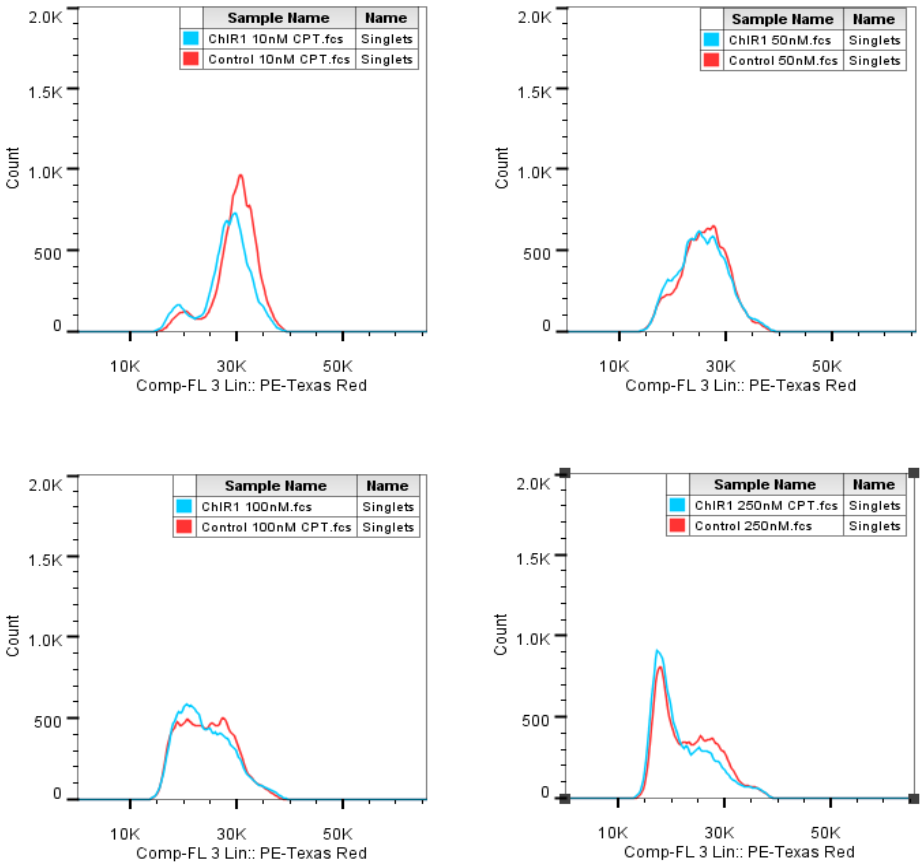

Figure 4.14. Flow cytometry analysis of hTERT-RPE1 cells transfected with either ChlR1 or control siRNA. Propidium iodide profiles showing DNA content of (A) asynchronous hTERT-RPE1 cells or cells treated for 24h with 250ng/ml nocodazole to arrest cells in mitosis and allow analysis of one single cell cycle. Cells were treated with increasing doses of either HU (B) or CPT (C) for 24 hours in the presence of nocodazole to allow analysis of cell cycle progression in the presence of replication stress. Graphs as are plotted as DNA content, determined by propidium iodide staining and detected in the PE-Texas red channel (X axis) versus cell count (Y axis). A total of 30000 events were captured per sample with the healthy singlet population then gated for subsequent analysis. This is representative of 3 independent experiments.

This conclusion is supported by western blot analysis. Cells were treated for 3h with increasing doses of either hydroxyurea or camptothecin and total lysates were then probed for various checkpoint proteins (**figure 4.15**). There is no increase in Chk1 phosphorylation at serine 345 in response to increasing doses of camptothecin. While from the western blots shown in this figure it appears as though there may be a very subtle increase in the levels of Chk1 phosphorylation in response to hydroxyurea, repeats of this experiment showed no difference. Lysates were also probed for Timeless, a known interacting protein of ChlR1 that is known to have an important role in replication fork stability and in checkpoint activation [65]. Levels of Timeless were consistently lower in ChlR1-depleted cells even in untreated samples. In this experiment, total Chk1 also seemed to be reduced in the ChlR1 knockdown although it is possible this was due to inaccurate quantification of the samples by Bradford assay prior to running the gels as actin was also slightly reduced in the hydroxyurea experiment. However, with regards to the camptothecin treated cells, quantification and loading seemed satisfactory and total Chk1 still appeared reduced. Repeats of these western blots confirmed that total Chk1 appeared to be consistently lower in ChlR1-depleted cells (**figure 4.16**), a phenomenon that had been also observed previously by K. Feeney in earlier experiments. Currently, an off-target effect of the ChlR1-specific siRNA cannot be conclusively ruled out however it should be noted that this effect is not always consistently apparent in the ChlR1 knock down as evidenced by previous western blots shown in **figure 4.13.** At present, there is no clear explanation for these observations.

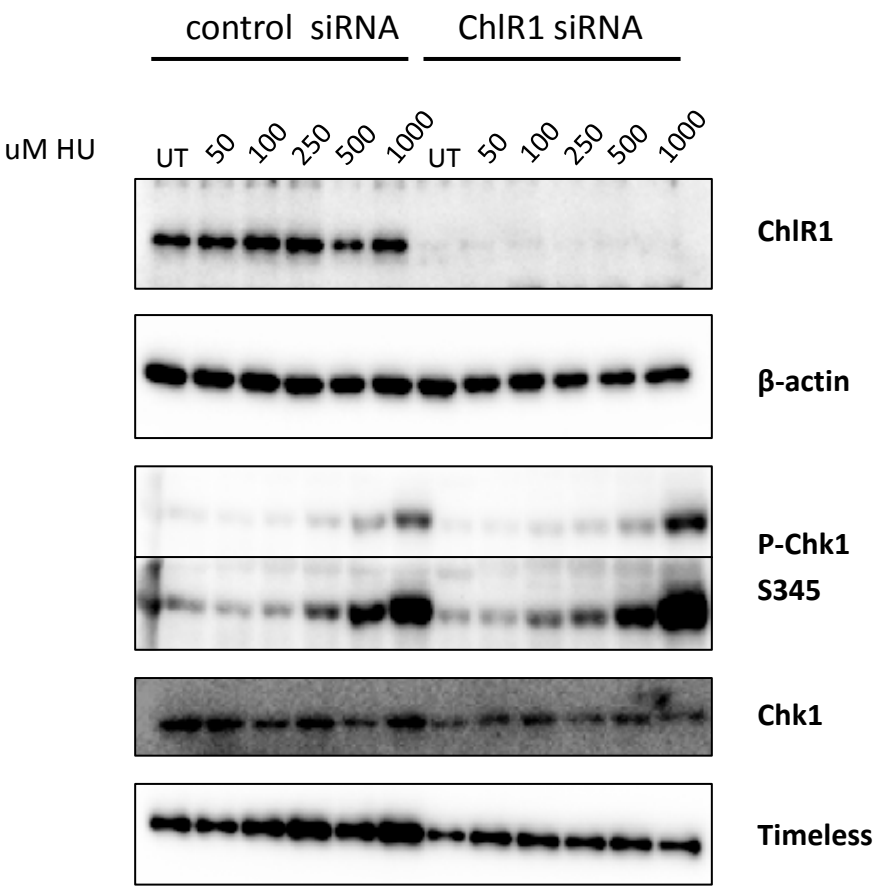
control siRNA
ChlR1 siRNA
uM HU
UT 50 100 250 500 1000 UT 50 100 250 500 1000
ChlR1
β-actin
P-Chk1
S345
Chk1
Timeless

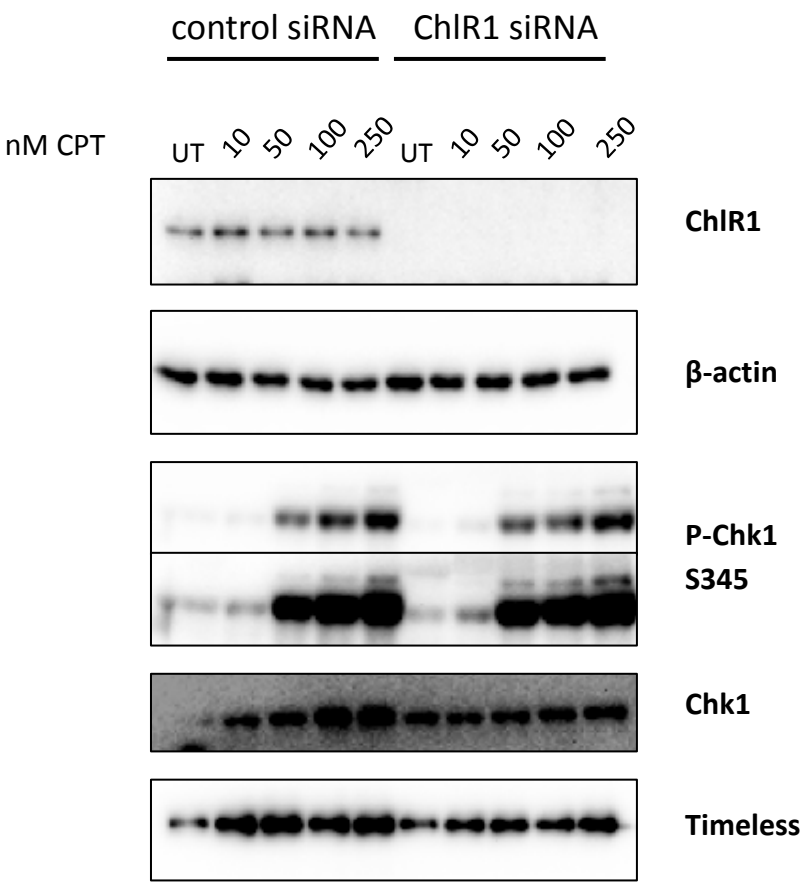
control siRNA
ChlR1 siRNA
nM CPT
UT 10 50 100 250 UT 10 50 100 250
ChlR1
β-actin
P-Chk1
S345
Chk1
Timeless

Figure 4.15. Representative western blots showing HU (top panel) and CPT (bottom panel) induced checkpoint activation in hTERT-RPE1 cells that have been transfected with ChlR1-specific siRNA compared with cells transfected with control siRNA. Cells were treated with increasing doses of each drug for 3 hours prior to harvesting and lysis. Whole cell lysates were probed for both total and phosphorylated forms of Chk1 and Timeless as well as for ChlR1. Two exposures are shown for p-Chk1. β-actin was used as a loading control. The western blot shown is representative of two independent experiments.

Evidence in the literature suggested that ChlR1 deficient cells, both from patients and in a knock-down model [139, 178] are particularly sensitive to DNA crosslinking agents. However no evidence to that effect was observed in the cell survival data generated in the Parish lab. Nevertheless, mitomycin-C treated cells were included in the panel of checkpoint western blots shown in **figure 4.16**. These repeats confirmed the observations discussed above with regards to total Chk1 but also show that Chk1 S345 phosphorylation remains unaffected. Again, no significant differences in Chk1 phosphorylation were observed following MMC treatment in ChlR1-depleted cells versus controls although Timeless is once again reduced. This appears to be a general effect of ChlR1 knock-down and is not drug specific.

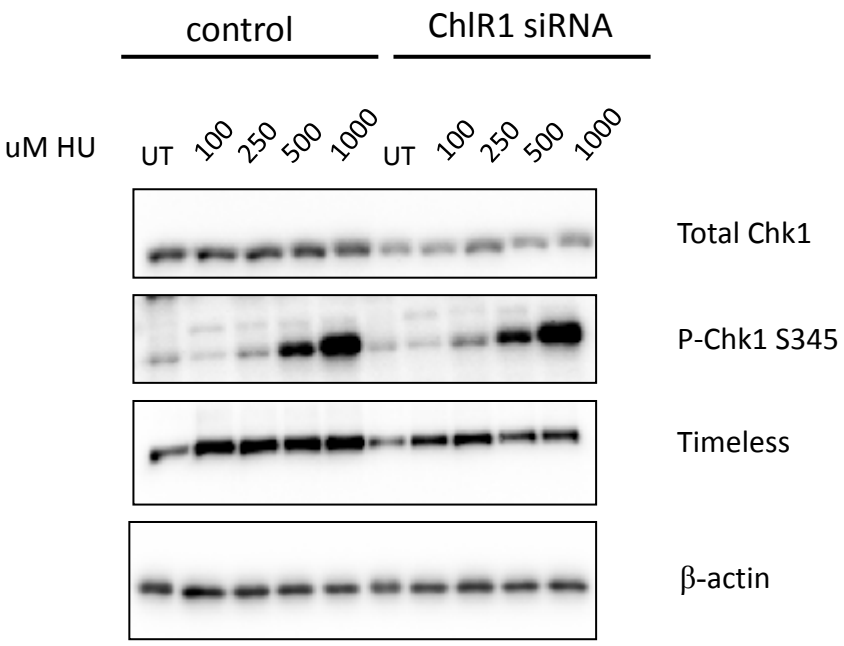
control
ChlR1 siRNA
uM HU
UT
100
250
500
1000
UT
100
250
500
1000
Total Chk1
P-Chk1 S345
Timeless
β-actin

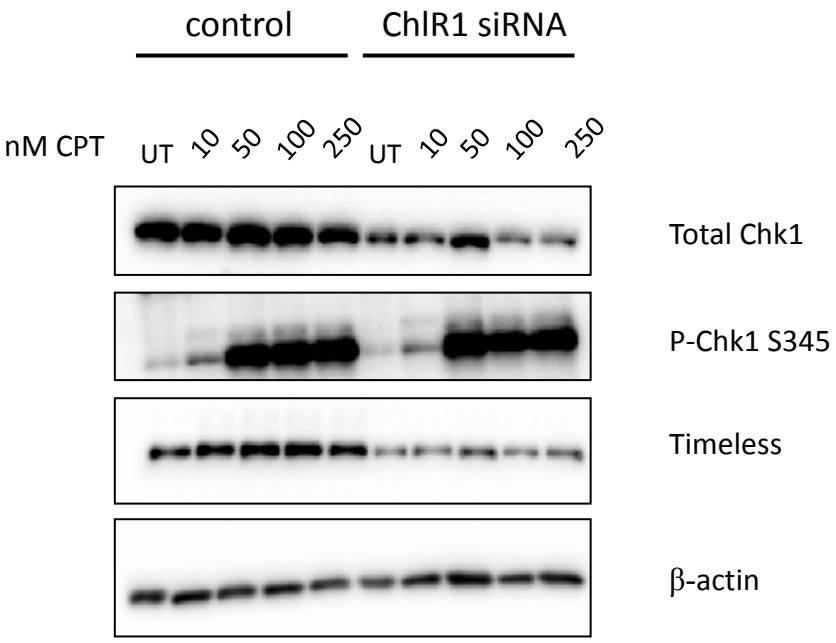
control
ChlR1 siRNA
nM CPT
UT
10
50
100
250
UT
10
50
100
250
Total Chk1
P-Chk1 S345
Timeless
β-actin

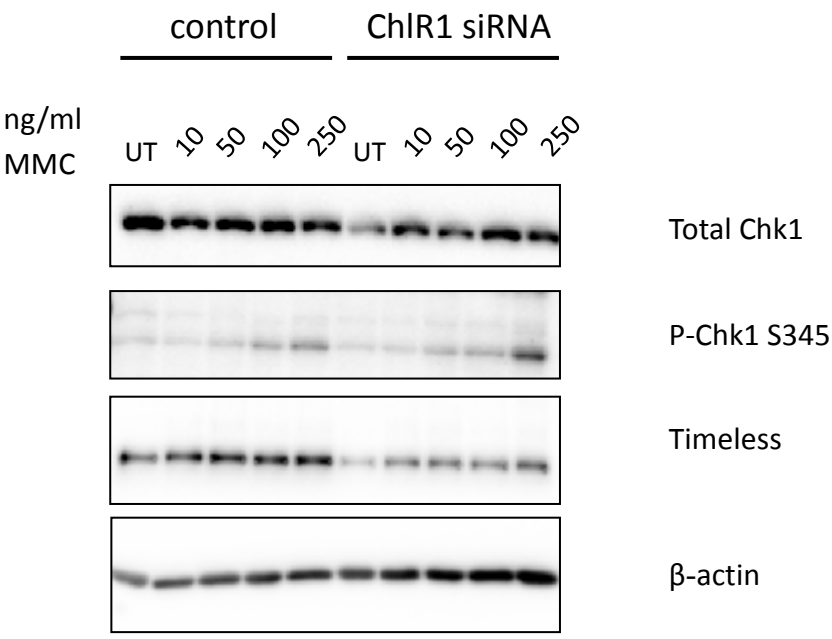
control
ChlR1 siRNA
ng/ml
MMC
UT
10
50
100
250
UT
10
50
100
250
Total Chk1
P-Chk1 S345
Timeless
β-actin

Figure 4.16. Representative western blots showing HU, CPT and MMC induced checkpoint activation in hTERT-RPE1 cells that have been transfected with ChlR1-specific siRNA compared with cells transfected with control siRNA. Cells were treated with increasing doses of each drug for 3 hours prior to harvesting and lysis. Whole cell lysates were probed for both total and phosphorylated forms of Chk1 and Timeless. β-actin was used as a loading control. The western blot shown is representative of three independent experiments.

4.7 ChlR1 depletion does not affect the recruitment of cohesin subunits to chromatin

Previous evidence published by various groups strongly indicates a role for ChlR1 in the establishment of sister chromatid cohesion [21, 131, 175]. Coupled with the evidence pointing to a role for ChlR1 in the cellular tolerance of replication stress, it was hypothesised that ChlR1 may function at the interface between DNA replication and establishment of chromatid cohesion. In an attempt to test this, sub-cellular fractionation was carried out to isolate chromatin-associated fractions from ChlR1 depleted cells before and after treatment with 2mM hydroxyurea for 2 hours. The chromatin-associated fractions were then probed with antibodies specific to the cohesin subunits Rad21 and SMC1 to determine whether their recruitment to chromatin was affected by the absence of ChlR1. **Figure 4.17** shows a panel of control western blots to confirm that the sub-cellular fractionation kit (Pierce) used for these experiments was reliable. A kit was chosen over the previous fractionation method for these experiments to ensure consistency of results. ChlR1 was included in this control experiment to determine which fractions ChlR1 primarily localised to. Interestingly there appeared to be an abundance of ChlR1 present in the cytoplasmic and membrane fractions with only a small amount seemingly associated

with chromatin under normal conditions. Unfortunately, confirmation of endogenous ChlR1 localisation by immunofluorescence has not been possible as there are currently no anti-ChlR1 antibodies available which work well for this application.

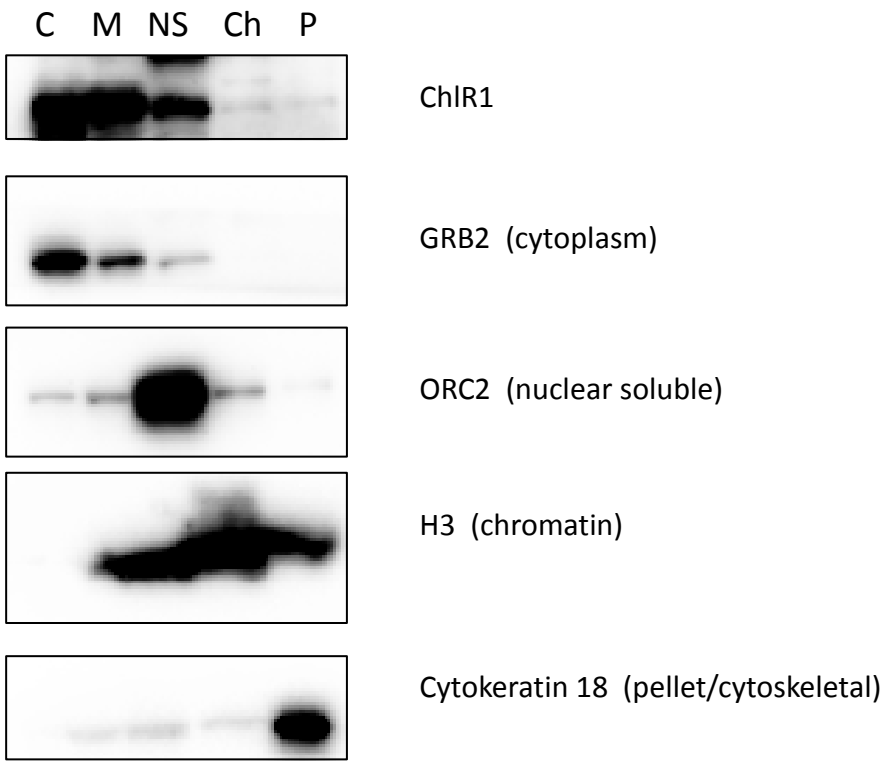

Figure 4.17. Panel of control western blots to confirm that the Pierce sub-cellular fractionation protocol can reliably differentiate between fractions. C=cytoplasm, M=membrane bound, NS=nuclear soluble, Ch=chromatin-associated and P=pellet/cytoskeletal components. Standard marker proteins, known to be present in specific sub-cellular fractions as indicated by parentheses, were blotted for to determine how effective the fractionation process was at separating fractions. ChlR1 was also included to ascertain which fractions the protein predominantly localised to.

From the H3 western blot shown in **figure 4.17,** the majority of the marker protein does localise to the chromatin fraction with only small amounts present in the nuclear soluble and the pellet. This was deemed satisfactory for proceeding with the analysis of the chromatin fraction to evaluate association of the cohesin subunits Rad21 and SMC1. **Figure 4.18** shows the chromatin-associated fraction, isolated using the Pierce fractionation kit, before and after treatment with 2mM HU for 2 hours. There is no difference in the chromatin association of either cohesin subunit in the absence of ChlR1, either under normal conditions or following hydroxyurea treatment. This suggests that ChlR1 is not involved in the loading of cohesin subunits onto DNA, rather its function is probably required in the downstream process of establishing cohesion between chromatids. This is consistent with previously published data[117, 121, 134]. Interestingly, there appears to be an increase in chromatin-associated ChlR1 in response to hydroxyurea treatment. This was reproducible across three independent experiments. This result could indicate that ChlR1 is important in the maintenance of replication fork stability in response to replicative stress which concurs with previous data (**figures 4.9-4.12)** that shows cells lacking ChlR1 are more sensitive to hydroxyurea-induced damage.

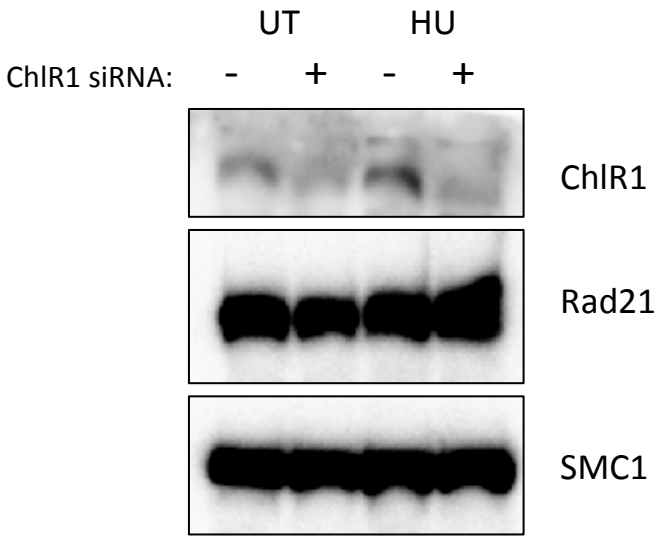

Figure 4.18. hTERT-RPE1 cells were transfected with either control or ChlR1 siRNA before being treated with 2mM HU for 2 hours and subjected to sub-cellular fractionation using the Pierce kit. Representative western blot panel shows the chromatin-associated fractions which were probed with anti Rad21 and anti-SMC1 antibodies, two major components of the cohesin complex as well as with anti-ChlR1 antibody. Western blot is representative of two independent experiments.

The effect of ChlR1 depletion on the chromatin association of a wider panel of proteins known to be involved in DNA replication and replication fork stability was also analysed using this subcellular fractionation method. **Figure 4.19** shows the proportion of various replication proteins which localise to the chromatin fraction before and after hydroxyurea treatment. As shown in **figure 4.18**, the proportion of cellular ChlR1 that is associated with chromatin increases after exposure to hydroxyurea. In ChlR1 depleted cells there is an increase in the amount of ubiquitinated PCNA and chromatin associated RPA compared

with control cells which corroborates the data in **figures 4.11** and **4.12**. The fraction of chromatin bound Timeless is significantly reduced in the ChlR1 depleted cells, however from previous experiments it was apparent that total Timeless is also reduced in the absence of ChlR1. Whether ChlR1 depletion affects the expression of Timeless or whether it has an effect on protein stability remains to be investigated. Topbp1, which is a known activator of ATR signalling in response to replication stress, is also increased in the chromatin associated fraction as is Rad9 which binds to RPA and becomes heavily phosphorylated following stalled replication. From the western blots it seems that both its association with chromatin and an increase in phosphorylation occur in response to ChlR1-depletion and that this effect is exacerbated by treatment with hydroxyurea. Fen1 was included in the panel as it has been previously published that Fen1 interacts with ChlR1 and that this interaction stimulates Fen1 endonuclease activity. However, the Fen1 western blots were not conclusive even on repetition and any effect is extremely subtle. H3 acts as a loading control for the chromatin enriched fraction.

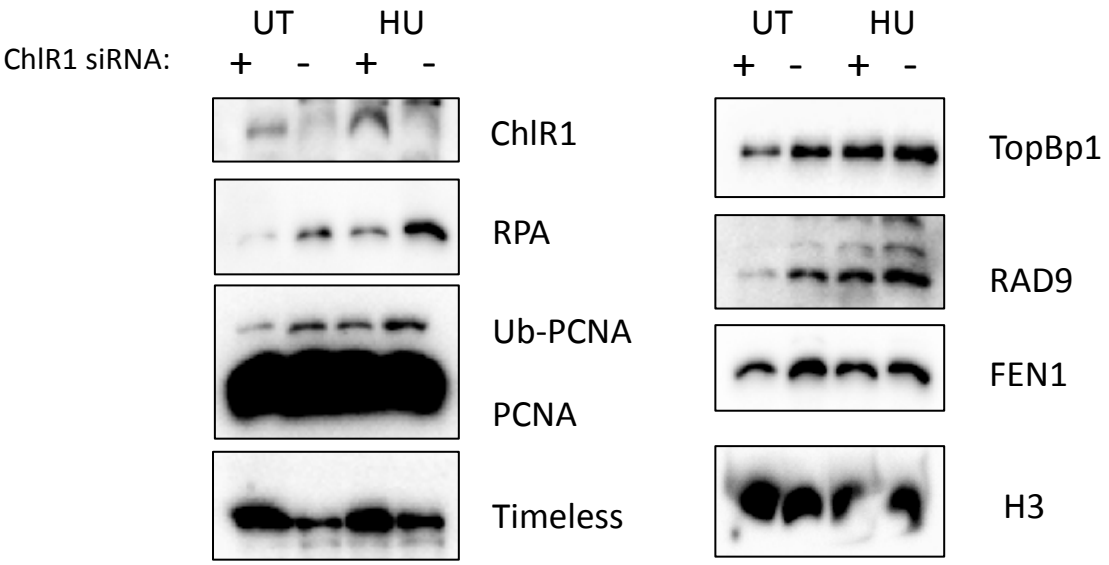

Figure 4.19. hTERT-RPE1 cells were transfected with either control or ChlR1 siRNA before being treated with 2mM HU for 2 hours and subjected to sub-cellular fractionation using the Pierce kit. Representative western blot panel shows the chromatin-associated fractions which were probed with antibodies against various proteins involved in DNA replication or in the cellular response to replication stress. These blots are representative of three independent experiments.

A co-immunoprecipitation was performed to determine whether ChlR1 interacted with RPA either in unperturbed cells or under conditions of replication stress. The results are shown in **figure 4.20.** While no association is apparent in undamaged cells or cells exposed to HU for 2h, following a longer HU treatment there is some evidence of an interaction between the two proteins. This might be because the treatment has enriched for stalled replication forks or it might be the case that ChlR1 is involved in the repair of forks which have begun to collapse after prolonged stalling.

ChlR1 has previously been shown to have roles in the process of cohesion establishment, in DNA replication and potentially in maintenance of replication fork stability [131, 178]. The proposed involvement of ChlR1 in such closely-coupled processes is intriguing and lends itself to speculation regarding the specifics of ChlR1 function in DNA metabolism. While there is evidence that suggests ChlR1 depletion leads to sensitivity to replication stress and that the absence of ChlR1 leads to major defects in sister chromatid cohesion, how ChlR1 functions to link these two cellular processes remains unclear and is undoubtedly worthy of further investigation. The implications of the data described above and how this contributes to the further understanding of ChlR1 function will be discussed below.

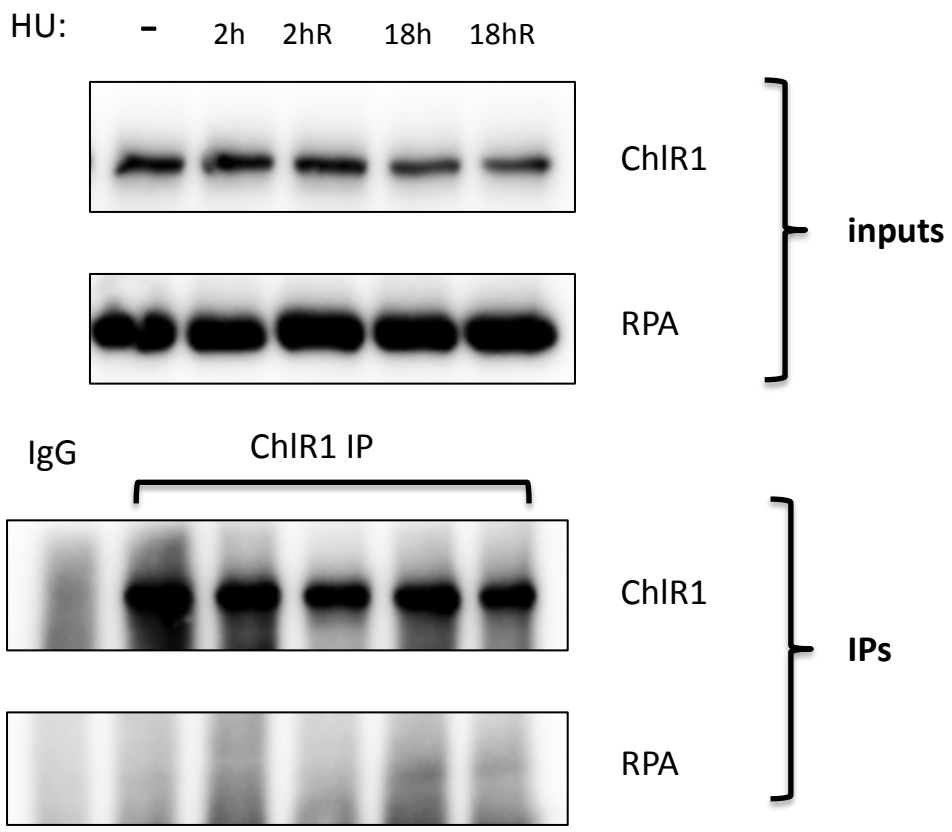

Figure 4.20. Co-immunoprecipitation showing an interaction between ChlR1 and RPA following an 18h treatment with 2mM HU. IgG was used as a control antibody for IP. Inputs are shown in the top panel and IPs on the bottom. This experiment was repeated multiple times however reproducibility was limited to around 50%.

4.7 Discussion

The involvement of Chl1p, the yeast homologue of ChlR1, in the process of sister chromatid cohesion establishment has been well-characterised over the years. The observation of major cohesion defects in mammalian cells deficient for ChlR1 in addition to the interaction of ChlR1 with cohesin subunits strongly suggests a similar role for this protein in human cells [131, 139]. Studies have also shown that ChlR1 interacts with components of the replisome as well as the Timeless/Tipin fork protection complex suggesting that ChlR1 may be involved at the interface between DNA replication and cohesion establishment [21, 65, 68]. Furthermore, recruitment of cohesin has been shown to be important in DNA repair processes, particularly in homologous recombination repair, and with the recent discovery that ChlR1 mutations are responsible for the phenotypes observed in patients with the genetic disorder Warsaw Breakage Syndrome (WBS/WABS), the potential role for ChlR1 in the DNA damage response also provides scope for exploration.

Does ChlR1 have a function in DNA damage repair?

Despite evidence published by other groups using patient-derived cells to investigate the sensitivity of ChlR1 mutant cells to various DNA damaging agents [139, 177], no significant increase in sensitivity to any of the cytotoxic agents tested was observed in our siRNA-mediated ChlR1 depleted cells. However, while the siRNA treatment does generally result in a very effective reduction in protein levels, it is possible that in primary cells any effect of ChlR1 depletion is much more apparent than in cell lines. Moreover, in WABS patients, typically any protein that is present is not fully functional which may well result in a more detrimental effect in cells than just depletion of the protein alone.

However, while no effect of ChlR1 depletion was observed in cell survival assays, direct quantification of DNA damage using the comet assay yielded more interesting data. Here, it appeared that in HeLa cells at least, there was a delay in the ability of ChlR1 depleted cells to repair damage caused by ionising radiation. Nevertheless, after 3 hours post-IR the cells had in fact managed to repair the damage to the same level as the control cells which may explain the lack of obvious phenotype in cell survival assays (**figures 4.2-4.5**).

The alkaline comet assay quantifies both double and single strand breaks and nicks as well as damage caused by alkali labile sites in the DNA. It is therefore a measure of global DNA damage in contrast to the adapted neutral comet assay which specifically quantifies DNA double strand breaks. As ionising radiation causes a range of molecular lesions in DNA, it is possible that the relatively modest effect of ChlR1 depletion could be due to the lack of specificity of the assay employed. If ChlR1 is involved in the repair or processing of a particular type of DNA lesion, for example, in the processing of a stalled replication fork or the repair of a double strand break then this may partially explain the subtle nature of the observed defect.

Sister chromatid cohesion established during S-phase has been shown to be crucial for the efficient repair of double strand breaks in S-phase and G2 by facilitating homologous recombination [148, 151, 163]. Repair by HR typically requires the sister chromatid to be maintained in close proximity for use as a template and thus promoting error-free repair of the DNA lesion. However, it has been suggested that in addition to the canonical role of cohesin in sister chromatid cohesion, the complex may also be recruited directly to the sites of DNA double strand breaks and thus have a role in the DNA repair process that is independent from its function in chromatid cohesion [153, 158]. Therefore, one hypothesis is that the absence of ChlR1 results in the inability of cells to efficiently recruit cohesin to these sites leading to the observed repair defect. Alternatively, the repair delay could

simply be the downstream consequence of the impaired sister chromatid cohesion in ChlR1 depleted cells which indirectly affects the cells capacity to successfully utilise homologous recombination as a repair mechanism. No increased effect of ChlR1 depletion on the repair kinetics was observed in cells synchronised by double thymidine block to early S-phase, however as HR predominantly occurs only in late-S and G2, repeating the experiment during this phase of the cell cycle may be more informative.

Interestingly, it has been proposed that the process of homologous recombination is an important cellular mechanism of replication fork stabilisation and reactivation, distinct from its more familiar function in the repair of double strand breaks (reviewed in [17]). Mutations in several HR proteins including BRCA2 and Rad51 have been shown to result in reduced fork velocity in mammalian cells, a phenotype also observed in ChlR1-depleted cells (Parish lab, unpublished). Results from the comet assay performed on cells treated with the replication inhibitor hydroxyurea indicate an accumulation of DNA damage in ChlR1-depleted cells. This sensitivity to replication stress could thus be linked to the impaired ability of ChlR1-depleted cells to efficiently utilise HR mechanisms to stabilise or repair damaged replication forks.

The role of ChlR1 in response to replication stress

In parallel to the work presented in this thesis, recent data in the Parish lab has shown that unperturbed ChlR1 depleted cells have a mild replication defect characterised by their reduced replication fork speed as measured by the DNA fibre assay. In addition to this, these cells have also been shown to be less efficient at restarting stalled replication forks following treatment with hydroxyurea. It was therefore hypothesised that the repair defect observed in the ChlR1 depleted cells using the comet assays could be replication-dependent. ChlR1 may potentially function to stabilise inactivated forks or to promote fork

restart. This would be consistent with the published interaction between ChlR1 and the Timeless/Tipin replication fork protection complex.

While the accumulation of damage in hydroxyurea treated cells is apparent using the alkaline comet assay, the nature of the assay does not allow us to distinguish between damage due to forks which have stalled but which can be reactivated and forks that have destabilised and collapsed leading to double strand breaks. If ChlR1 is involved in replication fork stabilisation it might be expected that in ChlR1 depleted cells there would be an increase in double strand break formation as a consequence of replication fork collapse. 53bp1 foci are detectable by immunofluorescence at sites of double strand breaks and were used as a measure of DSB formation in cells treated with hydroxyurea to induce replication stress.

There was some concern that a 2mM dose of hydroxyurea for 2 hours would not necessarily induce fork collapse as it is known that forks treated with either low doses or short durations of replication inhibitors can simply stall transiently and then restart after removal of the block [37]. However, from the 53bp1 foci assay, a modest increase in foci formation is observed after 2 hours of treatment, while after removal of the drug the number of foci continued to increase. This suggests that a proportion of the stalled replication forks were unable to restart and instead collapsed into DSBs, to which 53bp1 was subsequently recruited. Western blot analysis also showed that Chk2 phosphorylation occurs following a 2 hour treatment of 2mM HU which further confirms that the ATM DSB response pathway is activated at this dose.

The observed increase in foci formation was consistently attenuated in the ChlR1 depleted cells after a 1 hour release from hydroxyurea treatment, however at later time points following removal of the drug ChlR1 depleted cells appeared to have accumulated an

increased number of foci compared with the control cells. This could potentially indicate a delay in the response to double strand breaks generated by collapsed replication forks in ChlR1 deficient cells. This supports the hypothesis that ChlR1 functions to promote repair of destabilised replication forks, either due to its role in the establishment of cohesion which facilitates repair via HR mechanisms, by recruiting cohesin to the sites of DNA damage or even perhaps by a more direct role in the repair process. Alternatively this increase in 53bp1 foci formation 4-8 hours post-HU may be indicative that in the ChlR1 depleted cells, forks that have been stalled during treatment with HU have been stalled indefinitely and are unable to restart compared with the majority of forks in the control cells which stalled transiently and recovered after the inhibitor was removed. It has been well established that forks which remain stalled for prolonged periods do not restart and usually collapse into DSBs. In these instances global replication is generally rescued by new origin firing [60, 62]. It would be extremely interesting to utilise the DNA fibre technique to ascertain whether this is indeed the case for ChlR1 depleted cells and this would certainly further support the theory that ChlR1 is important for replication fork stability and/or restart rather than repair per se.

53bp1 performs various functions at double strand break sites including the recruitment of other DNA repair factors and signalling proteins, checkpoint activation as well as the regulation of DNA repair pathway choice [78, 196, 197]. Recruitment of 53bp1 to DSBs inhibits end resection by cellular nucleases [78]. This action thus promotes the non-homologous end joining (NHEJ) repair pathway rather than repair by HR, due to the requirement of the latter for end resection to occur. This then allows the association of Rad51 to the exposed single stranded DNA, which is one of the key mediators of HR repair. Removal of 53bp1 to allow nucleases to gain access to DNA ends is thought to be mediated by BRCA1 in a cell cycle dependent manner [79]. Thus, NHEJ is the preferred

DSB repair pathway in G1 but preference then shifts to repair by HR in S phase and G2 in the presence of a replicated sister chromatid for use as a template. The level of 53bp1 foci in ChlR1-depleted cells remains elevated up to 4-8 hours post-hydroxurea treatment which could indicate that 53bp1 is not efficiently removed from DSB sites to allow HR to occur. Inappropriate repair of replication induced breaks by error-prone NHEJ could lead to downstream mutations and rearrangements which could be deleterious to cells. ChlR1 has been shown to be essential in mammalian embryonic development and an inability to tolerate replication associated DNA damage leading to genomic instability could explain the embryonic lethality observed in the mouse model [175].

As well as an apparent increase in DNA damage following replication stress as evidenced by the comet assay, an increase in PCNA ubiquitination is also observed. This, coupled with the comet assay on HU treated cells, supports the idea that ChlR1-depleted cells are more sensitive to replication stress. PCNA mono-ubiquitination by the Rad18 ubiquitin ligase occurs in response to DNA damage or stalled replication. This mono-ubiquitination is traditionally thought to activate the translesion synthesis (TLS) pathway. This pathway is responsible for bypassing lesions caused by damaged DNA via recruitment of specialised low-fidelity DNA polymerases which are more tolerant of aberrant templates, hence allowing replication to bypass the damage [29]. Mono-ubiquitination of PCNA in response to hydroxyurea however presents something of a conundrum as no DNA lesion is generated that would benefit from the recruitment of alternative polymerases. In this instance it is probable that ubiquitination of PCNA acts as a signal or scaffold for the recruitment of other repair factors or proteins required to stabilise the replication complex at the stalled fork. Interestingly, ChlR1 has been shown to interact with PCNA as well as with components of the Timeless/tipin complex which has been shown to be important in maintaining replication fork stability, further suggesting that ChlR1 also functions in this

process [21, 65]. Additionally, when replication stalls the replicative helicase continues to unwind the DNA duplex ahead of the stalled fork leading to long tracts of single-stranded DNA that become coated with RPA. Increased association of RPA with chromatin is also observed in ChlR1-depleted cells treated with HU, which similarly suggests an increase in stalled replication in these cells compared with controls.

Despite indications that absence of ChlR1 results in an accumulation of replication coupled damage, whether this can be attributed to an increase in fork stalling, a decrease in fork stability or a defect in the repair processes associated with replication stalling, analysis of checkpoint activation and recovery in response to replication stress in these cells appears to be normal. Both western blot analyses of checkpoint proteins as well as flow cytometry analysis of cell cycle progression in response to HU and CPT is comparable with control siRNA treated cells. Since the ChlR1-depleted cells appear to activate the intra S-phase replication checkpoint normally after damage and also arrest appropriately in response to replication inhibitors, cells are likely prevented from continuing through the cell cycle with unrepaired damage or incomplete replication as a result of the increase in stalled or collapsed forks. This could suggest that ChlR1 depleted cells employ some compensatory mechanisms to rescue replication or to repair the damage caused by fork collapse. The former could be facilitated by an increase in new origin firing while the utilisation of the NHEJ repair pathway in preference to HR in S-phase to repair collapsed forks could circumvent problems caused by the diminished cohesion in ChlR1 deficient cells and the impact this has on the ability to carry out HR mediated repair. Both of these hypotheses could be tested experimentally.

Experiments evaluating the chromatin association of various proteins in both unperturbed ChlR1-depleted cells as well as in cells treated with 2mM HU for 2 hours also yielded some interesting data. Encouragingly, ChlR1 appeared to consistently accumulate in the

chromatin fraction in response to the HU treatment. This supports much of the previously discussed data indicating a role for the protein in replication fork stability or maintenance. Unfortunately direct localisation of endogenous ChlR1 by immunofluorescence-based techniques was not possible due to lack of appropriate antibodies. The in-house rabbit anti-ChlR1 antibody was tested for IF using control and ChlR1-specific siRNAs to deplete ChlR1 in hTERT-RPE1 cells. Although the knock-down of the protein was approximately 90% efficient by western blot, there was no reduction in the level or specificity of staining as visualised by IF (data not shown).

Chromatin-association of the cohesin subunits SMC1 and Rad21 did not appear to be reduced in ChlR1 depleted cells, which remains consistent with the current body of evidence implicating ChlR1 in the process of replication-coupled cohesion establishment as opposed to cohesin loading which has been shown to be a separate and temporally distinct process in mammalian cells [117, 134]. It was thought that exposure to hydroxyurea could potentially lead to an increase in chromatin associated cohesin in normal cells due to the phenomenon known as damage-induced cohesion which has been extensively characterised in yeast models but which lacks convincing evidence in higher eukaryotes [153, 198, 199]. The theory was that in ChlR1-depleted cells this association may be reduced if ChlR1 has a role in the specific recruitment of cohesin to double strand break sites. Treatment with HU had no effect on the levels of cohesin on the chromatin however. This could be a number of explanations for this. As mentioned previously, there is little evidence in mammalian systems to suggest that cohesin is actually recruited to sites of DNA damage. It is also possible that the level of damage induced by the HU treatment is not significant enough to observe any effect, particularly because cohesin is so abundant on the chromatin under normal conditions. Any subtle effect is therefore likely to be masked when using a basic fractionation method.

Timeless, one of the components of the Timeless/Tipin replication fork protection complex, showed reduced chromatin association in ChlR1 depleted cells. However, levels of Timeless protein in whole cell lysate were also reduced in ChlR1 depleted cells so it is possible that ChlR1 is involved in stabilising Timeless, perhaps via its recruitment to chromatin in response to endogenous as well as exogenous replication stress. In control cells the level of Timeless associated with the chromatin did not appear to increase in response to the HU treatment, however in whole cell lysates it was clear that expression of Timeless increased in response to both HU and CPT in control cells and to a significantly reduced extent in ChlR1 depleted cells. These observations are intriguing and support the notion that ChlR1 may somehow be required for the stability of the Timeless/Tipin complex. Interestingly, a previous study has shown that reduction of Timeless also leads to a reciprocal reduction in the association of ChlR1 with chromatin [65].

Depletion of Timeless and/or Tipin has been shown to lead to both G2 and intra S-phase checkpoint defects [200]. However, as far as can be determined from the experiments in this thesis, despite the reduction in Timeless protein levels evident in the ChlR1-depleted cells, there is no discernable impact on checkpoint function. It is probable that the relatively modest reduction in Timeless protein observed when ChlR1 is knocked down is not enough to significantly impact on checkpoint function. Unlike the Timeless binding partner Tipin, which associates directly with the replicative helicase and depletion of which results in destabilisation of Timeless and leads to major checkpoint defects, it is possible that the interaction between ChlR1 and Timeless is important for stabilisation of the complex under more specific circumstances, such as at regions of DNA with significant secondary structure or highly transcribed regions i.e. conditions which cause endogenous replication stress. In co-immunopreciptiation experiments, Timeless and Tipin interact both in the presence and absence of HU suggesting their interaction is not

mediated or enhanced by replication stress conditions. It would be interesting to investigate whether the reported interaction between Timeless and ChlR1 is amplified after treatment with agents which induce DNA damage and/or replication stress.

When investigating the increased monoubiquitination of PCNA in ChlR1-depleted cells, it was observed that during treatment with HU, a significant proportion of PCNA appeared to dissociate from the chromatin in both control and ChlR1 deficient cells (**Figure 4.11**). The fraction that did remain bound appeared to be the fraction modified by ubiquitin. This dissociation is probably indicative of the down-regulation of replication in response to the inhibitor, which is more apparent in the ChlR1 depleted cells. While the fractionation experiments performed using the commercial Pierce kit showed no visible reduction in chromatin association of PCNA (**figure 4.19**), it should be noted that in any sub-cellular fractionation protocol stringency can vary such that what is described as the chromatin-associated fraction in one experiment may well be a slightly different pool of cellular protein than in another experiment using an alternative protocol.

Conversely, Rad9, a component of the trimeric protein clamp known as the 9-1-1 complex (Rad9-Rad1-Hus1) which exhibits significant structural homology to PCNA, appears to increase its association with chromatin in response to HU. This is consistent with published reports which show 9-1-1 is a sensor of DNA damage which is recruited to stalled replication forks and subsequently loaded onto DNA by the Rad17-RFC complex [201]. 9-1-1 is then thought to facilitate the phosphorylation-dependent recruitment of Topbp1 which is known to up-regulate the activity of ATR in response to replication stress. ChlR1-depleted cells show a greater accumulation of both Rad9 and Topbp1 on the chromatin both in the absence and presence of HU which is consistent with our other findings suggesting ChlR1-depleted cells are more vulnerable to the effects of replication stress, whether endogenous or exogenous.

Finally, while these observations have certainly shed further light on the complex role of ChlR1 in DNA replication and the response to replication stress, in depth study of the function of this protein is still essential to understand the complex nature of its involvement in the various aspects of DNA metabolism in which it has so far been implicated. Thus far the actual biochemical mechanisms by which ChlR1 carries out its function in the processes of cohesion establishment and maintenance of replication fork stability have remained elusive and only recently have researchers succeeded in a thorough *in vitro* biochemical analysis of the helicase and its substrates [179]. How this data can be interpreted in the context of the current biological evidence informing ChlR1 function will be discussed in later chapters. Additionally, by investigating the impact of ChlR1 mutations associated with the genetic disorder Warsaw Breakage Syndrome an attempt will be made to further elucidate the role of ChlR1 in the genome stability maintenance in a wider disease setting.

Chapter 5

Characterisation of patient-derived ChlR1 mutations using stable transfected fibroblast cell lines

5.1. ChlR1 mutations and Warsaw Breakage Syndrome (WABS)

For many years, much of the understanding of the function of ChlR1 came from genetic and biochemical studies of the yeast homologue Chl1. Few studies were carried out in mammalian cells directly looking at the role of ChlR1, although data from Jo Parish and others largely concluded that the mammalian ChlR1, like it's yeast counterpart, played a crucial role in cohesion establishment. The exact mechanism and biological function of the protein, however, remained unclear.

In 2010, Van der Lelij and colleagues identified a patient with a novel human genetic disorder directly attributed to mutations in the ChlR1 gene [139]. The patient presented with severe growth defects, abnormal skin pigmentation and microcephaly. This disease, which they named Warsaw Breakage Syndrome (WABS) after the location of the affected individual, displayed features of both known cohesinopathies such as Roberts Syndrome as well as Fanconi Anaemia. Cytogenetic analysis indicated severe sister chromatid cohesion defects as well as sensitivity to MMC-induced chromosomal breakage. The patient was found to have biallelic mutations in the ChlR1 gene with the paternal mutation resulting in an in-frame deletion of a highly conserved lysine residue (ΔK897) at the C-terminus of the protein, and a maternal splice site mutation which results in the deletion of the last 10 base pairs of exon 22. The maternal mutation is thought to lead to nonsense-mediated decay of this product. Very little protein was detectable by western blot from these patient cells suggesting that the ΔK897 mutant protein product is also likely to be unstable. Later biochemical studies on the ΔK897 protein confirmed that it was indeed less stable than the wild-type in thermostability assays as well as consistently producing a significantly lower yield in recombinant expression systems.

Subsequently, three more patients were identified with a similar phenotype to the original WABS patient, all within the same Lebanese family [177]. All were found to have a homozygous point mutation in the ChlR1 gene (R263Q). Biochemical analysis of the purified protein showed that this resulted in a protein with perturbed DNA binding and DNA-dependent ATP hydrolysis, upon which the helicase activity is dependent. Separate biochemical studies carried out by Brosh *et al* using the ΔK897 mutant have shown that this protein has a similarly impaired helicase function suggesting that these clinically relevant mutations share this feature and also serves to emphasise the probable *in vivo* importance of the helicase function of ChlR1, the exact biological function of which is still unclear [179].

Recently, yet another patient has been identified with a WABS-like phenotype (G.Stewart, University of Birmingham). Although originally diagnosed with the chromosomal instability disorder Nijmegen breakage syndrome, this patient was later found to harbour a point mutation in the coding sequence of one allele of the ChlR1 gene (c.169G>C p.Gly57Arg) while the other allele contains a second point mutation affecting the last base of intron 26 (c.2692-1G>A). At the protein level, the major effect of this mutation appears to be increased retention of intron 26 resulting in an in-frame insertion of an additional 25 amino acids. How this affects protein function or stability has not been characterised. Western blots for ChlR1 in these patient cells however revealed barely detectable levels of a protein which showed no decreased mobility by SDS PAGE. Therefore, it was initially assumed that the splice mutation leads to an unstable protein product and the small amount of detectable protein present is due to transcription from the G57R mutant allele. However, further western blots on patient-derived fibroblasts using our in-house anti-ChlR1 antibody do result in multiple higher molecular weight bands and the possibility that a small amount of the larger protein is also expressed cannot be definitively excluded.

While *in vitro* biochemical analysis has so far been carried out on two of the known patient-derived mutant ChlR1 proteins, little functional cell biology has been undertaken with these mutants to determine the actual biological role of ChlR1 in cellular processes. Additionally, the G57R mutation has yet to be fully characterised. With this in mind, by making use of two patient-derived mutant proteins, as well as an artificially generated helicase dead construct (K50R), work was undertaken to try to further our understanding of the functional relevance of ChlR1 and the mechanism by which ChlR1 mutations result in genomic instability phenotypes.

5.2. Characterisation of patient-derived ChlR1 mutations

5.2.1. Generation of stable cell lines in G57R patient background

In order to study the biological significance of these patient-derived ChlR1 mutations, a strategy was developed whereby stable cell lines were generated using the G57R mutant patient fibroblasts as a genetic background. Using a retroviral-based system, G.Stewart and K. Feeney (University of Birmingham) established a panel of five fibroblast cell lines each re-expressing either HA-tagged vector only, wild-type ChlR1 or either of three ChlR1 mutants: K50R, G57R and ΔK897.

Stable expression of these constructs was determined by western blot analysis using our in-house anti-ChlR1 antibody (**figure 5.1**).

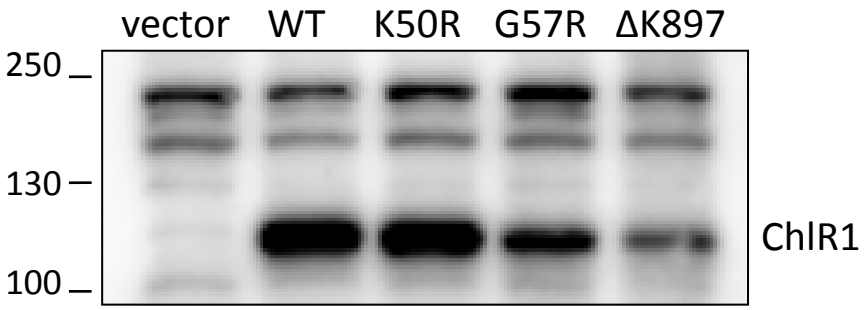

Figure 5.1. Western blot analysis showing the relative expression of the various ChlR1 constructs in the G57R patient background. There is a faint visible band in the vector only lane, indicating a small amount of endogenously expressed G57R ChlR1 in this background. However, the identity of the higher molecular weight bands is not known and it is possible that one of these, perhaps the faint band running at 130 kDa, is the larger protein product expressed from the c.2692-1G>A allele. Protein concentration was determined by Bradford assay and 20ug of total protein loaded in each lane.

From the western blot it seems there remains a small amount of endogenously expressed G57R ChlR1 protein present in the vector only cell line as expected. While the re-introduced wild-type and K50R mutant proteins both express well, the G57R and ΔK897 protein levels are significantly reduced by comparison. It is possible that, like the ΔK897 mutation, the G57R point mutation also affects protein stability.

Localisation of endogenous ChlR1 had previously been attempted in both RPE1 and HeLa cell lines, however the lack of availability of an antibody which works well for immunofluorescence led to limited success of previous localisation studies. The panel of

fibroblast cell lines presented an opportunity to study the localisation of the wild-type and ChlR1 mutant proteins by utilising their HA epitope tag. Immunofluorescence images showing the differential localisation of the ChlR1 mutants are shown in **figure 5.2.**

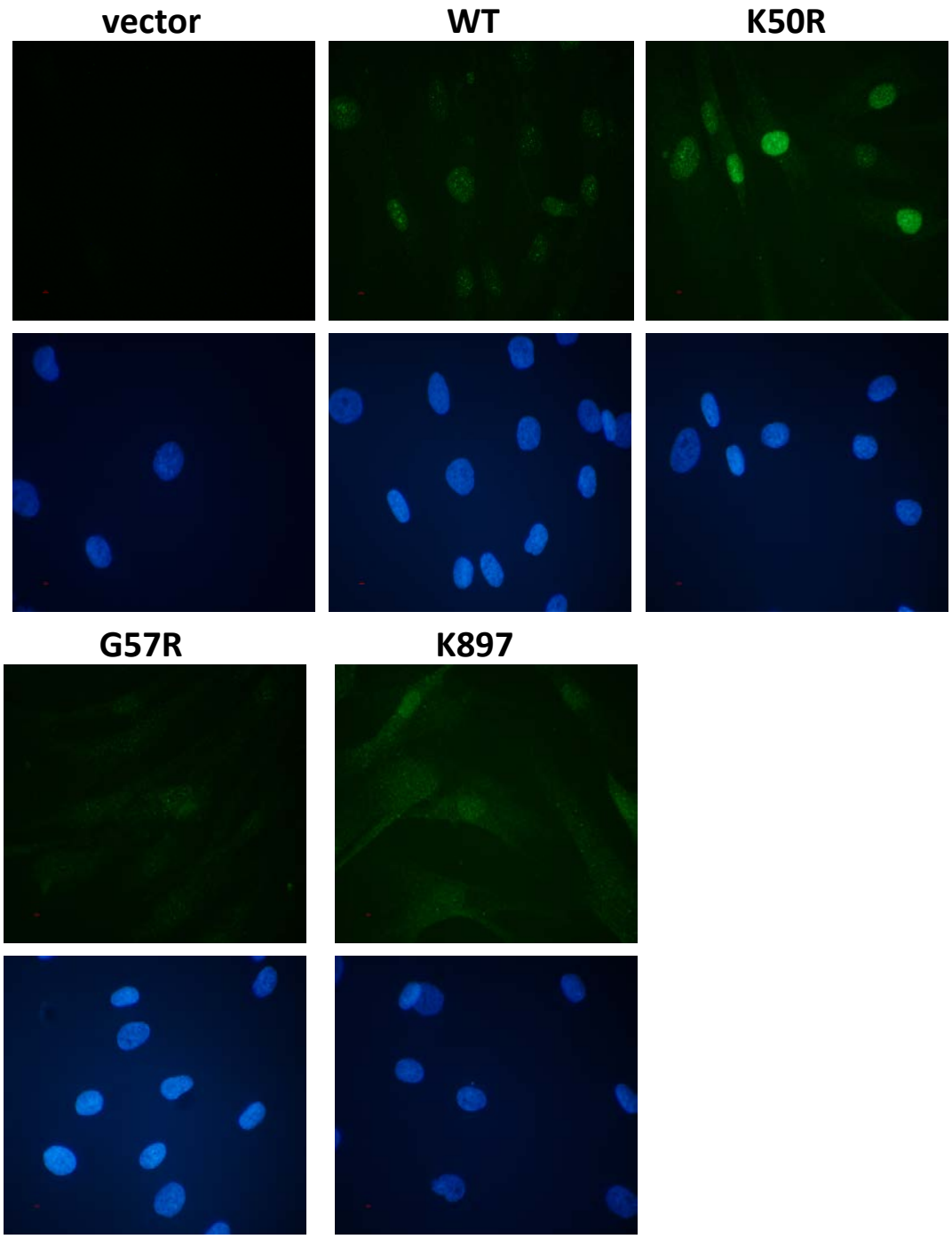
vector
WT
K50R
G57R
K897

Figure 5.2. Immunofluorescence images showing the localisation of the HA-ChlR1 proteins. Coverslips were stained with a commercially available HA 9110 antibody (Abcam) followed by detection with Alexa 488 conjugated secondary antibody (Invitrogen). Hoescht 33342 was used as a nuclear counterstain. All images were taken at the same exposure using a Zeiss inverted epifluorescent microscope fitted with a 60x oil immersion objective. Images shown are representative of two independent experiments.

Wild-type and the K50R mutant ChlR1 proteins are predominantly localised to the nucleus, with particularly strong nuclear staining apparent in the K50R mutant. There also appears to be some enrichment in the nucleolus which correlates with the original observations of Lahti and colleagues. This may be cell type dependent as nucleolar enrichment was not observed in a subsequent publication by Parish *et al*. This might also be explained by differences in the slide preparation and staining procedures. Although it is clear from the western blot that the G57R and ΔK897 proteins are less well expressed, it still appears that the localisation of these proteins is more diffuse with increased cytoplasmic staining compared with wild-type or K50R.

5.2.2. Cohesion defects in fibroblast cell lines are rescued by wild-type ChlR1

Metaphase spread analysis of the vector only line and the three ChlR1 mutant fibroblast cell lines indicated the presence of severe cohesion defects, either ‘rail-road’ type chromosomes or premature chromatid separation (PCS), consistent with the WABS phenotype (**figure 5.3a**). The cell line stably expressing wild-type ChlR1 however showed

significant rescue of the cohesion defect (**figure 5.3b**). Interestingly, upon analysing the percentage of metaphases displaying the more severe PCS phenotype across the different cell lines, it appeared that both the K50R mutation and the ΔK897 may have a slightly higher incidence of PCS (**figure 5.3c**). It must be noted that the number of metaphases counted for each cell line was relatively low due to the very slow proliferation of these cells and it was difficult to accumulate enough metaphase cells to perform the experiment. Indeed, for many subsequent experiments the point must be made that statistical significance was not obtained due to the technical difficulties in culturing these particular cells.

a

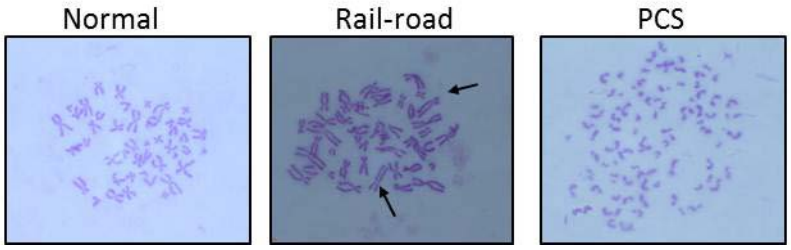
Normal
Rail-road
PCS

b

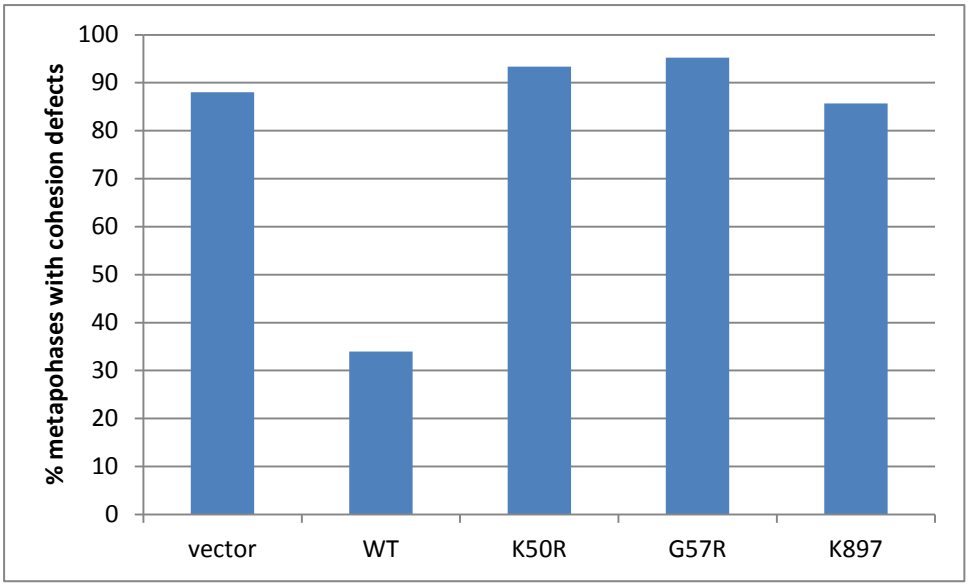
% metapohases with cohesion defects
100
90
80
70
60
50
40
30
20
10
0
vector
WT
K50R
G57R
K897

c

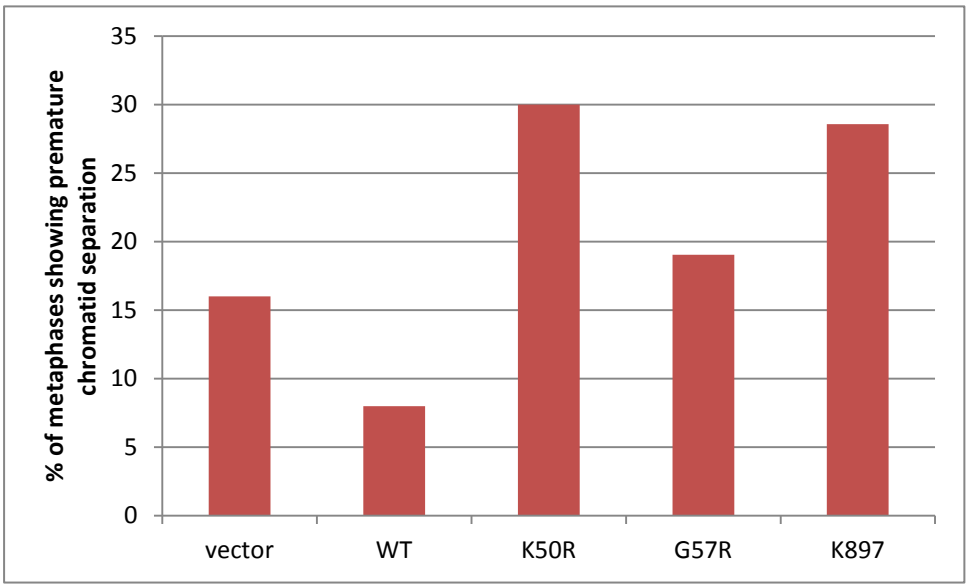
% of metaphases showing premature chromatid separation
35
30
25
20
15
10
5
0
vector
WT
K50R
G57R
K897

Figure 5.3. Quantification of metaphase spreads on the five fibroblast cell lines. Metaphases showing 1 or more 'railroad' chromosome were scored as having a cohesion defect, as were metaphases displaying premature chromatid separation (PCS). Examples of these cohesion defects are shown in (a). The total percentage of metaphases in each cell line with cohesion defects is shown in (b) while (c) indicates the percentage of metaphases with PCS only. N=30-50 for each cell line. This experiment was only performed once due to the difficulty in culturing the fibroblast cell lines.

5.2.3. Sustained checkpoint activation in ChlR1 mutant cell lines

To further understand the functional significance of the ChlR1 mutations and to relate the patient cell phenotypes to what had been observed in the knock-down system described in results chapter 2, each of the fibroblast cell lines were treated with 2mM HU for 2 hours to perturb DNA replication. This leads to rapid activation of the Chk1 pathway as well as phosphorylation of H2AX (γ-H2AX) at stalled forks. **Figure 5.4** shows a panel of western blots analysing Chk1 activation in the fibroblast cell lines.

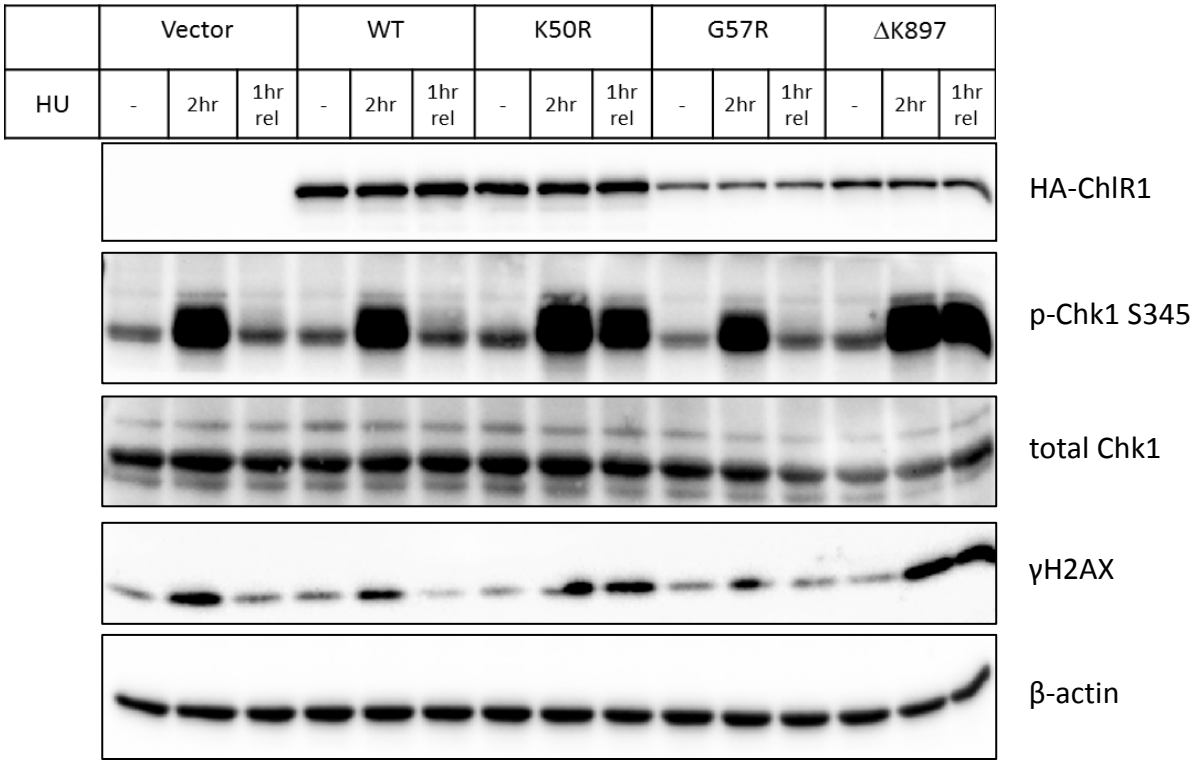

Figure 5.4. Western blot panel showing Chk1 and H2AX phosphorylation in response to HU across the panel of fibroblast cell lines. β-Actin is included as a loading control. Western blots are representative of three independent experiments.

All five cell lines show normal activation of Chk1 in response to HU, however the K50R and the ΔK897 mutants appear to show sustained activation of the pathway following removal of the drug. They also both show sustained γ-H2AX in response to the HU treatment. Interestingly, these are the same mutants that show an increased incidence of PCS upon analysis of metaphase spreads. Biochemical analysis carried out on purified samples of these proteins confirmed that they both lack the ability to hydrolyse ATP and are thus effectively helicase-dead[174, 179]. On the other hand no such biochemical data is

available as yet for the G57R mutant so it is potentially feasible that this protein retains its helicase function thus allowing for normal checkpoint recovery.

5.2.4. Helicase dead K50R mutant still interacts with the cohesin complex

The fact that two of the known ChlR1 patient mutations linked to WABS result in proteins with impaired helicase activity strongly suggests that the helicase function of the protein is crucial and when absent has serious biological consequences. It is still unclear exactly what role this helicase function plays in either cohesion establishment or during DNA replication or damage repair. For example, do the helicase dead mutant proteins still interact with the cohesin complex? Co-immunoprecipitation experiments using the fibroblast cell lines were carried out using an anti-HA antibody to immunoprecipitate (IP) the ChlR1 proteins. IPs were then probed with anti-ChlR1 or anti-Rad21 antibodies to observe any interaction with the Rad21 cohesin subunit (**figure 5.5**).

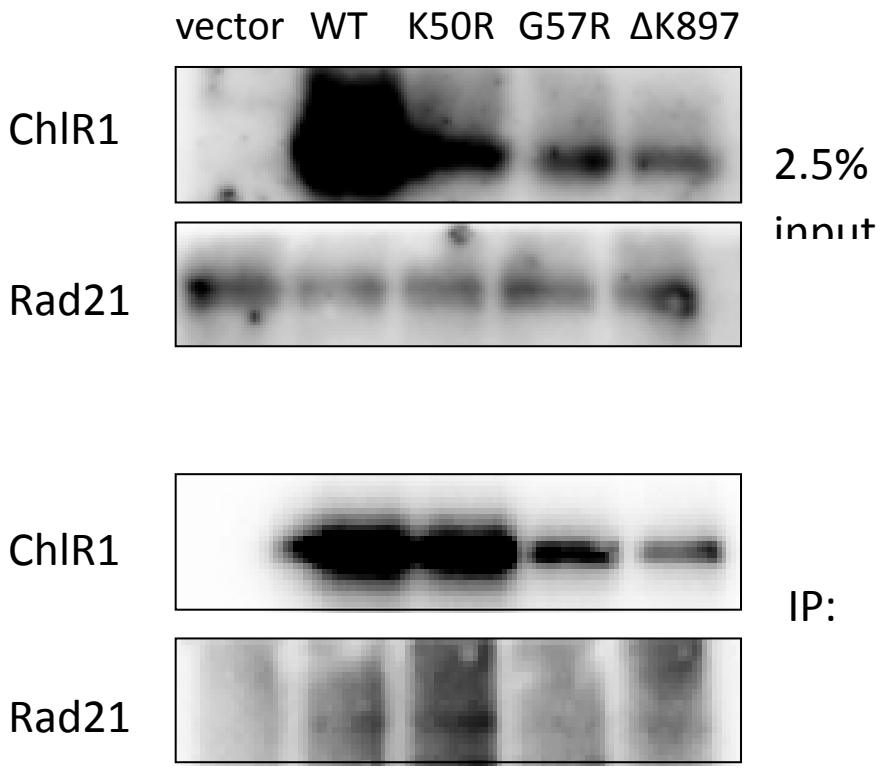

Figure 5.5. Co-immunoprecipitation (Co-IP) experiment using anti-HA antibody (Abcam) to immunoprecipitate the HA-tagged ChlR1 proteins. Inputs (2.5%) are shown in the top panel, IPs are shown in bottom panel. Different exposures were used for the inputs and IPs. This experiment was only performed once due to difficulties in culturing the fibroblast cell lines.

The co-IPs show that the K50R mutant still interacts with the Rad21 component of the cohesin complex. The wild-type protein also co-IPs Rad21 as expected. It is less clear whether this is true for either of the patient mutations on the panel. Even though there is no clear band visible in the co-IP for either the G57R or the ΔK897, this may simply be due to the relatively low expression of these proteins and the fact that the co-IP conditions may not be optimal. For example, the interaction between ChlR1 and the cohesin complex me be specific to S-phase when sister chromatid cohesion is established. The fibroblast cell lines on the other hand grow very slowly and are likely to be predominantly in G1 at any given time.

These data suggest that, at least in the case of the K50R mutation, absence of helicase activity does not impact on its ability to interact with the cohesin complex. The fact that cohesion defects are still prominent in the K50R mutant even though interaction with Rad21 is not disrupted suggests that inability to interact with the cohesin complex is not the most likely mechanism behind the ChlR1 mutant phenotype. Rather, this suggests that it is probably the intrinsic helicase activity of ChlR1 that is crucial for its biological function in DNA metabolic processes. This will be explored in detail in the discussion section of this chapter.

5.2.5. G2 checkpoint defect in ChlR1 mutant cells

Having found evidence of severe cohesion defects in all the mutant cell lines, rescued only by re-expressing wild-type protein, the G2 checkpoint was targeted for investigation to determine whether these cells were perhaps entering into mitosis when they shouldn't due to a defective checkpoint. Cells were treated with 3gy of gamma-IR and allowed to recover for 2 hours and 8 hours before being fixed and analysed by flow cytometry for the

presence of mitotic cells. After 2 hours post-IR it would be expected that the majority of cells should have arrested in G2 if the checkpoint is intact. This is evidently the case in the wild-type, however it appears that the vector-only and the three mutant lines do indeed have a partially defective G2 checkpoint with more cells continuing to enter mitosis despite IR treatment (**figure 5.6**). This defect is more prominent in the vector-only cell line, which as discussed above, only express a very small amount of mutant protein. This differs from our knock-down system described in chapter 4, in which no checkpoint defect is apparent, in that the residual protein remaining after siRNA treatment is obviously wild-type. The reduction at the 8 hour time point may be caused by a G1 arrest that prevents cells from cycling back into mitosis. Or taking into account the timing, could be more likely attributed to activation of an intra-S phase checkpoint that prevents mutant cell lines from completing S phase and entering mitosis after 8 hours while the wild-type cells would be able to repair the damage and enter mitosis normally.

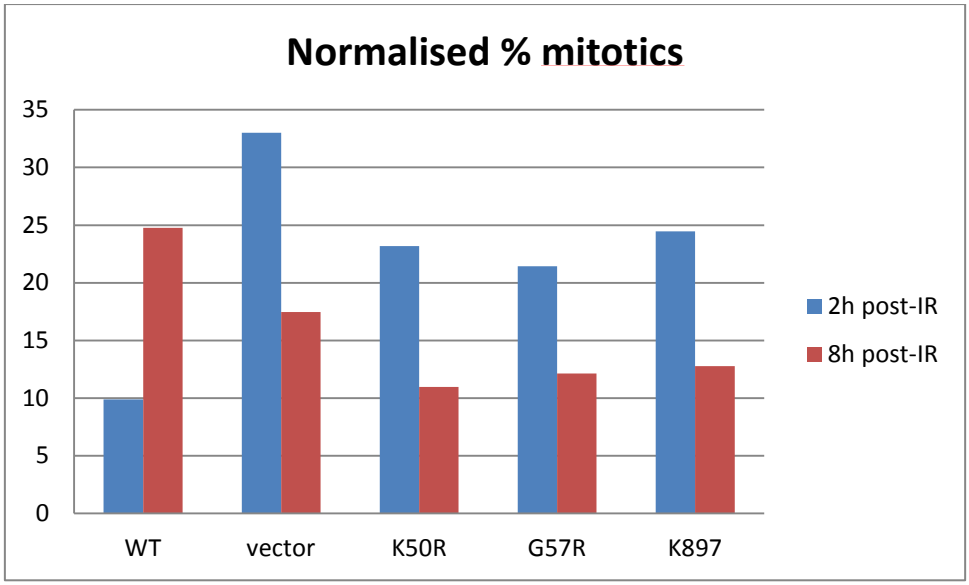

Figure 5.6. IR-induced G2 checkpoint arrest is deficient in the mutant fibroblast cell lines. Flow cytometric analysis of mitotic entry using phospho-H3 staining to detect mitotic cells. Each cell line was normalised to its own untreated sample which was set to 100%. The number of mitotic cells post-IR was then expressed as a proportion of that initial 100%. This data

5.3. Summary

Characterisation of these patient mutations has been hindered by the technical difficulties encountered through working with this particular cell system. As such, much of the above data is very preliminary and requires further confirmation. However, it is clear that the cohesion defect phenotype and G2 checkpoint defect exhibited by the patient cells can be rescued by re-expressing wild-type ChlR1 protein, further confirming the functional importance of ChlR1 in these WABS patients. Over-expression of either the G57R, or the two helicase-dead mutants K50R and ΔK897, does not appear to have the same effect.

Furthermore, while the G57R mutant has yet to be biochemically characterised, there appeared to be a striking difference between this mutation and the confirmed helicase dead mutants upon analysis of Chk1 activation in response to HU. The G57R cells (in case of both the vector-only and the G57R over-expressing cell line) showed the same rapid de-phosphorylation of Chk1 as wild-type upon removal of the drug. It will be interesting to discover whether this difference in some way corresponds to some retention of helicase activity in this mutant. This mutant also showed a lower incidence of PCS, perhaps indicating some milder abrogation of function compared with those which have previously been biochemically characterised.

5.4 Discussion

As discussed above, one of the main difficulties in studying the *in situ* effects of these ChlR1 mutations was successfully culturing and maintaining the patient-derived fibroblast cell lines which were the system chosen for these experiments. Their slow proliferation and tendency to rapidly senesce after only a few passages posed a challenge for experiments where significant cell numbers were required, for example the analysis of metaphase spreads. Because of this, statistical significance was unfortunately not obtained in the majority of the experiments discussed here. However, despite this caveat, the observations made do support previously published findings regarding the association of ChlR1 mutations with the cellular WABS phenotype as well as hinting at the possibility of phenotypic differences, at least at the cellular level, depending upon the nature of the mutation.

While there were certainly some difficulties with the stable cell lines, the availability of the HA epitope tag on the re-expressed proteins did provide an opportunity to analyse the localisation of these ChlR1 mutant proteins, albeit in an overexpression system. Although the proteins all expressed at different levels, a comparison between the wild-type and K50R mutant showed no obvious difference in localisation, both displaying strong nuclear staining. On the other hand, despite the G57R and ΔK897 proteins obviously reduced levels of expression, both did appear to show more diffuse cytoplasmic staining. Interestingly, the *in vitro* biochemical study carried out by Brosh and colleagues indicated that the ΔK897 protein was unable to bind DNA, unlike the artificially generated K50R mutant which still bound DNA despite lacking the ability to hydrolyse ATP. The observed differences in subcellular localisation could be taken to correlate with the Brosh data as it is conceivable that the inability of the ΔK897 to bind DNA in the cell might thus lead to increased nuclear exclusion and/or decreased protein stability. As there is currently no

biochemical data available for the G57R protein, it is possible that this protein may also have perturbed DNA binding. This, however, along with the potential helicase function of the G57R mutant, remains to be determined.

Metaphase spread analysis of the fibroblast panel confirmed that re-expressing the wild-type protein rescued the cohesion defects present in the mutant cell lines. This supports the evidence in the literature linking ChlR1 mutations with the WABS phenotype. However, overexpression of the mutant proteins did not rescue the defect. While the helicase activity status is unknown in the case of the G57R mutant, both the K50R and the ΔK897 have been shown in biochemical studies to be helicase-dead. In addition, the ΔK897 protein has also been shown to be unstable [179], data which is supported by its comparatively low expression in western blot analyses (**fig 5.1**). The K50R mutant protein on the other hand, expresses as well as wild-type and has been shown to be equally stable in *in vitro* experiments [174, 179]. Therefore it can be concluded that the helicase activity of ChlR1 is essential to its biological function and abrogation of this activity likely leads to the cohesion defects observed in WABS patients. Furthermore, although attempts to determine whether the panel of ChlR1 mutants could still interact with the cohesin complex were hindered by the low expression levels of the ΔK897 and G57R proteins, it was clear that the K50R mutant still interacted with the Rad21 subunit. This suggests that the cohesion defects observed in WABS patient cells are unlikely to be a direct consequence of abolishing the interaction between ChlR1 and cohesin and more likely due to loss of helicase function.

While attempting to explore whether the WABS cohesion defect was the result of an underlying problem with DNA replication or the ability of cells to tolerate replication stress, it became apparent that while all of the cell lines responded to HU treatment by activating Chk1 as expected, only the wild-type, the vector only and the G57R mutant

appeared to show the corresponding de-phosphorylation and continuation of replication following removal of the drug. This is consistent with data obtained using siRNA to knock down endogenous ChlR1 in the RPE1 cell system where no difference in Chk1 activation and recovery was observed between ChlR1 and control siRNA-treated cells. The two confirmed helicase-dead mutants on the other hand showed sustained Chk1 activation, presumably indicating continued stalling of replication and S-phase arrest. This could potentially be explained by considering that the presence of an overexpressed inactive mutant is more detrimental that having little or no active protein present at all (as would be the case in the knock-down system or in the vector only cell line). Particularly in the case of the K50R mutant which can still bind DNA and might therefore present a physical obstacle to the use of alternative pathways for replication recovery. Moreover, while the ΔK897 has been shown not to bind DNA *in vitro* there is still the possibility that it retains the ability to interact with other ChlR1 binding partners and in doing so prevent efficient resolution of replication-coupled damage.

The intriguing observation that the G57R mutant protein behaves similarly to wild-type protein in this assay raises the possibility that this particular mutant may well retain some or all of its helicase activity. This would suggest that the WABS phenotype observed in this patient is due to either the reduction in total ChlR1 protein levels or a partial reduction in helicase activity rather than complete abrogation of function. It is perplexing however that despite this apparently normal response to HU treatment and recovery, overexpression of the G57R mutant does not actually rescue the cohesion defect. Whether this is because the protein is in fact helicase-dead or only partially functional, or whether this is indicative of an additional helicase-independent function of ChlR1 requires further investigation. Interestingly, analysis of the G2 checkpoint in the fibroblast panel indicated that all the mutants had a slightly defective checkpoint in response to IR with the vector only cell line

exhibiting a more severe defect than the others. This lends some credence to the notion that there may well be an alternative helicase-independent checkpoint function for ChlR1 that has yet to be thoroughly explored.

As discussed in the introduction to this chapter, there does remain some ambiguity with regards to the potential product of the second mutant allele (c.2692-1G>A) in the G57R patient fibroblasts and its effect on protein expression and function. While highly speculative, it is possible that the addition of an extra twenty-five amino acids at the extreme C-terminus of the protein results in an unstable product that is rapidly degraded. While there is no tangible evidence of this, the somewhat surprisingly severe biochemical consequences of a single amino acid deletion at the C-terminus represented by the ΔK897 mutation would suggest that the protein is highly sensitive to disruption at this location.

In choosing to perform the experiments described above in this patient background, interpretation of the results becomes somewhat challenging. The biochemical properties of the G57R mutant protein have not been characterised and it is still not entirely clear if a protein product is produced from the second mutant allele. If both protein products are in fact present in the patient cells, albeit at low levels, drawing any concrete conclusions with regards to the G57R mutation and its function is untenable. In an attempt to circumvent this issue, stably-transfected RPE1 cell lines were generated using the same mutant constructs used to transfect the fibroblasts. It would therefore be possible in future to use these cells to repeat some of the experiments discussed above and further characterise the mutants without the uncertainty of the patient background. Using RPE1 cells instead of primary fibroblasts would also avoid many of the technical difficulties experienced when culturing the fibroblast lines. However, the caveat to this as an alternative system is that the endogenous wild-type ChlR1 would have to be knocked down with siRNA which is

not ideal from a practical perspective as well as inevitably resulting in a small amount of wild-type protein remaining in cells and thus potentially complicating matters further.

Finally, while the novel G57R mutant has not yet been biochemically characterised, at least two clinically relevant ChlR1 mutations are known to abrogate the helicase activity of the protein. It is therefore tempting to speculate that this enzymatic function of ChlR1 is crucial for the *in vivo* functions of the protein, some of which have been investigated in previous chapters of this thesis. Furthermore, the data from these biochemical studies has provided invaluable information on ChlR1 substrate specificity that allows important insight into how ChlR1 potentially functions in DNA metabolism and genome maintenance. The concluding chapter of this thesis will attempt to discuss the functional biological data presented thus far in the context of these recent biochemical studies with the aim of providing a clearer insight into the role of ChlR1 in these cellular processes.

Chapter 6

Concluding Remarks

ChlR1 is a member of a family of proteins known as the DEAD/H box helicases which also includes other helicases known to have important roles in genome stability maintenance such as RTEL, XPD and FANCJ (reviewed in [202]). Structurally, these proteins all contain a conserved iron-sulphur (Fe-S) cluster motif that appears to be crucial for protein function. Indeed, one of the fundamental concerns when attempting to purify *S. pombe* Chl1 was preserving the structural integrity of this Fe-S motif by preventing oxidation. Although purification to the standard of homogeneity required for biochemical or structural analysis was never achieved, the observation that the protein preparations were coloured with a yellow-green tinge strongly suggested the presence of an iron-binding protein with an intact binding cluster. Several classes of proteins with diverse cellular functions are known to contain this Fe-S motif and as a result both structural and functional roles have been proposed for this domain. Structural and biochemical studies of other Fe-S helicases however, coupled with site-directed mutagenesis to disrupt the domain integrity, have provided insight into how the Fe-S cluster in this instance potentially functions to allow the recognition of the boundary between single and double stranded DNA and promote the strand displacement critical to duplex unwinding [203, 204]. Additionally, clinically relevant mutations that disrupt the integrity of the Fe-S cluster have been identified in both XPD and FANCJ, leading to the genetic disorders trichothiodystrophy (TTD) and Fanconi Anaemia respectively [204]. At least one recently described patient derived mutation in ChlR1, which leads to the WABS phenotype, also disrupts the Fe-S cluster and severely abrogates the helicase function [177].

In the cases of both XPD and FANCJ, different mutations have the potential to lead to different disease phenotypes. In fact mutations in XPD are linked to three distinct genetic disorders: Xeroderma Pigmentosum, Cockayne's Syndrome and TTD. FANCJ mutations on the other hand have been linked to both Fanconi Anaemia and an increase in breast

cancer susceptibility. Currently it is not known whether the same may be true of mutations in ChlR1 however the recent data generated in the Parish lab suggests that the novel G57R mutation may represent a variant with a biochemical phenotype distinct from the patient mutations which have so far been characterised. The patient from whom this mutation was derived was originally diagnosed with Nijmegen Breakage Syndrome (NBS) which has a very similar clinical presentation to WABS although no mutation in NBS1 was subsequently detected [205]. This patient, unlike the other WABS patients who have been identified thus far, displayed hypersensitivity to X-rays which normally confirms a diagnosis of NBS in conjunction with the other clinical features. It is therefore possible that, similar to other related helicases, mutations in ChlR1 can lead to a spectrum of clinical phenotypes depending upon the nature and function of the particular mutation. Remarkably, a variant of FANCJ identified in women with early-onset breast cancer actually showed an increase in ATPase and helicase activities compared with wild-type protein in *in vitro* assays [206]. How this apparent gain of function mutation contributes to cancer development or progression is not yet understood but interestingly, recent experiments in the Parish lab have suggested that in terms of replication fork speed the G57R re-expressing mutant appears to be slightly faster than wild-type and the cells themselves also seem to proliferate at a faster rate (K. Feeney, unpublished). Whether this is a truly gain of function mutation has yet to be determined and only through purification and biochemical analysis will better understanding of the nature of this mutation be achieved.

Biochemical characterisation of the substrate preference of purified recombinant ChlR1 protein showed that the helicase preferentially unwound forked duplex structures and that it favours a 3’ overhang of 5-10 nucleotides for optimal activity. In the same study the ΔK897 patient-derived mutant protein was also purified and characterised but showed no

catalytic activity on any of the substrates tested [179]. This is in contrast to a second study that attempted to characterise another clinically relevant mutant of ChlR1, R263Q, which at high concentrations showed some residual helicase activity on forked duplex structures [177]. The WABS patients with the homozygous R263Q mutation did not display the same skin pigmentation abnormality observed in the original WABS patient and also had a more severe intellectual disability, further underlining the potentially heterogeneous nature of ChlR1-associated disease phenotypes. Interestingly, the R263Q mutation results in the substitution of glutamine for a highly conserved arginine residue in the Fe-S domain. The Fe-S motif has been shown to be essential for the helicase activity of FANCJ and XPD and in fact the equivalent mutation in XPD results in loss of helicase activity, defective nucleotide excision repair as well as a reduction in the protein levels of the transcription factor TFIIH of which XPD is a crucial component [204]. It is possible that disruption of the structural integrity of the Fe-S domain not only abrogates the helicase activity of ChlR1 but also disrupts other important protein-protein interactions that further impacts upon function. This is particularly important to consider as some of our data could be taken to indicate a helicase-independent checkpoint function for ChlR1, although this requires further verification. With this in mind, more in depth biochemical and functional characterisation of the novel G57R mutation could be crucial in further defining the biological role(s) of ChlR1. **Table 5** summarises the biochemical properties of ChlR1 mutant proteins.

Mutation	Properties
K50R	Point mutation in Walker A box. Binds DNA but cannot hydrolyse ATP. Helicase dead.
G57R	Point mutation near the helicase domain. Biochemically uncharacterised.
ΔK897	Deletion of a lysine residue at the extreme C terminus. Does not bind DNA *in vitro*
R263Q	Point mutation of a conserved arginine residue in Fe-S domain. Some residual helicase activity at high concentrations *in vitro*

Table 5. Table explaining the biochemical properties of the ChlR1 mutant proteins

The *in vitro* biochemical characterisation of wild-type ChlR1 also suggested that ChlR1 was able to unwind some varieties of G4 quadruplex DNA structures. These are DNA secondary structures thought to arise in G-rich tracts of DNA sequence which may thus impede crucial cellular processes such as replication, transcription and repair if not successfully resolved by the cellular machinery [207]. However, treatment of ChlR1-depleted U2OS cells with the G4 stabilising ligand telomestatin did not result in any increase in markers of DNA damage compared with control cells [208]. Depletion of the related helicase FANCJ on the other hand showed a marked increase in γH2AX foci following treatment with the drug. It is therefore not conclusive whether the *in vitro* G4 unwinding ability of ChlR1 has real physiological relevance *in vivo*. Nevertheless, in *C. elegans*, a double mutant of CHL-1 and DOG-1 (the putative FANCJ homologue in worms) showed an increase in the number of deletions upstream of polyguanine tracts compared with those observed in the DOG-1 mutant alone, although no deletions were apparent in the CHL-1 single mutant. The authors suggest that this points to a potential role for CHL-1 in resolving G4 structures that lead to genomic instability either in the

absence of DOG-1 or in specific circumstances such as during DNA replication [209]. It must be noted however that additional mutations in cohesin subunits as well as in HR proteins also lead to an exacerbation of the DOG-1 mutant phenotype which could also suggest that it is the more general homologous recombination repair pathway that is utilised to compensate for or prevent potentially deleterious genomic deletions that occur in the absence of DOG-1. This does not negate a role for CHL-1 in the specific resolution of G4 quadruplex structures but perhaps the downstream cohesion defect and its impact on HR repair presents an equally viable alternative explanation for the above observations. It would nonetheless be interesting to test the effects of telomestatin treatment on a ChlR1 FANCJ double knockdown to determine whether a similar additive effect on DNA damage can be observed in human cells.

In the same study by Brosh and colleagues, ChlR1-depleted cells treated with an inter-strand crosslinking agent did show an increase in DNA damage which would seem to be consistent with the observation that cells derived from WABS patients are sensitive to MMC. Although in our hands ChlR1-depleted cells showed no increased sensitivity to MMC, it should be noted that both the cell type and biological endpoint used were different. Use of the comet assay to analyse the response of ChlR1-depleted cells to cross-linking agents such as MMC or cisplatin may well yield different results compared with the cell survival assays that we initially employed. Our comet assay data which shows that ChlR1-depleted cells are more sensitive to hydroxyurea mediated replication stress, as well as the published data indicating WABS patient cells are also sensitive to camptothecin which causes stabilisation of the topoisomerase-DNA intermediate rather than a DNA crosslink, supports the hypothesis that the observed cellular sensitivity to MMC is probably replication-dependent rather than arising directly from a defect in the ICL repair pathway.

Comet assay data published recently by the Noguchi lab appears to confirm that following treatment with cisplatin, ChlR1-depleted cells show elevated levels of DNA damage [178]. They follow this up with evidence that suggests ChlR1-depleted cells which have been arrested by hydroxyurea are less able to resume replication when released into fresh growth medium containing cisplatin compared with control-treated cells. Presumably, this indicates that ChlR1 is required for processing cisplatin-induced DNA crosslinks during DNA replication but does not necessarily confirm that ChlR1 is required for replication restart. Another caveat to this experiment is that prolonged treatment with hydroxyurea has been shown to lead to fork collapse whereby rescue is only possible through new origin firing. It is therefore difficult to definitively conclude that restart of stalled forks is actually being measured in this instance rather than simply re-initiation of replication from new origins. Perhaps a better approach to answer that particular question would be to simply transiently arrest cells with hydroxyurea and then assay for replication restart in the absence of further drug treatment. Although using an alternative assay to Noguchi and colleagues, DNA fibre data from the Parish lab has attempted to shed further light on the potential role of ChlR1 in the restart of stalled replication forks. Our data suggest that depletion of ChlR1 does lead to an impaired ability to resume replication following hydroxyurea treatment, supporting a role for ChlR1 either in replication fork restart or in stabilisation of the stalled fork.

Finally, another potentially exciting observation was reported by the Brosh and colleagues in their biochemical analysis of ChlR1 activity [179]. In addition to the traditional ability of a helicase to unwind DNA duplex structures, ChlR1 was also able to successfully disrupt the interaction between a tetrameric streptavidin complex bound to a biotinylated single stranded oligonucleotide. Other functionally related helicases were unable to successfully disrupt the complex as effectively under similar conditions suggesting that

this novel ability to remodel protein-DNA structures may be mechanistically important for the *in vivo* function of ChlR1. Indeed, in another recent publication, the Brosh lab reported that in the case of several helicases, including FANCJ and RECQ1, their ability to facilitate the displacement of proteins from DNA is stimulated by interaction with the single-strand binding protein RPA [210]. There is some evidence to suggest that under certain circumstances ChlR1 also interacts with RPA and it is therefore possible that this association somehow promotes the ChlR1-mediated removal of proteins from DNA to promote the successful completion of cellular processes such as replication recovery and damage repair. Although helicases are well-characterised in terms of their ability to unwind DNA, currently there is relatively little understanding of the mechanisms by which they might also utilise their intrinsic ATPase motor activity to disrupt DNA-protein interactions and how this may be biologically relevant. This presents yet another avenue for potential further study in terms of ChlR1 function, particularly given the well-characterised roles of the protein in sister chromatid cohesion and DNA replication, processes where it can easily be imagined that this remodelling function of ChlR1 could be biologically important.

It has been shown in this work and by others that ChlR1 has a role in the cellular response to replication stress. Clinically relevant ChlR1 mutations have also been identified in patients with a severe genetic disorder characterised by a cellular sensitivity to agents which cause replication stress. Furthermore, a recent study has indicated that ChlR1 is not only highly expressed in both primary and metastatic melanomas but that ChlR1 knockdown in these cells results in reduced proliferation, cohesion defects and apoptosis [211]. Thus ChlR1 may be an important candidate gene for targeted treatment in the case of this extremely aggressive type of cancer. Further biological characterisation of ChlR1 and patient-derived variants will therefore be central to furthering our understanding of the

precise molecular mechanisms underlying ChlR1 function and allow exploitation of its potential as a cancer target.

Future work

Biochemical characterisation of the novel ChlR1 WABS-associated mutation, G57R, will be crucial to furthering our understanding and interpretation of the differences in checkpoint function observed in the complemented fibroblast cell lines. Determining whether this protein retains its helicase activity despite the clear manifestation of a clinical WABS phenotype in these patients could shed new light on the potential mechanism by which ChlR1 mutations lead to this disease. In addition, comprehensive analysis of replication fork dynamics in these complemented patient cells using the DNA fibre technique could also be important for investigating the *in vivo* consequences of ChlR1 mutations on replication fork progression and stability. It could also allow analysis of how these mutations impact on the replication checkpoint. However, the limitations of the stable fibroblast cell lines have been discussed in detail within this thesis and development of an alternative cell system in which to carry out these analyses may prove to be essential.

Bibliography

1. Hoeijmakers, J.H., *Genome maintenance mechanisms for preventing cancer.* Nature, 2001. **411**(6835): p. 366-74.
2. Mannini, L., S. Menga, and A. Musio, *The expanding universe of cohesin functions: a new genome stability caretaker involved in human disease and cancer.* Hum Mutat, 2010. **31**(6): p. 623-30.
3. Aguilera, A. and B. Gomez-Gonzalez, *Genome instability: a mechanistic view of its causes and consequences.* Nat Rev Genet, 2008. **9**(3): p. 204-17.
4. Jackson, D.A. and A. Pombo, *Replicon clusters are stable units of chromosome structure: evidence that nuclear organization contributes to the efficient activation and propagation of S phase in human cells.* J Cell Biol, 1998. **140**(6): p. 1285-95.
5. Gilbert, D.M., *Replication origin plasticity, Taylor-made: inhibition vs recruitment of origins under conditions of replication stress.* Chromosoma, 2007. **116**(4): p. 341-7.
6. Gavin, K.A., M. Hidaka, and B. Stillman, *Conserved initiator proteins in eukaryotes.* Science, 1995. **270**(5242): p. 1667-71.
7. Bell, S.P. and B. Stillman, *ATP-dependent recognition of eukaryotic origins of DNA replication by a multiprotein complex.* Nature, 1992. **357**(6374): p. 128-34.
8. Ohta, S., et al., *The ORC1 cycle in human cells: II. Dynamic changes in the human ORC complex during the cell cycle.* J Biol Chem, 2003. **278**(42): p. 41535-40.
9. Vashee, S., et al., *Sequence-independent DNA binding and replication initiation by the human origin recognition complex.* Genes Dev, 2003. **17**(15): p. 1894-908.
10. Lei, M., et al., *Mcm2 is a target of regulation by Cdc7-Dbf4 during the initiation of DNA synthesis.* Genes Dev, 1997. **11**(24): p. 3365-74.
11. Krude, T., et al., *Cyclin/Cdk-dependent initiation of DNA replication in a human cell-free system.* Cell, 1997. **88**(1): p. 109-19.
12. Tanaka, S., et al., *CDK-dependent phosphorylation of Sld2 and Sld3 initiates DNA replication in budding yeast.* Nature, 2007. **445**(7125): p. 328-32.
13. Mimura, S. and H. Takisawa, *Xenopus Cdc45-dependent loading of DNA polymerase alpha onto chromatin under the control of S-phase Cdk.* EMBO J, 1998. **17**(19): p. 5699-707.
14. Takayama, Y., et al., *GINS, a novel multiprotein complex required for chromosomal DNA replication in budding yeast.* Genes Dev, 2003. **17**(9): p. 1153-65.
15. Ilves, I., et al., *Activation of the MCM2-7 helicase by association with Cdc45 and GINS proteins.* Mol Cell, 2010. **37**(2): p. 247-58.
16. Gambus, A., et al., *GINS maintains association of Cdc45 with MCM in replisome progression complexes at eukaryotic DNA replication forks.* Nat Cell Biol, 2006. **8**(4): p. 358-66.
17. Jones, R.M. and E. Petermann, *Replication fork dynamics and the DNA damage response.* Biochem J, 2012. **443**(1): p. 13-26.
18. Stukenberg, P.T., P.S. Studwell-Vaughan, and M. O'Donnell, *Mechanism of the sliding beta-clamp of DNA polymerase III holoenzyme.* J Biol Chem, 1991. **266**(17): p. 11328-34.
19. Stukenberg, P.T., J. Turner, and M. O'Donnell, *An explanation for lagging strand replication: polymerase hopping among DNA sliding clamps.* Cell, 1994. **78**(5): p. 877-87.
20. Lehmann, A.R., et al., *Translesion synthesis: Y-family polymerases and the polymerase switch.* DNA Repair (Amst), 2007. **6**(7): p. 891-9.
21. Farina, A., et al., *Studies with the human cohesin establishment factor, ChlR1. Association of ChlR1 with Ctf18-RFC and Fen1.* J Biol Chem, 2008. **283**(30): p. 20925-36.
22. Cuvier, O., et al., *A topoisomerase II-dependent mechanism for resetting replicons at the S-M-phase transition.* Genes Dev, 2008. **22**(7): p. 860-5.

23. Santamaria, D., et al., *Bi-directional replication and random termination.* Nucleic Acids Res, 2000. **28**(10): p. 2099-107.
24. Moreno, S.P., et al., *Polyubiquitylation drives replisome disassembly at the termination of DNA replication.* Science, 2014. **346**(6208): p. 477-81.
25. Petermann, E. and T. Helleday, *Pathways of mammalian replication fork restart.* Nat Rev Mol Cell Biol, 2010. **11**(10): p. 683-7.
26. Labib, K. and B. Hodgson, *Replication fork barriers: pausing for a break or stalling for time?* EMBO Rep, 2007. **8**(4): p. 346-53.
27. Boudsocq, F., et al., *Investigating the role of the little finger domain of Y-family DNA polymerases in low fidelity synthesis and translesion replication.* J Biol Chem, 2004. **279**(31): p. 32932-40.
28. Chandani, S., C. Jacobs, and E.L. Loechler, *Architecture of y-family DNA polymerases relevant to translesion DNA synthesis as revealed in structural and molecular modeling studies.* J Nucleic Acids, 2010. **2010**.
29. Andersen, P.L., F. Xu, and W. Xiao, *Eukaryotic DNA damage tolerance and translesion synthesis through covalent modifications of PCNA.* Cell Res, 2008. **18**(1): p. 162-73.
30. Hoege, C., et al., *RAD6-dependent DNA repair is linked to modification of PCNA by ubiquitin and SUMO.* Nature, 2002. **419**(6903): p. 135-41.
31. Bienko, M., et al., *Ubiquitin-binding domains in Y-family polymerases regulate translesion synthesis.* Science, 2005. **310**(5755): p. 1821-4.
32. Kannouche, P.L., J. Wing, and A.R. Lehmann, *Interaction of human DNA polymerase eta with monoubiquitinated PCNA: a possible mechanism for the polymerase switch in response to DNA damage.* Mol Cell, 2004. **14**(4): p. 491-500.
33. Branzei, D., M. Seki, and T. Enomoto, *Rad18/Rad5/Mms2-mediated polyubiquitination of PCNA is implicated in replication completion during replication stress.* Genes Cells, 2004. **9**(11): p. 1031-42.
34. Unk, I., et al., *Role of yeast Rad5 and its human orthologs, HLTF and SHPRH in DNA damage tolerance.* DNA Repair (Amst), 2010. **9**(3): p. 257-67.
35. Unk, I., et al., *Human HLTF functions as a ubiquitin ligase for proliferating cell nuclear antigen polyubiquitination.* Proc Natl Acad Sci U S A, 2008. **105**(10): p. 3768-73.
36. Motegi, A., et al., *Polyubiquitination of proliferating cell nuclear antigen by HLTF and SHPRH prevents genomic instability from stalled replication forks.* Proc Natl Acad Sci U S A, 2008. **105**(34): p. 12411-6.
37. Petermann, E., et al., *Hydroxyurea-stalled replication forks become progressively inactivated and require two different RAD51-mediated pathways for restart and repair.* Mol Cell, 2010. **37**(4): p. 492-502.
38. Byun, T.S., et al., *Functional uncoupling of MCM helicase and DNA polymerase activities activates the ATR-dependent checkpoint.* Genes Dev, 2005. **19**(9): p. 1040-52.
39. Ira, G., et al., *DNA end resection, homologous recombination and DNA damage checkpoint activation require CDK1.* Nature, 2004. **431**(7011): p. 1011-7.
40. Li, L. and L. Zou, *Sensing, signaling, and responding to DNA damage: organization of the checkpoint pathways in mammalian cells.* J Cell Biochem, 2005. **94**(2): p. 298-306.
41. O'Driscoll, M., et al., *A splicing mutation affecting expression of ataxia-telangiectasia and Rad3-related protein (ATR) results in Seckel syndrome.* Nat Genet, 2003. **33**(4): p. 497-501.
42. Zou, L. and S.J. Elledge, *Sensing DNA damage through ATRIP recognition of RPA-ssDNA complexes.* Science, 2003. **300**(5625): p. 1542-8.
43. Guo, Z., et al., *Requirement for Atr in phosphorylation of Chk1 and cell cycle regulation in response to DNA replication blocks and UV-damaged DNA in Xenopus egg extracts.* Genes Dev, 2000. **14**(21): p. 2745-56.
44. Ward, I.M. and J. Chen, *Histone H2AX is phosphorylated in an ATR-dependent manner in response to replicational stress.* J Biol Chem, 2001. **276**(51): p. 47759-62.

45. Tibbetts, R.S., et al., *A role for ATR in the DNA damage-induced phosphorylation of p53.* Genes Dev, 1999. **13**(2): p. 152-7.
46. Cimprich, K.A. and D. Cortez, *ATR: an essential regulator of genome integrity.* Nat Rev Mol Cell Biol, 2008. **9**(8): p. 616-27.
47. Sanchez, Y., et al., *Conservation of the Chk1 checkpoint pathway in mammals: linkage of DNA damage to Cdk regulation through Cdc25.* Science, 1997. **277**(5331): p. 1497-501.
48. Zhao, H., J.L. Watkins, and H. Piwnica-Worms, *Disruption of the checkpoint kinase 1/cell division cycle 25A pathway abrogates ionizing radiation-induced S and G2 checkpoints.* Proc Natl Acad Sci U S A, 2002. **99**(23): p. 14795-800.
49. Shirahige, K., et al., *Regulation of DNA-replication origins during cell-cycle progression.* Nature, 1998. **395**(6702): p. 618-21.
50. Zegerman, P. and J.F. Diffley, *Checkpoint-dependent inhibition of DNA replication initiation by Sld3 and Dbf4 phosphorylation.* Nature, 2010. **467**(7314): p. 474-8.
51. Santocanale, C. and J.F. Diffley, *A Mec1- and Rad53-dependent checkpoint controls late-firing origins of DNA replication.* Nature, 1998. **395**(6702): p. 615-8.
52. Bahassi, E.M., et al., *The checkpoint kinases Chk1 and Chk2 regulate the functional associations between hBRCA2 and Rad51 in response to DNA damage.* Oncogene, 2008. **27**(28): p. 3977-85.
53. Zou, L., D. Cortez, and S.J. Elledge, *Regulation of ATR substrate selection by Rad17-dependent loading of Rad9 complexes onto chromatin.* Genes Dev, 2002. **16**(2): p. 198-208.
54. Unsal-Kacmaz, K., et al., *The human Tim/Tipin complex coordinates an Intra-S checkpoint response to UV that slows replication fork displacement.* Mol Cell Biol, 2007. **27**(8): p. 3131-42.
55. Yoshizawa-Sugata, N. and H. Masai, *Human Tim/Timeless-interacting protein, Tipin, is required for efficient progression of S phase and DNA replication checkpoint.* J Biol Chem, 2007. **282**(4): p. 2729-40.
56. Kumagai, A. and W.G. Dunphy, *Claspin, a novel protein required for the activation of Chk1 during a DNA replication checkpoint response in Xenopus egg extracts.* Mol Cell, 2000. **6**(4): p. 839-49.
57. Furuya, K., et al., *Chk1 activation requires Rad9 S/TQ-site phosphorylation to promote association with C-terminal BRCT domains of Rad4TOPBP1.* Genes Dev, 2004. **18**(10): p. 1154-64.
58. Ohashi, E., et al., *Interaction between Rad9-Hus1-Rad1 and TopBP1 activates ATR-ATRIP and promotes TopBP1 recruitment to sites of UV-damage.* DNA Repair (Amst), 2014. **21**: p. 1-11.
59. Sorensen, C.S., et al., *ATR, Claspin and the Rad9-Rad1-Hus1 complex regulate Chk1 and Cdc25A in the absence of DNA damage.* Cell Cycle, 2004. **3**(7): p. 941-5.
60. Shechter, D., V. Costanzo, and J. Gautier, *ATR and ATM regulate the timing of DNA replication origin firing.* Nat Cell Biol, 2004. **6**(7): p. 648-55.
61. Syljuasen, R.G., et al., *Inhibition of human Chk1 causes increased initiation of DNA replication, phosphorylation of ATR targets, and DNA breakage.* Mol Cell Biol, 2005. **25**(9): p. 3553-62.
62. Petermann, E., M. Woodcock, and T. Helleday, *Chk1 promotes replication fork progression by controlling replication initiation.* Proc Natl Acad Sci U S A, 2010. **107**(37): p. 16090-5.
63. Zachos, G., M.D. Rainey, and D.A. Gillespie, *Chk1-deficient tumour cells are viable but exhibit multiple checkpoint and survival defects.* EMBO J, 2003. **22**(3): p. 713-23.
64. Scorah, J. and C.H. McGowan, *Claspin and Chk1 regulate replication fork stability by different mechanisms.* Cell Cycle, 2009. **8**(7): p. 1036-43.
65. Leman, A.R., et al., *Human Timeless and Tipin stabilize replication forks and facilitate sister-chromatid cohesion.* J Cell Sci, 2010. **123**(Pt 5): p. 660-70.

66. Cortez, D., G. Glick, and S.J. Elledge, *Minichromosome maintenance proteins are direct targets of the ATM and ATR checkpoint kinases.* Proc Natl Acad Sci U S A, 2004. **101**(27): p. 10078-83.
67. Leman, A.R. and E. Noguchi, *Local and global functions of Timeless and Tipin in replication fork protection.* Cell Cycle, 2012. **11**(21): p. 3945-55.
68. Ansbach, A.B., et al., *RFCCtf18 and the Swi1-Swi3 complex function in separate and redundant pathways required for the stabilization of replication forks to facilitate sister chromatid cohesion in Schizosaccharomyces pombe.* Mol Biol Cell, 2008. **19**(2): p. 595-607.
69. Noguchi, E., et al., *Swi1 and Swi3 are components of a replication fork protection complex in fission yeast.* Mol Cell Biol, 2004. **24**(19): p. 8342-55.
70. Katou, Y., et al., *S-phase checkpoint proteins Tof1 and Mrc1 form a stable replication-pausing complex.* Nature, 2003. **424**(6952): p. 1078-83.
71. Cho, W.H., et al., *Human Tim-Tipin complex affects the biochemical properties of the replicative DNA helicase and DNA polymerases.* Proc Natl Acad Sci U S A, 2013. **110**(7): p. 2523-7.
72. Urtishak, K.A., et al., *Timeless Maintains Genomic Stability and Suppresses Sister Chromatid Exchange during Unperturbed DNA Replication.* J Biol Chem, 2009. **284**(13): p. 8777-85.
73. Daley, J.M. and P. Sung, *53BP1, BRCA1, and the choice between recombination and end joining at DNA double-strand breaks.* Mol Cell Biol, 2014. **34**(8): p. 1380-8.
74. Chapman, J.R., M.R. Taylor, and S.J. Boulton, *Playing the end game: DNA double-strand break repair pathway choice.* Mol Cell, 2012. **47**(4): p. 497-510.
75. Dynan, W.S. and S. Yoo, *Interaction of Ku protein and DNA-dependent protein kinase catalytic subunit with nucleic acids.* Nucleic Acids Res, 1998. **26**(7): p. 1551-9.
76. Lieber, M.R., *The mechanism of double-strand DNA break repair by the nonhomologous DNA end-joining pathway.* Annu Rev Biochem, 2010. **79**: p. 181-211.
77. Aylon, Y., B. Liefshitz, and M. Kupiec, *The CDK regulates repair of double-strand breaks by homologous recombination during the cell cycle.* EMBO J, 2004. **23**(24): p. 4868-75.
78. Bunting, S.F., et al., *53BP1 inhibits homologous recombination in Brca1-deficient cells by blocking resection of DNA breaks.* Cell, 2010. **141**(2): p. 243-54.
79. Chapman, J.R., et al., *BRCA1-associated exclusion of 53BP1 from DNA damage sites underlies temporal control of DNA repair.* J Cell Sci, 2012. **125**(Pt 15): p. 3529-34.
80. San Filippo, J., P. Sung, and H. Klein, *Mechanism of eukaryotic homologous recombination.* Annu Rev Biochem, 2008. **77**: p. 229-57.
81. Lundin, C., et al., *Different roles for nonhomologous end joining and homologous recombination following replication arrest in mammalian cells.* Mol Cell Biol, 2002. **22**(16): p. 5869-78.
82. Marechal, A. and L. Zou, *DNA damage sensing by the ATM and ATR kinases.* Cold Spring Harb Perspect Biol, 2013. **5**(9).
83. Ogawa, T., et al., *Similarity of the yeast RAD51 filament to the bacterial RecA filament.* Science, 1993. **259**(5103): p. 1896-9.
84. Baumann, P., F.E. Benson, and S.C. West, *Human Rad51 protein promotes ATP-dependent homologous pairing and strand transfer reactions in vitro.* Cell, 1996. **87**(4): p. 757-66.
85. Nimonkar, A.V., et al., *Human exonuclease 1 and BLM helicase interact to resect DNA and initiate DNA repair.* Proc Natl Acad Sci U S A, 2008. **105**(44): p. 16906-11.
86. Nimonkar, A.V., et al., *BLM-DNA2-RPA-MRN and EXO1-BLM-RPA-MRN constitute two DNA end resection machineries for human DNA break repair.* Genes Dev, 2011. **25**(4): p. 350-62.
87. Bishop, D.K., et al., *Xrcc3 is required for assembly of Rad51 complexes in vivo.* J Biol Chem, 1998. **273**(34): p. 21482-8.

88. Sartori, A.A., et al., *Human CtIP promotes DNA end resection.* Nature, 2007. **450**(7169): p. 509-14.
89. Huertas, P. and S.P. Jackson, *Human CtIP mediates cell cycle control of DNA end resection and double strand break repair.* J Biol Chem, 2009. **284**(14): p. 9558-65.
90. Marmorstein, L.Y., T. Ouchi, and S.A. Aaronson, *The BRCA2 gene product functionally interacts with p53 and RAD51.* Proc Natl Acad Sci U S A, 1998. **95**(23): p. 13869-74.
91. Tarsounas, M., A.A. Davies, and S.C. West, *RAD51 localization and activation following DNA damage.* Philos Trans R Soc Lond B Biol Sci, 2004. **359**(1441): p. 87-93.
92. Yu, D.S., et al., *Dynamic control of Rad51 recombinase by self-association and interaction with BRCA2.* Mol Cell, 2003. **12**(4): p. 1029-41.
93. Ip, S.C., et al., *Identification of Holliday junction resolvases from humans and yeast.* Nature, 2008. **456**(7220): p. 357-61.
94. Wu, L. and I.D. Hickson, *The Bloom's syndrome helicase suppresses crossing over during homologous recombination.* Nature, 2003. **426**(6968): p. 870-4.
95. Constantinou, A., et al., *Werner's syndrome protein (WRN) migrates Holliday junctions and co-localizes with RPA upon replication arrest.* EMBO Rep, 2000. **1**(1): p. 80-4.
96. Karow, J.K., et al., *The Bloom's syndrome gene product promotes branch migration of holliday junctions.* Proc Natl Acad Sci U S A, 2000. **97**(12): p. 6504-8.
97. Seigneur, M., et al., *RuvAB acts at arrested replication forks.* Cell, 1998. **95**(3): p. 419-30.
98. Hanada, K., et al., *The structure-specific endonuclease Mus81 contributes to replication restart by generating double-strand DNA breaks.* Nat Struct Mol Biol, 2007. **14**(11): p. 1096-104.
99. Chandramouly, G., N.A. Willis, and R. Scully, *A protective role for BRCA2 at stalled replication forks.* Breast Cancer Res, 2011. **13**(5): p. 314.
100. Lomonosov, M., et al., *Stabilization of stalled DNA replication forks by the BRCA2 breast cancer susceptibility protein.* Genes Dev, 2003. **17**(24): p. 3017-22.
101. Costanzo, V., et al., *Mre11 protein complex prevents double-strand break accumulation during chromosomal DNA replication.* Mol Cell, 2001. **8**(1): p. 137-47.
102. Trenz, K., et al., *ATM and ATR promote Mre11 dependent restart of collapsed replication forks and prevent accumulation of DNA breaks.* EMBO J, 2006. **25**(8): p. 1764-74.
103. Sobeck, A., et al., *Fanconi anemia proteins are required to prevent accumulation of replication-associated DNA double-strand breaks.* Mol Cell Biol, 2006. **26**(2): p. 425-37.
104. Bryant, H.E., et al., *PARP is activated at stalled forks to mediate Mre11-dependent replication restart and recombination.* EMBO J, 2009. **28**(17): p. 2601-15.
105. Yin, J., et al., *BLAP75, an essential component of Bloom's syndrome protein complexes that maintain genome integrity.* EMBO J, 2005. **24**(7): p. 1465-76.
106. Feeney, K.M., C.W. Wasson, and J.L. Parish, *Cohesin: a regulator of genome integrity and gene expression.* Biochem J, 2010. **428**(2): p. 147-61.
107. Michaelis, C., R. Ciosk, and K. Nasmyth, *Cohesins: chromosomal proteins that prevent premature separation of sister chromatids.* Cell, 1997. **91**(1): p. 35-45.
108. Haering, C.H., et al., *Molecular architecture of SMC proteins and the yeast cohesin complex.* Mol Cell, 2002. **9**(4): p. 773-88.
109. Uhlmann, F., et al., *Cleavage of cohesin by the CD clan protease separin triggers anaphase in yeast.* Cell, 2000. **103**(3): p. 375-86.
110. Uhlmann, F., F. Lottspeich, and K. Nasmyth, *Sister-chromatid separation at anaphase onset is promoted by cleavage of the cohesin subunit Scc1.* Nature, 1999. **400**(6739): p. 37-42.
111. Waizenegger, I.C., et al., *Two distinct pathways remove mammalian cohesin from chromosome arms in prophase and from centromeres in anaphase.* Cell, 2000. **103**(3): p. 399-410.

112. Gimenez-Abian, J.F., et al., *Regulation of sister chromatid cohesion between chromosome arms.* Curr Biol, 2004. **14**(13): p. 1187-93.
113. Sumara, I., et al., *The dissociation of cohesin from chromosomes in prophase is regulated by Polo-like kinase.* Mol Cell, 2002. **9**(3): p. 515-25.
114. Hornig, N.C. and F. Uhlmann, *Preferential cleavage of chromatin-bound cohesin after targeted phosphorylation by Polo-like kinase.* EMBO J, 2004. **23**(15): p. 3144-53.
115. Lengronne, A., et al., *Cohesin relocation from sites of chromosomal loading to places of convergent transcription.* Nature, 2004. **430**(6999): p. 573-8.
116. Darwiche, N., L.A. Freeman, and A. Strunnikov, *Characterization of the components of the putative mammalian sister chromatid cohesion complex.* Gene, 1999. **233**(1-2): p. 39-47.
117. Ciosk, R., et al., *Cohesin's binding to chromosomes depends on a separate complex consisting of Scc2 and Scc4 proteins.* Mol Cell, 2000. **5**(2): p. 243-54.
118. Skibbens, R.V., et al., *Ctf7p is essential for sister chromatid cohesion and links mitotic chromosome structure to the DNA replication machinery.* Genes Dev, 1999. **13**(3): p. 307-19.
119. Kenna, M.A. and R.V. Skibbens, *Mechanical link between cohesion establishment and DNA replication: Ctf7p/Eco1p, a cohesion establishment factor, associates with three different replication factor C complexes.* Mol Cell Biol, 2003. **23**(8): p. 2999-3007.
120. Toth, A., et al., *Yeast cohesin complex requires a conserved protein, Eco1p(Ctf7), to establish cohesion between sister chromatids during DNA replication.* Genes Dev, 1999. **13**(3): p. 320-33.
121. Lengronne, A., et al., *Establishment of sister chromatid cohesion at the S. cerevisiae replication fork.* Mol Cell, 2006. **23**(6): p. 787-99.
122. Moldovan, G.L., B. Pfander, and S. Jentsch, *PCNA controls establishment of sister chromatid cohesion during S phase.* Mol Cell, 2006. **23**(5): p. 723-32.
123. Skibbens, R.V., M. Maradeo, and L. Eastman, *Fork it over: the cohesion establishment factor Ctf7p and DNA replication.* J Cell Sci, 2007. **120**(Pt 15): p. 2471-7.
124. Guacci, V., D. Koshland, and A. Strunnikov, *A direct link between sister chromatid cohesion and chromosome condensation revealed through the analysis of MCD1 in S. cerevisiae.* Cell, 1997. **91**(1): p. 47-57.
125. Gruber, S., C.H. Haering, and K. Nasmyth, *Chromosomal cohesin forms a ring.* Cell, 2003. **112**(6): p. 765-77.
126. Mc Intyre, J., et al., *In vivo analysis of cohesin architecture using FRET in the budding yeast Saccharomyces cerevisiae.* EMBO J, 2007. **26**(16): p. 3783-93.
127. Zhang, N., et al., *A handcuff model for the cohesin complex.* J Cell Biol, 2008. **183**(6): p. 1019-31.
128. Chang, C.R., et al., *Targeting of cohesin by transcriptionally silent chromatin.* Genes Dev, 2005. **19**(24): p. 3031-42.
129. Skibbens, R.V., *Chl1p, a DNA helicase-like protein in budding yeast, functions in sister-chromatid cohesion.* Genetics, 2004. **166**(1): p. 33-42.
130. Petronczki, M., et al., *Sister-chromatid cohesion mediated by the alternative RF-CCtf18/Dcc1/Ctf8, the helicase Chl1 and the polymerase-alpha-associated protein Ctf4 is essential for chromatid disjunction during meiosis II.* J Cell Sci, 2004. **117**(Pt 16): p. 3547-59.
131. Parish, J.L., et al., *The DNA helicase ChlR1 is required for sister chromatid cohesion in mammalian cells.* J Cell Sci, 2006. **119**(Pt 23): p. 4857-65.
132. Ivanov, D., et al., *Eco1 is a novel acetyltransferase that can acetylate proteins involved in cohesion.* Curr Biol, 2002. **12**(4): p. 323-8.
133. Rolef Ben-Shahar, T., et al., *Eco1-dependent cohesin acetylation during establishment of sister chromatid cohesion.* Science, 2008. **321**(5888): p. 563-6.

134. Unal, E., et al., *A molecular determinant for the establishment of sister chromatid cohesion.* Science, 2008. **321**(5888): p. 566-9.
135. Zhang, J., et al., *Acetylation of Smc3 by Eco1 is required for S phase sister chromatid cohesion in both human and yeast.* Mol Cell, 2008. **31**(1): p. 143-51.
136. Terret, M.E., et al., *Cohesin acetylation speeds the replication fork.* Nature, 2009. **462**(7270): p. 231-4.
137. Rowland, B.D., et al., *Building sister chromatid cohesion: smc3 acetylation counteracts an antiestablishment activity.* Mol Cell, 2009. **33**(6): p. 763-74.
138. Schmidt, C.K., N. Brookes, and F. Uhlmann, *Conserved features of cohesin binding along fission yeast chromosomes.* Genome Biol, 2009. **10**(5): p. R52.
139. van der Lelij, P., et al., *Warsaw breakage syndrome, a cohesinopathy associated with mutations in the XPD helicase family member DDX11/ChlR1.* Am J Hum Genet, 2010. **86**(2): p. 262-6.
140. Misulovin, Z., et al., *Association of cohesin and Nipped-B with transcriptionally active regions of the Drosophila melanogaster genome.* Chromosoma, 2008. **117**(1): p. 89-102.
141. Kagey, M.H., et al., *Mediator and cohesin connect gene expression and chromatin architecture.* Nature, 2010. **467**(7314): p. 430-5.
142. Bausch, C., et al., *Transcription alters chromosomal locations of cohesin in Saccharomyces cerevisiae.* Mol Cell Biol, 2007. **27**(24): p. 8522-32.
143. Gullerova, M. and N.J. Proudfoot, *Cohesin complex promotes transcriptional termination between convergent genes in S. pombe.* Cell, 2008. **132**(6): p. 983-95.
144. Parelho, V., et al., *Cohesins functionally associate with CTCF on mammalian chromosome arms.* Cell, 2008. **132**(3): p. 422-33.
145. Klenova, E.M., et al., *Characterization of the chicken CTCF genomic locus, and initial study of the cell cycle-regulated promoter of the gene.* J Biol Chem, 1998. **273**(41): p. 26571-9.
146. Kim, T.H., et al., *Analysis of the vertebrate insulator protein CTCF-binding sites in the human genome.* Cell, 2007. **128**(6): p. 1231-45.
147. Wendt, K.S., et al., *Cohesin mediates transcriptional insulation by CCCTC-binding factor.* Nature, 2008. **451**(7180): p. 796-801.
148. Sjogren, C. and K. Nasmyth, *Sister chromatid cohesion is required for postreplicative double-strand break repair in Saccharomyces cerevisiae.* Curr Biol, 2001. **11**(12): p. 991-5.
149. Strom, L., et al., *Postreplicative formation of cohesion is required for repair and induced by a single DNA break.* Science, 2007. **317**(5835): p. 242-5.
150. Strom, L., et al., *Postreplicative recruitment of cohesin to double-strand breaks is required for DNA repair.* Mol Cell, 2004. **16**(6): p. 1003-15.
151. Unal, E., J.M. Heidinger-Pauli, and D. Koshland, *DNA double-strand breaks trigger genome-wide sister-chromatid cohesion through Eco1 (Ctf7).* Science, 2007. **317**(5835): p. 245-8.
152. Potts, P.R., M.H. Porteus, and H. Yu, *Human SMC5/6 complex promotes sister chromatid homologous recombination by recruiting the SMC1/3 cohesin complex to double-strand breaks.* EMBO J, 2006. **25**(14): p. 3377-88.
153. Kim, J.S., et al., *Specific recruitment of human cohesin to laser-induced DNA damage.* J Biol Chem, 2002. **277**(47): p. 45149-53.
154. De Piccoli, G., et al., *Smc5-Smc6 mediate DNA double-strand-break repair by promoting sister-chromatid recombination.* Nat Cell Biol, 2006. **8**(9): p. 1032-4.
155. Bauerschmidt, C., et al., *Cohesin promotes the repair of ionizing radiation-induced DNA double-strand breaks in replicated chromatin.* Nucleic Acids Res, 2010. **38**(2): p. 477-87.
156. Yazdi, P.T., et al., *SMC1 is a downstream effector in the ATM/NBS1 branch of the human S-phase checkpoint.* Genes Dev, 2002. **16**(5): p. 571-82.

157. Garg, R., et al., *Chromatin association of rad17 is required for an ataxia telangiectasia and rad-related kinase-mediated S-phase checkpoint in response to low-dose ultraviolet radiation.* Mol Cancer Res, 2004. **2**(6): p. 362-9.
158. Kim, S.T., B. Xu, and M.B. Kastan, *Involvement of the cohesin protein, Smc1, in Atm-dependent and independent responses to DNA damage.* Genes Dev, 2002. **16**(5): p. 560-70.
159. Bauerschmidt, C., et al., *Cohesin phosphorylation and mobility of SMC1 at ionizing radiation-induced DNA double-strand breaks in human cells.* Exp Cell Res, 2011. **317**(3): p. 330-7.
160. Kitagawa, R., et al., *Phosphorylation of SMC1 is a critical downstream event in the ATM-NBS1-BRCA1 pathway.* Genes Dev, 2004. **18**(12): p. 1423-38.
161. Luo, H., et al., *Regulation of intra-S phase checkpoint by ionizing radiation (IR)-dependent and IR-independent phosphorylation of SMC3.* J Biol Chem, 2008. **283**(28): p. 19176-83.
162. Brough, R., et al., *APRIN is a cell cycle specific BRCA2-interacting protein required for genome integrity and a predictor of outcome after chemotherapy in breast cancer.* EMBO J, 2012. **31**(5): p. 1160-76.
163. Watrin, E. and J.M. Peters, *The cohesin complex is required for the DNA damage-induced G2/M checkpoint in mammalian cells.* EMBO J, 2009. **28**(17): p. 2625-35.
164. Liras, P., et al., *Characterization of a mutation in yeast causing nonrandom chromosome loss during mitosis.* Genetics, 1978. **88**(4 Pt 1): p. 651-71.
165. Laha, S., et al., *The budding yeast protein Chl1p is required to preserve genome integrity upon DNA damage in S-phase.* Nucleic Acids Res, 2006. **34**(20): p. 5880-91.
166. Haber, J.E., *Bisexual mating behavior in a diploid of Saccharomyces cerevisiae: evidence for genetically controlled non-random chromosome loss during vegetative growth.* Genetics, 1974. **78**(3): p. 843-58.
167. Gerring, S.L., F. Spencer, and P. Hieter, *The CHL 1 (CTF 1) gene product of Saccharomyces cerevisiae is important for chromosome transmission and normal cell cycle progression in G2/M.* EMBO J, 1990. **9**(13): p. 4347-58.
168. Spencer, F., et al., *Mitotic chromosome transmission fidelity mutants in Saccharomyces cerevisiae.* Genetics, 1990. **124**(2): p. 237-49.
169. S, L.H., *CHL1 is a nuclear protein with an essential ATP binding site that exhibits a size-dependent effect on chromosome segregation.* Nucleic Acids Res, 2000. **28**(16): p. 3056-64.
170. Wu, Y., A.N. Suhasini, and R.M. Brosh, Jr., *Welcome the family of FANCJ-like helicases to the block of genome stability maintenance proteins.* Cell Mol Life Sci, 2009. **66**(7): p. 1209-22.
171. Ogiwara, H., et al., *Chl1 and Ctf4 are required for damage-induced recombinations.* Biochem Biophys Res Commun, 2007. **354**(1): p. 222-6.
172. Amann, J., et al., *Localization of chi1-related helicase genes to human chromosome regions 12p11 and 12p13: similarity between parts of these genes and conserved human telomeric-associated DNA.* Genomics, 1996. **32**(2): p. 260-5.
173. Amann, J., V.J. Kidd, and J.M. Lahti, *Characterization of putative human homologues of the yeast chromosome transmission fidelity gene, CHL1.* J Biol Chem, 1997. **272**(6): p. 3823-32.
174. Hirota, Y. and J.M. Lahti, *Characterization of the enzymatic activity of hChlR1, a novel human DNA helicase.* Nucleic Acids Res, 2000. **28**(4): p. 917-24.
175. Inoue, A., et al., *Loss of ChlR1 helicase in mouse causes lethality due to the accumulation of aneuploid cells generated by cohesion defects and placental malformation.* Cell Cycle, 2007. **6**(13): p. 1646-54.

176. van der Lelij, P., et al., *Diagnostic Overlap between Fanconi Anemia and the Cohesinopathies: Roberts Syndrome and Warsaw Breakage Syndrome.* Anemia, 2010. **2010**: p. 565268.
177. Capo-Chichi, J.M., et al., *Identification and biochemical characterization of a novel mutation in DDX11 causing Warsaw breakage syndrome.* Hum Mutat, 2013. **34**(1): p. 103-7.
178. Shah, N., et al., *Roles of ChlR1 DNA helicase in replication recovery from DNA damage.* Exp Cell Res, 2013. **319**(14): p. 2244-53.
179. Wu, Y., et al., *Biochemical characterization of Warsaw breakage syndrome helicase.* J Biol Chem, 2012. **287**(2): p. 1007-21.
180. Gould, K.L., et al., *Tandem affinity purification and identification of protein complex components.* Methods, 2004. **33**(3): p. 239-44.
181. Tasto, J.J., et al., *Vectors and gene targeting modules for tandem affinity purification in Schizosaccharomyces pombe.* Yeast, 2001. **18**(7): p. 657-62.
182. Huen, J., et al., *Rvb1-Rvb2: essential ATP-dependent helicases for critical complexes.* Biochem Cell Biol, 2010. **88**(1): p. 29-40.
183. Nguyen, V.Q., et al., *Molecular architecture of the ATP-dependent chromatin-remodeling complex SWR1.* Cell, 2013. **154**(6): p. 1220-31.
184. Tosi, A., et al., *Structure and subunit topology of the INO80 chromatin remodeler and its nucleosome complex.* Cell, 2013. **154**(6): p. 1207-19.
185. Morrison, A.J. and X. Shen, *Chromatin remodelling beyond transcription: the INO80 and SWR1 complexes.* Nat Rev Mol Cell Biol, 2009. **10**(6): p. 373-84.
186. Dunaway, S., H.-Y. Liu, and N.C. Walworth, *Interaction of 14-3-3 protein with Chk1 affects localization and checkpoint function.* J Cell Sci, 2005. **118**(1): p. 39-50.
187. Selvanathan, S.P., et al., *Schizosaccharomyces pombe Dss1p Is a DNA Damage Checkpoint Protein That Recruits Rad24p, Cdc25p, and Rae1p to DNA Double-strand Breaks.* Journal of Biological Chemistry, 2010. **285**(19): p. 14122-14133.
188. van Heusden, G.P.H. and H. Yde Steensma, *Yeast 14-3-3 proteins.* Yeast, 2006. **23**(3): p. 159-171.
189. Frank, S. and S. Werner, *The human homologue of the yeast CHL1 gene is a novel keratinocyte growth factor-regulated gene.* J Biol Chem, 1996. **271**(40): p. 24337-40.
190. Chomczynski, P. and N. Sacchi, *Single-step method of RNA isolation by acid guanidinium thiocyanate-phenol-chloroform extraction.* Anal Biochem, 1987. **162**(1): p. 156-9.
191. Bharti, S.K., et al., *Molecular functions and cellular roles of the ChlR1 (DDX11) helicase defective in the rare cohesinopathy Warsaw breakage syndrome.* Cell Mol Life Sci, 2014. **71**(14): p. 2625-39.
192. Moldovan, G.L., B. Pfander, and S. Jentsch, *PCNA, the maestro of the replication fork.* Cell, 2007. **129**(4): p. 665-79.
193. Chen, J., W. Bozza, and Z. Zhuang, *Ubiquitination of PCNA and its essential role in eukaryotic translesion synthesis.* Cell Biochem Biophys, 2011. **60**(1-2): p. 47-60.
194. Kumagai, A., et al., *Treslin collaborates with TopBP1 in triggering the initiation of DNA replication.* Cell, 2010. **140**(3): p. 349-59.
195. Lin, J.R., et al., *SHPRH and HLTF act in a damage-specific manner to coordinate different forms of postreplication repair and prevent mutagenesis.* Mol Cell, 2011. **42**(2): p. 237-49.
196. Wang, B., et al., *53BP1, a mediator of the DNA damage checkpoint.* Science, 2002. **298**(5597): p. 1435-8.
197. DiTullio, R.A., Jr., et al., *53BP1 functions in an ATM-dependent checkpoint pathway that is constitutively activated in human cancer.* Nat Cell Biol, 2002. **4**(12): p. 998-1002.
198. Heidinger-Pauli, J.M., et al., *The kleisin subunit of cohesin dictates damage-induced cohesion.* Mol Cell, 2008. **31**(1): p. 47-56.

199. Kim, B.J., et al., *Genome-wide reinforcement of cohesin binding at pre-existing cohesin sites in response to ionizing radiation in human cells.* J Biol Chem, 2010. **285**(30): p. 22784-92.
200. Chou, D.M. and S.J. Elledge, *Tipin and Timeless form a mutually protective complex required for genotoxic stress resistance and checkpoint function.* Proc Natl Acad Sci U S A, 2006. **103**(48): p. 18143-7.
201. Lee, J. and W.G. Dunphy, *Rad17 plays a central role in establishment of the interaction between TopBP1 and the Rad9-Hus1-Rad1 complex at stalled replication forks.* Mol Biol Cell, 2010. **21**(6): p. 926-35.
202. White, M.F., *Structure, function and evolution of the XPD family of iron-sulfur-containing 5'-->3' DNA helicases.* Biochem Soc Trans, 2009. **37**(Pt 3): p. 547-51.
203. Liu, H., et al., *Structure of the DNA repair helicase XPD.* Cell, 2008. **133**(5): p. 801-12.
204. Rudolf, J., et al., *The DNA repair helicases XPD and FancJ have essential iron-sulfur domains.* Mol Cell, 2006. **23**(6): p. 801-8.
205. Hiel, J.A., et al., *Nijmegen breakage syndrome in a Dutch patient not resulting from a defect in NBS1.* J Med Genet, 2001. **38**(6): p. E19.
206. Cantor, S.B. and S. Guillemette, *Hereditary breast cancer and the BRCA1-associated FANCJ/BACH1/BRIP1.* Future Oncol, 2011. **7**(2): p. 253-61.
207. Wu, Y., K. Shin-ya, and R.M. Brosh, Jr., *FANCJ helicase defective in Fanconia anemia and breast cancer unwinds G-quadruplex DNA to defend genomic stability.* Mol Cell Biol, 2008. **28**(12): p. 4116-28.
208. Bharti, S.K., et al., *Specialization among iron-sulfur cluster helicases to resolve G-quadruplex DNA structures that threaten genomic stability.* J Biol Chem, 2013. **288**(39): p. 28217-29.
209. Chung, G., N.J. O'Neil, and A.M. Rose, *CHL-1 provides an essential function affecting cell proliferation and chromosome stability in Caenorhabditis elegans.* DNA Repair (Amst), 2011. **10**(11): p. 1174-82.
210. Sommers, J.A., et al., *Novel function of the Fanconi anemia group J or RECQ1 helicase to disrupt protein-DNA complexes in a replication protein A-stimulated manner.* J Biol Chem, 2014. **289**(29): p. 19928-41.
211. Bhattacharya, C., X. Wang, and D. Becker, *The DEAD/DEAH box helicase, DDX11, is essential for the survival of advanced melanomas.* Mol Cancer, 2012. **11**: p. 82.